RUSSIAN GEOGRAPHICAL SOCIETY

FACULTY OF GEOGRAPHY,
LOMONOSOV MOSCOW STATE UNIVERSITY

INSTITUTE OF GEOGRAPHY,
RUSSIAN ACADEMY OF SCIENCE

Vol. 10 2017 No. 04

GEOGRAPHY ENVIRONMENT SUSTAINABILITY

EDITORIAL BOARD

CONTENTS

Svetlana A. Agafonova[1]*, Natalia L. Frolova[1], Galina V. Surkova[1], Klaus P. Koltermann[1]
[1]Faculty of Geography, Lomonosov Moscow State University, Moscow, Russia
*** Corresponding author:** sv_andreevna@mail.ru

MODERN CHARACTERISTICS OF THE ICE REGIME OF RUSSIAN ARCTIC RIVERS AND THEIR POSSIBLE CHANGES IN THE 21ST CENTURY

ABSTRACT. Changes in rivers ice regime features and the climatic resources of the winter period were examined for the territory of Russia northward from 60° N. Datasets from 220 gauging stations for the period from 1960 to 2014 have been used in the study both with the results of numerical experiments carried out using climate models in the framework of the international project CMIP5. A change in the duration of the ice phenomena period, the ice cover period and the maximum thickness of ice on the rivers for the scenario RCP 8.5 by the end of the 21st century for a spatial grid with a distance between the nodes of 1.75x1.75 degrees in latitude and longitude has been estimated. We elaborated series of the maps. Main features of the ice regime changes are consistent with the expected changes in the duration of the cold season and the accumulated negative air temperatures. The significant changes are expected for the rivers of the Kola Peninsula and the lower reaches of the rivers Northern Dvina and Pechora, whereas the lowest changes - for the center of Eastern Siberia.

KEY WORDS: river ice, climate change

CITATION: Svetlana A. Agafonova, Natalia L. Frolova, Galina V. Surkova Modern characteristics of the ice regime of Russian Arctic rivers and their possible changes in the 21st century. Geography, Environment, Sustainability, Vol.10, No 4, p. 4-15
DOI-10.24057/2071-9388-2017-10-4-4-15

INTRODUCTION

The study of current trends of the hydrological regime of the Arctic rivers is a relevant scientific and practical task. Ice phenomena can be observed on the Arctic rivers for most of the year. A lot of types of economic activities are related to the terms and duration of ice phenomena (navigation, the construction of ice crossings and the operation of various hydraulic structures). In many cases, ice phenomena cause dangerous hydrological processes, including floods (Agafonova et al. 2017). For the selected region, the population and the economy experience the greatest difficulties due to ice phenomena on the rivers during hanging ice dam or ice jam floods, in the case of a damage to hydraulic structures during a heavy ice run and high water levels, as well as when arranging navigation and ice crossings.

The change in the characteristics of the ice regime from year to year is primarily a function of meteorological characteristics and the characteristics of the river's water regime. There are a lot of studies of trends of the ice regime of rivers to date, including the Arctic zone, the results of which have been summarized in (IPCC 2014; Prowse et al. 2007, Prowse et al. 2011; Vuglinsky 2002; Vuglinsky 2017). There are also estimates of changes in the characteristics of the ice regime of the Russian rivers under various scenarios of climate changes. The studies using a simple model based on the relation between the terms of ice phenomena and the average air temperature of the preceding month, have obtained the probable characteristics of the future ice regime of rivers during the 21st century (Borshch et al. 2001; Ginzburg 2005).

The area under study is located to the north of 60° N and includes the Arctic zone of Russia and the neighboring regions: the Kola Peninsula, Karelia, the basins of the rivers Onega, Northern Dvina and Pechora, the middle and lower reaches of large Siberian rivers (Ob, Yenisei and Lena), the basins of the rivers Yana, Indigirka and Kolyma. The rivers of the area under study are important thruways, first of all, for the Northern Supply Haul. If the main settlements in the Republic of Karelia and the Murmansk region are located along the railway, then within the Arkhangelsk region and the Komi Republic - along the rivers. There are also most of the settlements along the rivers in Siberia. The transport accessibility of such settlements depends on the work of ferry crossings in summer and during ice crossings in winter.

The climate of the area is characterized mainly by a severe long winter and a short cool summer. The water runoff of the studied rivers is formed mainly during the melting of the snow cover with the addition of high mountain snowfields, glaciers and ice coating for a number of rivers. The spring-summer high water lasts, on average, from May to July. The winter low water is stable, its runoff reaches significant values in the north of the European part of Russia and near the rivers of the Kara Sea and decreases to rather low values in the catchment areas of the Laptev Sea, the East Siberian and the Chukchi Seas due to severe environmental conditions. A number of large and medium-sized northern rivers (the rivers Anabar, Olenek, Yana, Alazeya, Palyavaam, Amguema, etc.) are frozen to the bottom in winter (Alekseevsky et al. 2007).

MATERIALS AND METHODS

The observation data obtained at 220 hydrological stations (Fig. 1) for the period from 1960 to 2014 have been used in the study, the most common characteristics of the ice regime of rivers have been considered: the duration of the period with ice phenomena, the duration of ice cover period and the maximum ice thickness. The data omissions were restored by means of hydrological analogy using the information on the sections located on the rivers with similar physical and geographical conditions and characteristics of catchment areas.

To estimate future changes in the characteristics of the ice regime, the indicators of climatic resources for the cold period (October-May) were used: the accumulated negative air temperatures, the accumulated positive air temperatures, the number of days with the air temperature below 0° C and the amount of solid precipitation. The climatic resources were calculated on the basis of the results of numerical experiments carried out using climate models within the framework of the international project CMIP5 (Taylor et al. 2012). Among the main computational experiments of CMIP5 important in estimating the Arctic's further response to climate changes, the experiment historical and the experiment under the scenario RCP8.5 were used (Moss et al. 2008). The choice of the scenario RCP 8.5 is due to the fact that it is the most «severe» among the scenarios estimated in the numerical experiments of CMIP5 in terms of a possible impact of external factors, including anthropogenic ones, on the climate system, taking into account the greenhouse gas emission control policy. Such an intense external impact makes it possible to elicit large and statistically significant response to an increase in the concentration of greenhouse gases.

The climatic resource indicators were calculated based on model data on the daily

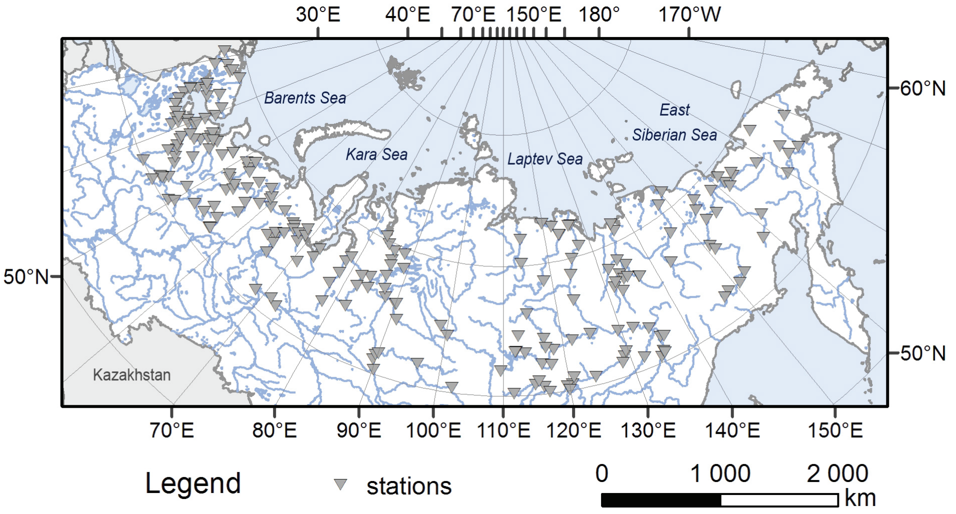

Fig. 1. The study area

values of the average daily temperature of the ground air and the daily precipitation. The results of each model were interpolated onto a single spatial grid with a distance between the nodes of 1.75×1.75 degrees in latitude and longitude, ensemble-averaged models were calculated for the grid nodes.

ICE REGIME OF RIVERS IN MODERN CONDITIONS

The rivers of the area under study are frozen up, on average, in October: in the first days – in the northeast (the rivers Anadyr and Kolyma), by the end of the first decade - within Western Siberia (the rivers Taz, Nadym and the lower reaches of the Ob River), in the middle of the month - the rivers of the European sector (the lower reaches of the rivers Pechora, Mezen and Onega) and by the end of the second decade of October - the rivers of the Kola Peninsula (the rivers Varzuga and Ponoy). Ice cover is on average formed on the rivers of the Asian part - in the middle of October, on the rivers of the European part - in the first days of November. The root-mean-square deviation of the autumnal periods of ice phenomena is 13 to 15 days for Karelia and the southern coast of the White Sea, 10-12 for the lower reaches of the north of the European part, 6-8 for the rivers of Western Siberia, and 3-5 days for the rest of the territory (Agafonova et al. 2016).

The rivers of the area under study are characterized by stable ice cover, the exceptions are rapids and sources of large lakes. There is no stable ice cover in the segments of industrial wastewater discharge, below the dams of hydroelectric power stations, either. The average duration of ice cover period varies from 150 days in the south-west to 240 or more on the rivers of the Taimyr Peninsula (Fig. 2). The isolines are mainly sub-latitudinal, except for the rivers Yana and Indigirka, in the upper reaches of which there is the zone of influence of the Siberian anticyclone. The duration of ice cover period for large rivers (the rivers Pechora, Ob, Yenisei, Lena, etc.) is somewhat lower than on the neighboring middle rivers. Due to the predominant direction of the flow of these rivers from south to north, the duration of ice cover period increases towards the mouth and is 230 days in the gauging sections of the rivers Lena and Yenisei, 210 days for the Ob River and 190 days for the Pechora River (Fig. 3).

For most of the rivers of the area under study, the thickness of the ice cover increases throughout the entire period of ice cover and reaches its maximum values in the last month of ice cover period, the intensity of increase in recent months being minimal. The sharp increases in the thickness of ice in February and March are usually caused by water outflow on the ice, in April – by thaws and the freezing of wet snow with the ice cover. The significant increase in the thickness of ice on small and medium rivers is often due to the freezing of the underlying layers to the bottom and lack of flow in the line of a station.

The wide spread of the values of the maximum ice thickness is characteristic for the northeast of the territory. The average maximum ice thickness for the values of the accumulation negative air temperatures below -5000° C is 0.8 to 2.0 m or more. For individual sections, the ice cover thickness increases due to the freezing of water on river ice, others are characterized

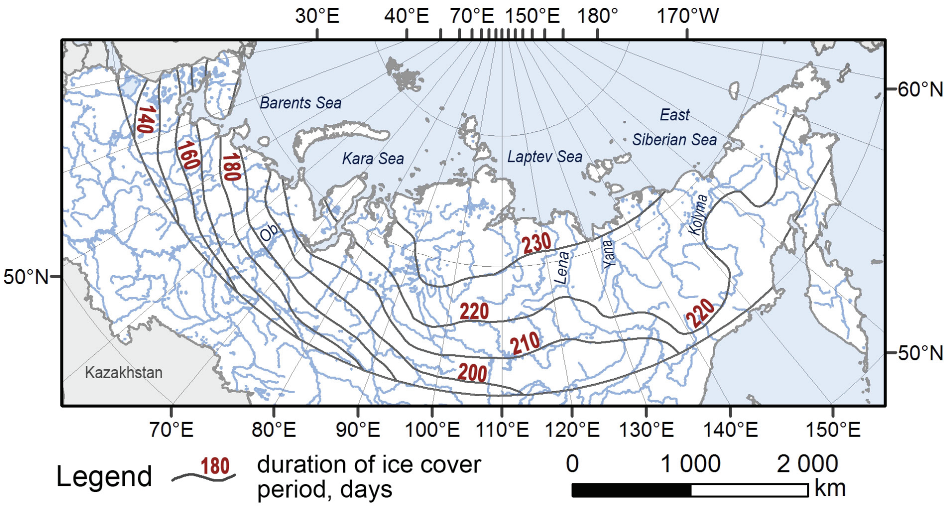

Fig. 2. Duration of ice cover period on middle rivers for the period of 1986-2005

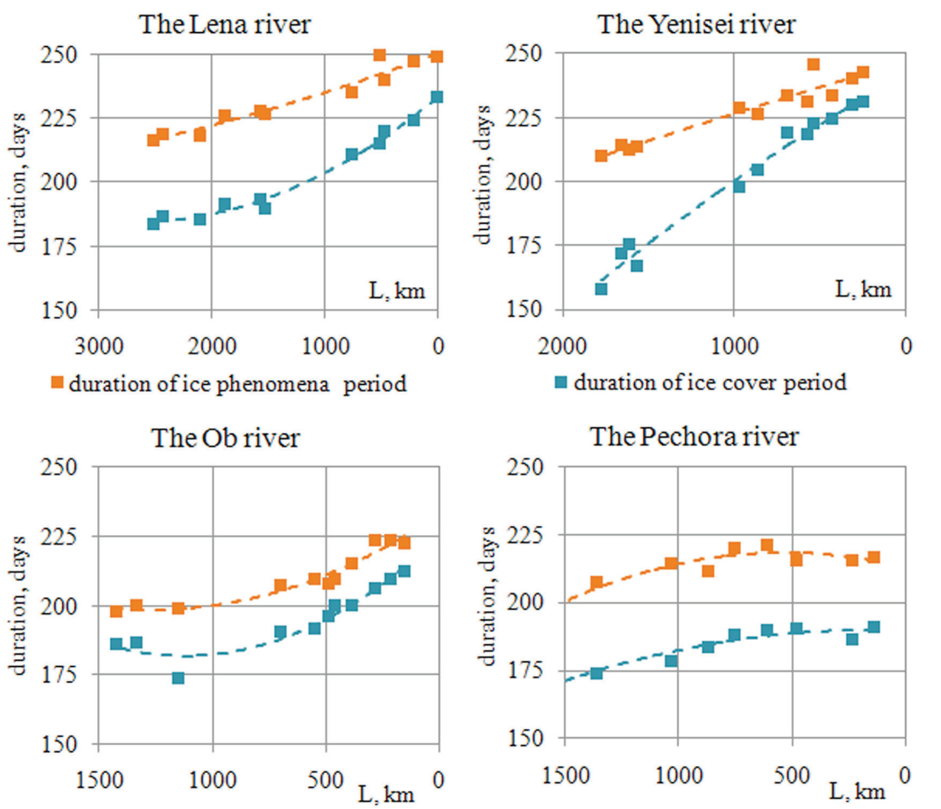

Fig. 3. Duration of ice phenomena and ice cover period by the length of large rivers for the period of 1986-2005 (L – distance from mouth, km).

by special hydrogeological conditions and, as a result, lower ice thickness values, and open leads during the winter period for individual sections of rivers.

For freezing rivers, the thickness of the ice cover ceases to grow long before the end of the winter period. In such cases, the ice thickness in the absence of icing is equal to the depth of the stream before ice cover period. It should be noted that within the European part of Russia, it is mainly small rivers (with a catchment area of up to 5000 km^2) that are frozen, within Siberia, especially in the north-eastern part, the freezing of sections of large rivers with a catchment area up to 200,000 km^2 is possible (Arzhakova 2001).

For the rivers of the Kola Peninsula, the highest values of ice thickness by the end of the ice cover period reach from 0.5 m in warm winters to 1.0 m in severe winters, for the Pechora River - from 0.7 to 1.4 m, respectively, for the rivers of Western Siberia - from 0.8 to 1.5 m, for the Lena River - from 1.3 to 2.0 m and on the rivers of the north-eastern part (the Amguema River and others) - from 1.7 to 2.5 m.

Due to the reduction in runoff in winter, the ice can be formed consisting of several layers separated by an empty, without water, space. Icings are formed on almost all the rivers in the zone of permafrost. River icings are formed when the rivers freeze, when the ice cover subsides under the pressure of snow or transport, when the bed is blocked by ice. In this case, the water flows out onto the surface of the ice cover and freezes. The melting of icing can continue throughout the warm period (Alekseev 1987).

On the rivers of the north-east, the ice cover period ends, on average, in the first decade of June, on the rivers of the Arctic part of Central and Western Siberia - at the end of May, and on the rivers of the Kola Peninsula - in mid-May. The root-mean-square deviation of the spring periods of ice phenomena for the rivers of the European sector of the Arctic zone is 9-11 days, for the rivers of Western Siberia - 6-8 days, for the rest of the territory - 3-5 days.

The average duration of the period with ice phenomena is from 180 days for the rivers of Karelia to 260 days for the rivers of the northeast and the Taimyr Peninsula, for the gauging sections of the Lena river - 250 days, for the Yenisei River - 245 days, for the Ob River - 225 days, and for the Pechora River - 220 days (Fig. 3).

OBSERVED CHANGES IN THE MAIN CHARACTERISTICS OF THE ICE REGIME OF RIVERS

The changes in the terms of ice phenomena are the result of a change in the water and thermal regime of rivers. The ice regime does not immediately react to climatic changes by reducing the duration of ice phenomena, changes in ice characteristics are often not so obvious and remain statistically insignificant for a long time. For the rivers of the area under study, some trends in the characteristics of the ice regime can be seen only after 1990 (Table 1).

In the autumn period, with a decrease in water consumption, the emergence of ice can be observed at a time close to the norm even with a slight increase in the air temperature. The similar situation is, for example, in the north of the European part. After the beginning of stable ice formation (early or near normal), the unstable pattern of the air temperature leads to a return of positive temperatures in November, resulting in floods due to the melting of snow and rainfall. The high levels during this period contribute to later ice formation, an increase in the duration of the autumn ice and sludge run, the formation of ice jams. It should be noted that the shift in the terms of ice formation within the European sector is primarily due to the increasingly frequent cases of extremely late ice cover formation, which significantly effects the duration of the ice cover period.

The greatest shift in the terms of ice emergence is observed on the rivers of Karelia and in the lower reaches of the Onega River (+7-8 days), for the rest of the rivers of the European sector - about +5 days; for Siberian rivers, the changes are statistically insignificant and are up to +2-4 days.

The important factors for the growth of the thickness of the ice cover and a change in its maximum values are the features of weather

Table 1. Change in the characteristics of the ice regime (when comparing 2 periods: 1961-1990 and 1991-2014)

Areas	Change in		
	the duration of		the maximum ice thickness (sm)
	the ice cover period, days	the period with ice phenomena, days	
Kola	–(12–13)	–(10–11)	–(5–10)
Karelia	–(13–14)	–(11–12)	–(10–15)
European North	–(11–12)	–(9–10)	–(5–10)
Western Siberia	–(9–10)	–(8–9)	–(5–10)
Middle Siberia	–(7–8)	–(6–7)	–(5–10)
Eastern Siberia	–(6–7)	–(4–5)	–(0–5)
Northeast	–(3–4)	–(3–4)	–(5–10)

conditions in winter. It is not only about the accumulation of negative air temperatures and snow cover on the ice, but also about the regime of thaws that become deeper and more prolonged in the European part of Russia. While thaws, with rare exceptions, do not lead to the breakup of ice in rivers in winter, snow melting on ice and the formation of snow ice, when negative air temperatures return, can be observed. Some softening of winter conditions does not lead to significant decreases in the average ice thickness values by the end of the winter season. On the rivers of Siberia, the thickness of the ice cover often reaches the values close to the limit ones; in the middle of the ice formation period, the further accumulation of negative air temperatures does not affect the maximum values of ice thickness any longer either. As a result, the change in the thickness of the ice cover on the rivers of Eastern Siberia is not more than -5 cm, on the rest of the rivers of Siberia and on the large rivers of the north of the European part - up to -10 cm, and only on the rivers of Karelia - –10-15 cm.

The ice cover is destroyed under the influence of two forces: 1. the surface and internal melting of ice under the influence of solar radiation, heat exchange with the atmosphere and the water mass; 2. the dynamic effect of the flow with a sufficiently high intensity and velocity of the flood wave. The nature of the spring breakup is determined by the thickness and strength of the ice cover by the time of breakup, the weather and hydrological conditions of the spring period. When the water flow rates are low and the fluctuations in the water level are slight during the breakup period, ice melts in place. On large and medium rivers, along with the weakening of ice strength, when effected by thermal factors, the integrity of the ice cover is disturbed under the influence of fluctuations of the water level and hydrodynamic load. For the rivers under study, most of which flow from south to north, the dynamic effect of the flow in breakup processes is crucial (Donchenko 1987).

The changes in the dates of the breakup of ice in rivers are statistically insignificant for almost all stations, except for the rivers of Karelia and the Kola Peninsula. The shift in the dates of breakup in the rivers of the Kola Peninsula and Karelia is –6-8 days, on the rivers of the north of the European part and Western Siberia - –4-5 days, the shift in the terms of ice clearing is also more pronounced for the rivers of the European sector of the Arctic zone and does not exceed –1-2 days for the rivers of the northeast.

As a result of a shift in the terms of ice phenomena, the change in the duration of ice cover period and the period with ice phenomena is –10-14 days for the European part and only –3-4 for the northeast part.

ESTIMATION OF CHANGES IN THE ICE REGIME

The total global warming predicted by the climate system models according to the scenarios RCP is manifested differently at the regional level. According to the IPCC assessment report (IPCC 2013), in the case of the scenario RCP 8.5, the average global surface temperature is expected to increase by about 2° C by the middle of the 21st century compared to 1986-2005, and by about 4° C by 2100. For the Arctic, according to this scenario, much more intensive climate warming is expected by the end of the 21st century, its value will be 5-10° C depending on the regions. On the larger territory of the Arctic, the anomalies of a lot of indicators of climatic resources are more pronounced during the cold period (Surkova et al. 2017).

To estimate possible future changes, empirical dependencies of indicators of climatic resources for the cold period (October-May), calculated on the basis of the results of numerical experiments carried out using climate models in the framework of the international project CMIP5, and the main characteristics of the ice regime at hydrological stations, were identified. As the initial data, the average (for 10 years) moving values for all stations were used: the accumulated negative air temperatures, the accumulated positive air temperatures, the number of days with the air temperature below 0° C, the amount of solid precipitation, as well as the duration of the period with ice phenomena, the duration of ice cover period and the maximum ice thickness for the period from 1986 to 2005.

For each empirical dependence, optimal combinations of predictors were selected (Table 2). As a result, about 2000 points were used for the dependencies of duration of ice cover period and the period with ice phenomena, and somewhat less for ice thickness. The sections, for which ice thickness increases due to icings or for which the effect of the groundwater outflow is decisive, were excluded. The averaging over the decades and the sharing of data of all stations within one dependence made it possible to smooth the effect of the local conditions of individual sections and the features of weather of individual years. The correlation coefficients of the obtained dependences are statistically significant.

Using the obtained dependences, the values of the ice regime characteristics for a spatial grid with a distance between the nodes 1.75x1.75 degrees in latitude and longitude for the time slices of 1986-2005 and 2081-2100 were calculated. The possible changes in the characteristics of the ice regime were estimated as the difference of the obtained fields. The results are presented in the form of maps (Fig. 4-6).

Table 2. Empirical dependencies of the characteristics of the ice regime

Characteristics of the ice regime of the rivers	Number of points	Predictors	Multiple correlation coefficient
Duration of ice cover period	2060	number of days with a negative air temperature, accumulated negative air temperatures	0.86
Duration of the period with ice phenomena	2050	number of days with a negative air temperature, accumulated positive air temperatures	0.91
Maximum ice thickness	1120	accumulated negative air temperatures, amount of solid precipitation	0.73

The estimates of changes in the main characteristics of the ice regime by the end of the 21st century are consistent with the expected changes in the duration of the cold period and the accumulated negative air temperatures. For Karelia and the Kola Peninsula, in the case of the scenario RCP 8.5, the accumulated negative temperatures is expected to be -700 ... -1000° C, for the north of Western Siberia -1500 ... -2000° C, for Eastern Siberia -3000 ... -3500. According to the estimates, the number of days with a negative air temperature will be reduced to 100-150 days for Karelia, the Kola Peninsula and the basin of the Northern Dvina River, up to 150-200 days for the basin of the Pechora River and the north of Western Siberia and will be 200 days or more for the north of Central and Eastern Siberia and the basins of the rivers Kolyma and Yana and for the north-east.

A significant reduction in the duration of the period with ice phenomena and the period of ice cover (when comparing two periods: 1986-2005 and 2081-2100) are expected for the rivers of the Kola Peninsula and the lower reaches

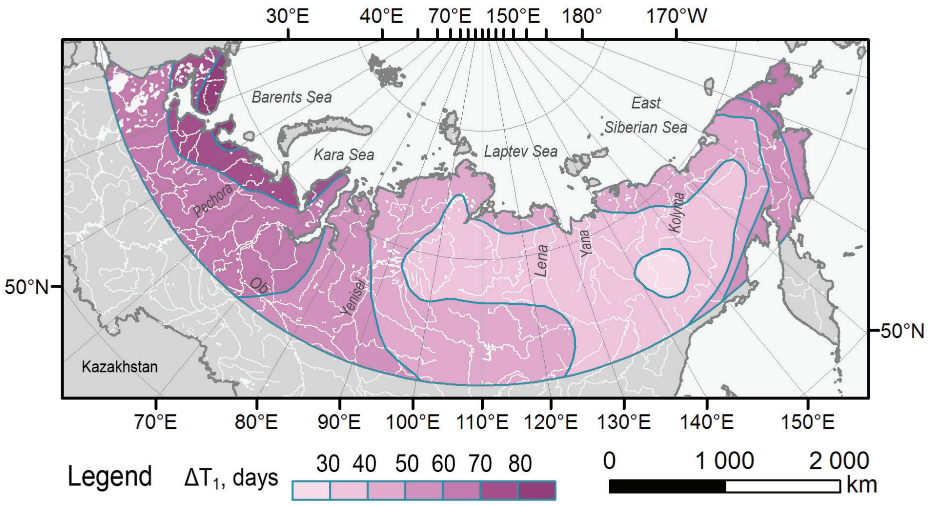

Fig. 4. Estimation of a change in the duration of the ice cover period (ΔT_1, days) by the end of the 21st century.in comparison with the period of 1986-2005

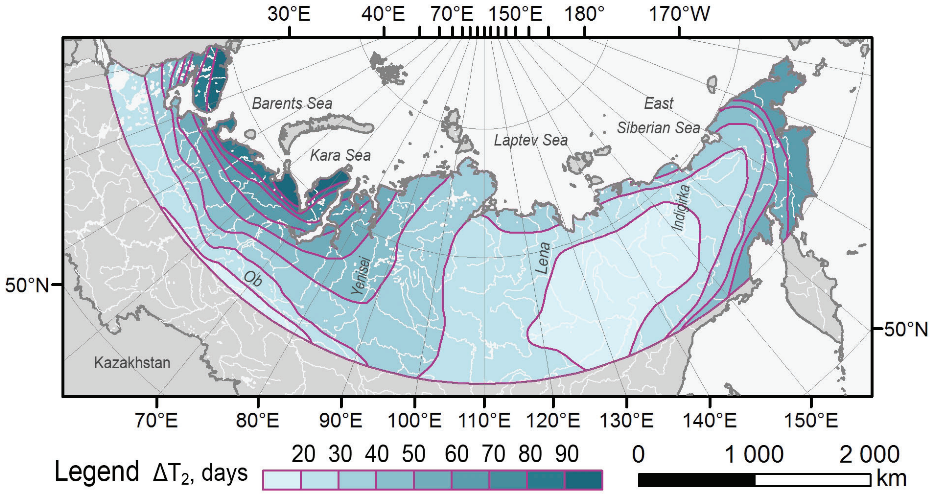

Fig. 5. Estimation of a change in the duration of ice phenomena period (ΔT_2, days) by the end of the 21st century.in comparison with the period of 1986-2005

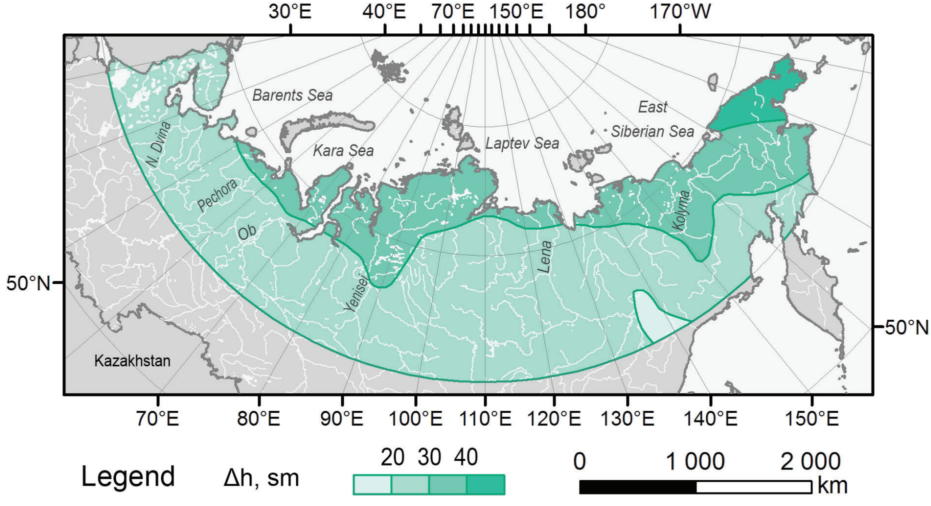

Fig. 6. Estimation of a change in the maximum ice thickness (Δh, sm) by the end of the 21st century.in comparison with the period of 1986-2005

of the rivers Northern Dvina and Pechora (80 days or more, which corresponds to 40-50%). The least changes are expected for the center of Eastern Siberia - about 30 days or 15-20%. For the European part, changes in the duration with ice phenomena are more pronounced, for the Asian part – changes in the period of ice cover are more pronounced (Figure 4, 5).

The reduction of the maximum ice thickness will be up to 30 cm for most of the territory, which is about 30-40% for the rivers of the European sector and Western Siberia (Fig. 6). The most pronounced changes are expected for the rivers of the Chukchi Peninsula (up to 50 cm). It should be noted that it is about a change in the contribution of accumulated negative air temperatures to the values of the maximum ice thickness. This paper does not estimate a change in the contribution of icing processes to the final values of the maximum thickness of the ice cover.

CONCLUSIONS

The analysis of the temporal variability of the main characteristics of the ice regime of Arctic rivers has shown that some trends of these characteristics can be seen only after 1990. As a result of a shift in the periods of ice phenomena and the change in the duration of ice cover period when comparing two periods (1961-1990 and 1991-2014) is 10-14 days for the European part and only 3-4 for the northeast. The duration of the ice cover period on the rivers of the European sector is reduced mainly due to more frequent cases of extremely late ice formation and its extremely early completion.

Some softening of winter conditions does not lead to significant decreases in the average ice thickness values by the end of the winter season. The thickness of the ice cover on the rivers of Siberia often reaches the values close to the limit ones; in the middle of the ice cover period, the further accumulation of negative temperatures does not affect the maximum values of ice thickness any longer either. As a result, the change in the thickness of the ice cover on the rivers of Eastern Siberia is not more than 5 cm, on the rest of the rivers of Siberia and on the large rivers of the north of the European part - up to 10 cm, and only on the rivers of Karelia - 10-15 cm.

According to the analysis of indicators of climate resources by the ensemble of models of the international project CMIP5 (the experiment under the scenario RCP 8.5), intensive warming of the climate is expected for the Arctic by the end of the XXI century. On the larger territory of the Arctic, the anomalies of a lot of indicators of climate resources are more pronounced in the cold period.

The dependences of the most general characteristics of the ice regime of rivers on the indicators of climatic resources for the cold period make it possible to estimate a change in the ice regime for different climatic scenarios and time slices. To elicit significant response, of the scenarios estimated in the numerical experiments of CMIP5 in terms of a possible impact on the climate system, the most «severe» one was chosen.

According to the estimates, by the end of the 21th century, the reduction in the duration of ice cover period and the period with ice phenomena for the rivers of the Kola Peninsula and the lower reaches of the rivers Northern Dvina and Pechora will have been 80 days or more in comparison with the period of 1986-2005, which is consistent with the expected reduction in the period with negative temperatures. The least changes are expected for the center of Eastern Siberia - about 30 days or 15-20%.

By 2081-2100, the reduction of the maximum thickness of the ice cover for the rivers of the European sector will have been about 30 cm or 30-40%. For the rivers of Siberia, the ice thickness provided by the accumulated negative temperatures will be reduced by 20-30%. The most pronounced changes are expected for the rivers of the Chukchi Peninsula (up to 50 cm). For the sections of rivers where the increase in ice thickness is mainly due to the freezing of water on river ice, the changes can be significant.

ACKNOWLEDGEMENTS

This study has been supported by the Russian Science Foundation: the modern changes in the ice regime of rivers have been studied within the framework of an RNF grant (Agreement No. 14-17-00155П); the future changes have been estimated according to the ensemble of models of the international project CMIP5 within the framework of an RNF grant (Agreement No. 14-37-00038П).

REFERENCES

Agafonova, S., Frolova, N., Vasilenko, A. and Shirokova, V. (2016). Ice regime and dangerous hydrological phenomena on rivers of the Arctic zone of European Russia. The Moscow University Bulletin. Series 5: Geography. 6, pp. 41–48. (in Russian with English summary)

Agafonova, S., Frolova, N., Krylenko, I., Sazonov, A. and Golovlyov, P. (2017). Dangerous ice phenomena on the lowland rivers of European Russia. Natural Hazards. 88, (S1), pp. 171–188.

Alekseev, V. (1987). Naledi [Aufeis]. Novosibirsk: Nauka. (in Russian)

Alekseevsky, N. et al. (2007). Geoecological state of the Arctic coast of Russia and safety of environmental management. Moscow: GEOS. (in Russian)

Arzhakova, S. (2001). The winter flow of the rivers of the permafrost zone of Russia. St. Petersburg: Gidrometeoizdat (in Russian)

IPCC (2014). Climate change 2014: impacts, adaptation, and vulnerability. Part B: Regional aspects. Contribution of working group II to the fifth assessment report of the intergovernmental panel on climate change. V. Barros, C. Field, D. Dokken et al., eds. Cambridge: Cambridge University Press

Borshch, S., Ginzburg, B. and Soldatova, I. (2001). Modeling the development of ice phenomena in rivers as applied to the assessment of probable changes in ice conditions at various Scenarios of the future climate. Water Resources, 28(2). pp. 194–200. DOI: 10.1023/A:1010387802874.

Donchenko, R. (1987). The ice regime of the rivers of the USSR. Leningrad: Gidrometeoizdat. (in Russian)

Ginzburg, B. (2005). River freeze-up and breakup dates in the late 20th century and their possible changes in the 21st century. Russian Meteorology and Hydrology, 12, pp. 65-72.

IPCC (2013). Climate Change 2013: The Physical Science Basis. Contribution of Working Group I to the Fifth Assessment Report of the Intergovernmental Panel on Climate Change. T. Stocker, D. Qin, G. Plattner et al., eds., Cambridge: Cambridge University Press

Moss, R., Babiker, M., Brinkman, S., Calvo, E., Carter, T. et al. (2008). Towards New Scenarios for Analysis of Emissions, Climate Change, Impacts, and Response Strategies. Intergovernmental Panel on Climate Change. Geneva.

Prowse, T., Alfredsen, K. and Beltaos S (2011). Changing lake and river ice regimes: trends, effects, and implications. In: C. Symon, J. Pawlak, T. Larson eds., Snow, Water, Ice, and Permafrost in the Arctic (SWIPA): climate change and the cryosphere. Oslo:AMAP, pp. 1 –52

Prowse, T., Bonsal, B., Duguay, C., Hessen, D. and Vuglinsky, V. (2007). River and lake ice. In: Global outlook for ice and snow. UNEP/GRID-Arendal, pp. 201–214

Surkova, G. and Krylov, A. (2017). The climate change in the hydrothermal resources in the Arctic amid warming of the XXI century. Arctic and Antarctic, 1, pp. 47-61. DOI: 10.7256/2453-8922.2017.1.22265. (in Russian with English summary)

Taylor, K., Stouffer, R. and Meehl, G. (2012). The CMIP5 experiment design. Bull. Amer. Meteor. Soc, 93, pp. 485–498.

Vuglinsky, V. (2002). Peculiarities of ice events in Russian Arctic rivers. Hydrological Process, 16, pp. 905–913.

Vuglinsky, V. (2017). Assessment of changes in ice regime characteristics of Russian lakes and rivers under current climate conditions. Natural Resources, 6 (8), pp. 416-431. DOI: 10.4236/nr.2017.86027

Hermann, A., Martinec, J. and Stichler, W. (1978). Study of snowmelt-runoff components using isotope measurements in Modeling of Snow Cover Runoff, Colbeck, S.C. and Ray, M., Eds., Hanover, U.S. Army Cold Regions Res. Eng. Lab, pp. 288–296.

Herrmann, A. Stichler, W. (1980). Groundwater-runoff relationships. Catena, vol. 7, pp. 251–263.

Lednik Dzhankuat: Tsentr. Kavkaz [Dzhankuat Glacier: Central Caucasus], Boyarskii, I.Ya, Ed., Leningrad: Gidrometeoizdat, 1978. 184 p. (in Russian).

Martinec, J., Siegenthaler, U., Oeschger, H. and Tongiorgi, E. (1974). New insights into the run-off mechanism by environmental isotopes, Proc. Sympos. Isotope Tech. in Groundwater Hydrol., Vienna: Int. Atomic Energy Agency, pp. 129–143.

Meiman, J., Friedman, I. and Hardcastle, K. (1973). Deuterium as a tracer in snow hydrology, The Role of Snow and Ice in Hydrology. Proc. Banff Symp., September, 1972, UNESCO-WHO-IASH, Int. Association of Sci. Hydrol. Association, Publ. 107, pp. 39–50.

Mook, W., Groeneveld, D., Brouwn, A. and Van Ganswijk, A. (1974). Analysis of a runoff hydrograph by means of natural 18O, in Isotope Techniques in Groundwater Hydrology, Proc. I.A.E.A. Symp., Vienna: Int. Atomic Energy Agency, pp. 145–156.

Ohlanders, N., Rodriguez, M. and McPhee, J. (2013). Stable water isotope variation in a Central Andean watershed dominated by glacier and snowmelt. Hydrol. Earth Syst. Sci., N. 17, pp.1035–1050, doi:10.5194/hess-17-1035-2013.

Received on November 2nd, 2017 Accepted on November 22nd, 2017

Natalia L. Frolova, is Professor of Hydrology at Lomonosov Moscow State University. She received her Doctor of Science degree (2013) in Hydrology from Lomonosov Moscow State University. She teaches hydrology undergraduate and graduate level courses («Hydrology», «Hydrology of Rivers", «Hydrological Forecasts») at the Universities in Russia and Kazakhstan, The focus of her research work is on dangerous hydrological processes and water resources with particular attention to the impact of climate change

Galina V. Surkova, is Associate Professor at the Department of Meteorology and Climatology, Faculty of Geography, Lomonosov Moscow State University, Russia. She received the PhD in 1998. Her research deals with the fields of Climatology and Meteorology, in particular, with extreme climate events, climate change, interaction of atmosphere and hydrosphere.

Svetlana A. Agafonova, is Researcher at the Department of Hydrology, Lomonosov Moscow State University. She received her PhD in Geography in 2009. Her research interests are in the area of climate change, hydrological hazards, and river ice.

Klaus P. Koltermann, studied oceanography, Meteorology and Geophysics at Hamburg University, graduating in 1968. He obtained Dr. rer.nat. degree from Hamburg University in 1988. He lectured at Hamburg University on Polar Oceanography, the Equation of State of Seawater. From 1987 to 1991 – director of the WOCE International Project Office at the IOS, Wormley, UK. Since 1991 his research was focused on the ocean's role in the climate system. In 2006–2010 he was leading the Tsunami Group of the Intergovernmental Oceanographic Commission, UNESCO. Since 2010 he is the Leading Scientist of the Natural Risk assessment laboratory at the Faculty of Geography, Moscow State University, established under the Russian Mega-grant programme.

Alexey V. Bobrov[1], Anton A. Iurmanov[1]*, David H. Lorence[2]
[1]Moscow State University, Faculty of Geography, Department of Biogeography, Leninskie Gory 1, Moscow, 119991, Russia
[2]National Tropical Botanical Garden, 3530 Papalina Rd, Kalaheo, HI 96741-9599, USA
*** Corresponding author:** yurmanov-anton.ya.ru@yandex.ru

PHYLOGENETIC BIOGEOGRAPHY OF THE FAMILY MONIMIACEAE

ABSTRACT. A complex cladistic analysis of molecular and morphological data of the Monimiaceae family is carried out. The hypothetic modes of the family dispersal are reconstructed basing on the data received for the studied representatives of the Monimiaceae family from all parts of the range and available fossils data. The family supposedly originated in Africa and penetrated into South America via the Antarctic way, and through the Arabian Peninsula and Sri-Lanka to South-Eastern Asia, Australia, New Zealand, New Caledonia, and further then to Madagascar.

KEY WORDS: dispersal history, cladistic analysis, Monimiaceae, molecular data

CITATION: Alexey V. Bobrov, Anton A. Iurmanov, David H. Lorence (2017) Phylogenetic biogeography of the family Monimiaceae. Geography, Environment, Sustainability, Vol.10, No 4, p. 16-26
DOI-10.24057/2071-9388-2017-10-4-16-26

INTRODUCTION

Molecular phylogenetics is a synthetic natural science discipline. It reveals the relationship between organisms on the basis of the sequence of the fragments of the nucleic acids - DNA and RNA (Judd et al. 2016; Wiley and Lieberman 2011). The result of a molecular genetic analysis is a phylogenetic tree formalized in the form of a cladogram - a scheme of successive divergences of the evolving group. At the present time, the concept that the data of molecular genetic analysis reflect the hypothetical evolution of the studied organisms is considered to be generally accepted (Judd et al. 2016; Wiley and Lieberman 2011).

This method of molecular analysis is widely used in biogeography (Crisci et al. 2003; Heads 2012, 2013). The analysis of the evolutionary relationships of different taxa within the key groups of angiosperms allows reconstructing the processes of their distribution and making the models of transformation of biogeosystems in the time and space (Crisci et al. 2003). So, with the aim to reconstruct the origin of the current distribution of the Monimiaceae family one of the most polymorphic families among magnoliids (Perkins and Gilg 1901; Philipson 2003; Takhtajan 2009) basing on the complex molecular and morphological analysis, this study was initiated.

Recent taxonomic treatment of Monimiaceae recognizes 27—28 genera, which include 200—270 species (Philipson 1993; Stevenson 2001). The family comprises two subfamilies – Hortonioideae (with single genus Hortonia) and Monimioideae, which includes three tribes: Hedycaryeae (7 genera – Xymalos, Decarydendron, Ephippiandra, Tambourissa, Hedycarya, Kibaropsis, Levieria), Monimieae (3 genera – Peumus, Monimia, Palmeria) and Mollinedieae (17 genera – Austromatthaea, Endressia, Hemmantia, Matthaea, Steganthera, Tetrasynandra, Hennecartia, Macropeplus, Macrotorus, Mollinedia, Grazielanthus, Wilkiea, Kairoa, Faika, Kibara, Parakibara, Lauterbachia) (Philipson 1993; Renner 1998; Renner and Chanderbali 2000; Stevenson 2001).

The representatives of Monimiaceae are woody plants with opposite leaves lacking stipules and the inflorescences formed by monoecious or dioecious, mostly polymerous flowers (Perkins and Gilg 1901; Philipson 1986, 1993; Takhtajan 2009). The fruit of most Monimiaceae are free from each other or submerged into the receptacle drupes of Laurus type (mostly red, orange or black) or apocarpous berries (Kibara, Steganthera) or inferior pyrenaria of Ilex type (Tambourissa only) (Romanov et al. 2007).

The representatives of the family Monimiaceae are mostly occurring in humid evergreen tropical and subtropical forests up to 3000 m above sea level and representing the forest subcanopy, lower woody level or making the forest canopy whereas some species are growing in dry forests and savannas (Lorence 1985; Philipson 1986, 1993; Whiffin and Foreman 2007). The reproductive biology of the representatives of Monimiaceae is studied insufficiently (Lorence 1985; Philipson 1986, 1993; Whiffin and Foreman 2007). The flowers are mostly small (up to 1 mm in diameter) and inconspicuous with strong smell, in multiflorous inflorescences and are mostly attractive for insects. Rarely the flowers are large and the segments of the perianth are petal-like (in Tambourissa perrieri Drake – up to 3,5 cm: (Lorence 1985)). The anther glands and cauliflory indicate the entomophilous syndrome of the flowers in most representatives of the family, on the other hand as well as the Monimiaceae representatives are mostly the plants of the understorey the anemophily is doubtful, but the data on any other visitors of the flowers are absent. The fruits of Monimiaceae are attractive for birds and supposedly are distributed by them, nevertheless only for Hedycarya arborea J. R. Forst. & G. Forst these data are based on the observations in the wild (Philipson 1993).

The most of biological diversity of Monimiaceae is distributed in South-East Asia as well as in Eastern Australia (Fig. 1) with endemic genera Austromatthaea, Endressia, Hemmantia, Steganthera, Tetrasynandra (and genus Wilkiea, which areal also covers the New Guinea) (Whiffin and Foreman 2007). The genera Kairoa, Faika, Lauterbachia are the endemics of New Guinea, where the genus Kibara is distributed both in New Guinea and on the islands in the broad region from Nicobar Islands and Thailand to Philippines and Queensland (Philipson 1986). The genera of Monimiaceae are widely distributed in Malesia in Philippines, Thailand, Malaya and Sumatra (Steganthera) and in Sulawesi, Solomon Islands and Queensland (Steganthera); whereas the genus Parakibara is the endemic of Halmahera Island (Philipson 1986). The genus Mollinedia is widely distributed in the New World (central and northern part of the South America), whereas the genus Hennecartia has narrower distribution (Paraguay, south Brazil, north-eastern Argentina); some genera (Macropeplus, Macrotorus and Grazielanthus) are distributed in south-east Brazil (Philipson 1993). Of particular interest is the distribution of the genera of Monimieae: the genus Peumus is distributed in South Chile, the genus Monimia occurs in Mauritius and Reunion, and the genus Palmeria is distributed in New Guinea, Sulawesi and Eastern Australia (Philipson 1993). In Africa, the family Monimiaceae is represented by the genus Xymalos (триба Hedycaryeae) with broad, but fragmented areal (Sudan, South Africa, the volcano Cameroon, Bioko Island) (Philipson 1993). There are three genera of the same tribe Hedycaryeae – Decarydendron, Ephippiandra, Tambourissa in Madagascar, whereas the last genus also occurs in the Mascarene Islands (Lorence 1985). The genus Kibaropsis is distributed at the New Caledonia, similar to Hedycarya, which is also occurs at the New Zealand, Eastern Australia and Fiji; the genus Levieria is represented in Queensland, New Guinea and Sulawesi (Philipson 1993). The genus Hortonia (subfamily Hortonioideae) is the endemic of Ceylon Island (Perkins and Gilg 1901; Philipson 1993).

The fossil records of the family Monimiaceae are scarce (Fig. 2). The fossils from Upper Senonian deposits in the eastern part of the Cape Province – Hedycaryoxylon hortonioides Mädel (Renner et al. 2010),

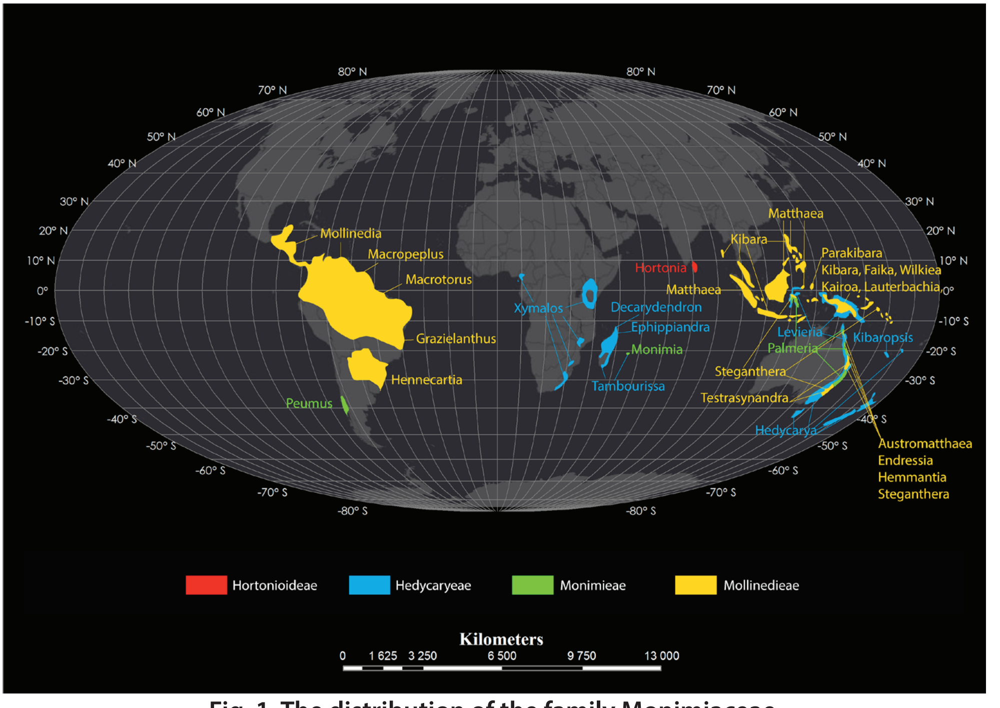

Fig. 1. The distribution of the family Monimiaceae

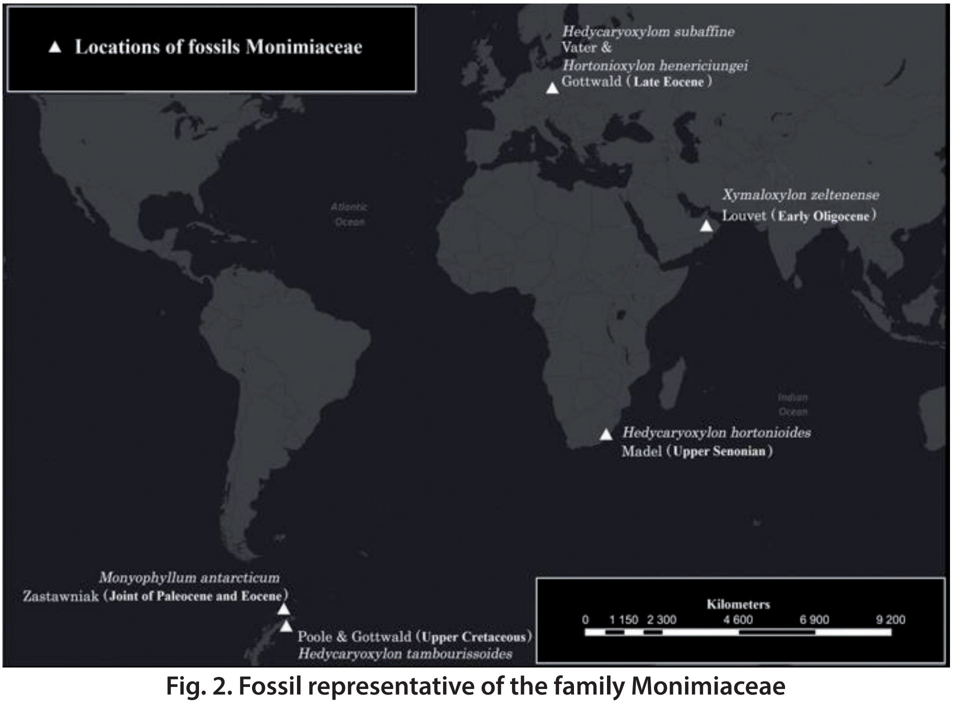

Fig. 2. Fossil representative of the family Monimiaceae

and those from Upper Cretaceous from the James Ross Island close to the Antarctic coasts – Hedycaryoxylon tambourissoides Poole & Gottwald (2001) are doubtlessly referred to Monimiaceae. The forest of fossil Xymaloxylon zeltenense Louvet are described from Oman (Knight and Wilf 2013). The Paleocene/Eocene leaves' reprints of Monimiophyllum antarcticum Zastawniak are found on the King Georgy Island at the Antarctic coasts (Renner et al. 2010). Interestingly, that Hedycaryoxylom subaffine Vater and Hortonioxylon henericiungeri Gottwald found in the most northern Upper Eocene deposits of Germany are similar with modern Hortonia and Hedycarya (Renner et al. 2010).

Basing on the data on morphology, ecology and geography of Monimiaceae mentioned above it is a relatively complicated task to build a reliable concept of the processes of historical distribution of the family even with attraction of data of the molecular analysis (Renner and Chanderbali 2000; Renner et al. 2010). The aim of present work is to combine molecular and morphological data and compare this complex phylogenetic data with the data on the family Monimiaceae distribution in the present time and in the past and thus to propose a verified model of origin of their modern distribution.

MATERIALS AND METHODS

To reconstruct the history of origin of modern distribution of Monimiaceae the representatives of 18 genera of the family occurring in different parts of the areal were analyzed. The object of the research were (The Plant List 2016): Hortonia floribunda Wight ex Arnott, Xymalos monospora (Harv.) Baill.*, Decarydendron ranomafanensis Lorence & Razafim.*, Ephippiandra madagascariensis (Danguy) Lorence*, Tambourissa amplifolia (Bojer ex Tul.) A. DC.*, Hedycarya arborea J. R. Forst. & G. Forst.*, H. angustifolia A. Cunningh.*, H. cupulata Baill., Kibaropsis caledonica (Guillaumin) J. Jérémie, Peumus boldus Molina*, Monimia amplexicaulis Lorence, Palmeria foremanii Whiffin, Austromatthaea elegans L. S. Sm.*, Steganthera macooraia (F.M. Bailey) P. K. Endress, Hennecartia omphalandra Poiss.*, Macropeplus ligustrinus (Tul.) Perkins var. friburgensis Perkins, Mollinedia widgrenii A. DC., Grazielanthus arkeocarpus Peixoto & Per.-Moura, Wilkiea huegeliana (Tul.) A. DC.*, Kibara moluccana Boerl. ex Perkins*. Gyrocarpus americanus Jacq.* from the Hernandiaceae family (sister to Monimiaceae: (APG IV 2016; Stevens 2001)) was selected as an outgroup in the analysis (Fig. 3). The following genes were selected for the molecular analysis: ITS 1 (internal transcribed spacer 1), 5.8S rRNA (5.8S ribosomal RNA gene) and ITS 2 (internal transcribed spacer 2), which had been sequences in all studied species. The rbcL gene (ribulose-1,5-bisphosphate carboxylase/oxygenase large subunit gene) was represented in GenBank (GenBank 2016) only for the taxa marked with an asterisk (*). The available molecular data were not enough for construction of a cladogram for all studied species, so the «molecular» and complex cladograms were built separately for two groups of taxa.

The principal method of the investigation is the construction of cladograms showing phylogenetic relationships by means of combination of molecular and morphological data of the taxa in Winclada program (Hall 2011; Wiens 2000; Wiley and Lieberman 2011). For the higher reliability of the reconstruction of the areal origin of Monimiaceae family three different models of phylogenetic relationships: molecular, morphological and the combined one.

Basing on the results of the nucleotide sequences analysis downloaded from the GenBank the «molecular-genetic» cladograms were built for 1) 20 species of Monimiaceae (Fig. 4) and 2) 11 species of Monimiaceae and Gyrocarpus americanus (Fig. 5). For estimation of the branch support of the cladograms the bootstrap analysis was conducted; the nodes with bootstrap values 80—100 are considered as highly supported, whereas the values of bootstrap > 65 are treated as acceptable (Hall 2011; Wiley and Lieberman, 2011).

With the aim to describe an alternative evolutionary scenario of the taxa involved in the present research the «morphological» cladogram was built (Fig. 6) basing on the

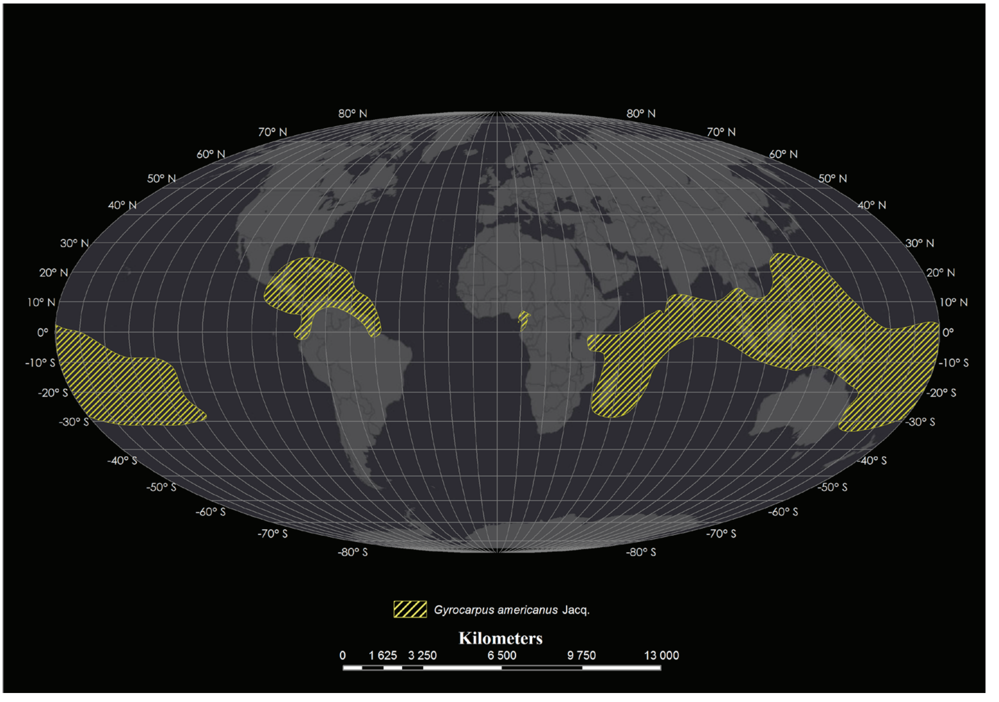

Fig. 3. The distribution of the Gyrocarpus americanus

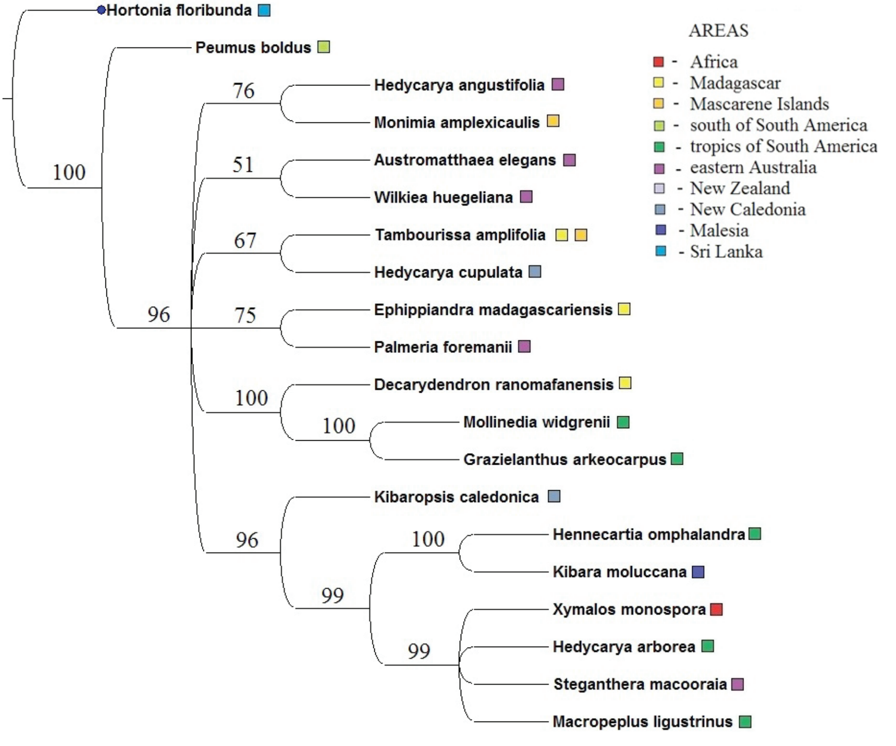

Fig. 4. Cladogram of Monimiaceae based on molecular data

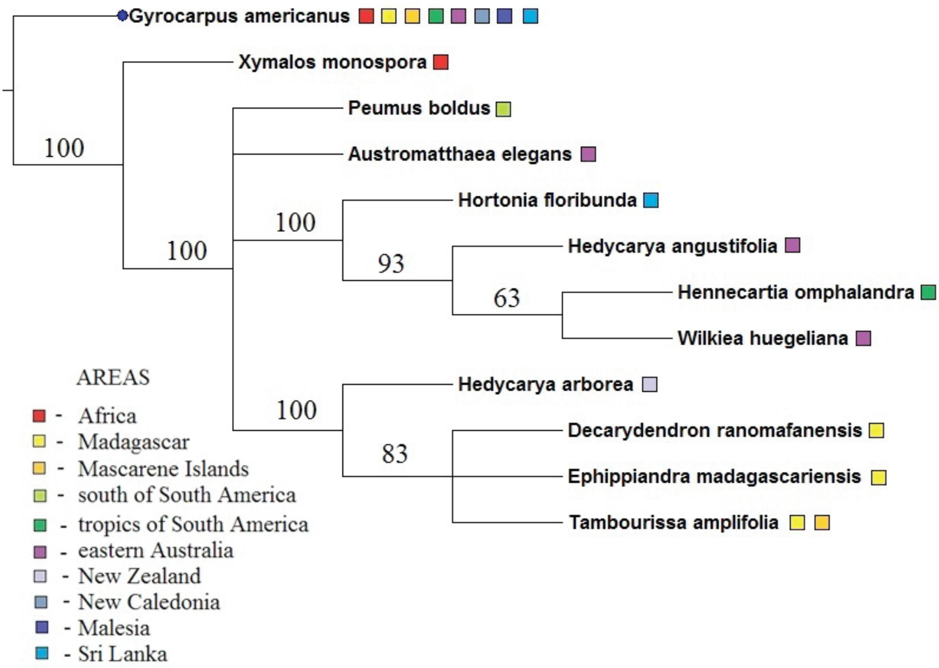

Fig. 5. Cladogram of Monimiaceae and Gyrocarpus (an outgroup) based on molecular data

tables of the morphological characters (Wiens 2000). Twenty-seven morphological characters were involved in the analysis, which are based on the original observations of plant morphology and the literature data (Lorence 1985; Money et al. 1950; Perkins and Gilg 1901; Philipson 1986; Philipson 1993). Both numerical (the number of perianth segments, stamens, carpels, cotyledons, etc.) and qualitative (the life form, leaf blade structure, pericarp type, presence of fleshy appendages of the fruitlet, etc.) characters were selected.

The combined cladograms (Fig. 7) are based on the complex analysis of data matrix including both molecular and morphological data (Hall 2011; Judd et al. 2016; Wiley and Lieberman 2011).

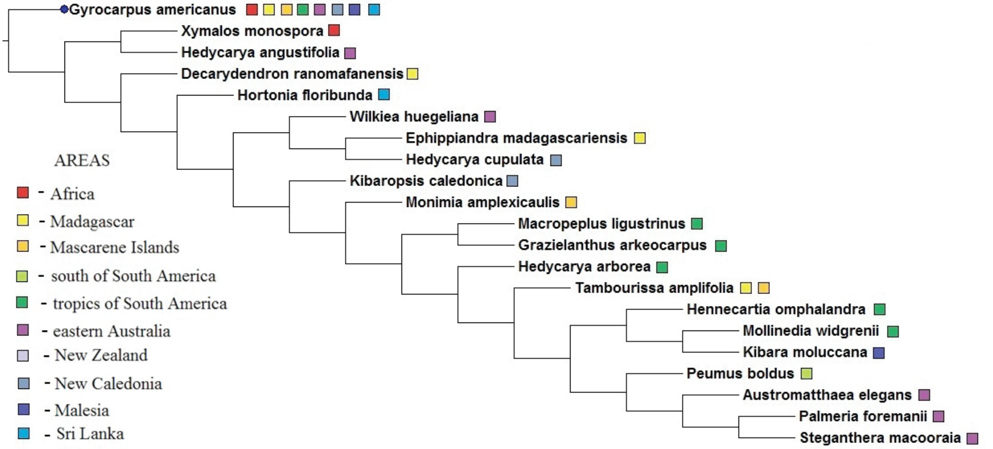

Fig. 6. Cladogram of Monimiaceae and Gyrocarpus (an outgroup) based on morphological data

RESULTS

The topology of «morphological» and «molecular» cladograms sufficiently differs – the «molecular» one provides better support for the genera delamination, whereas

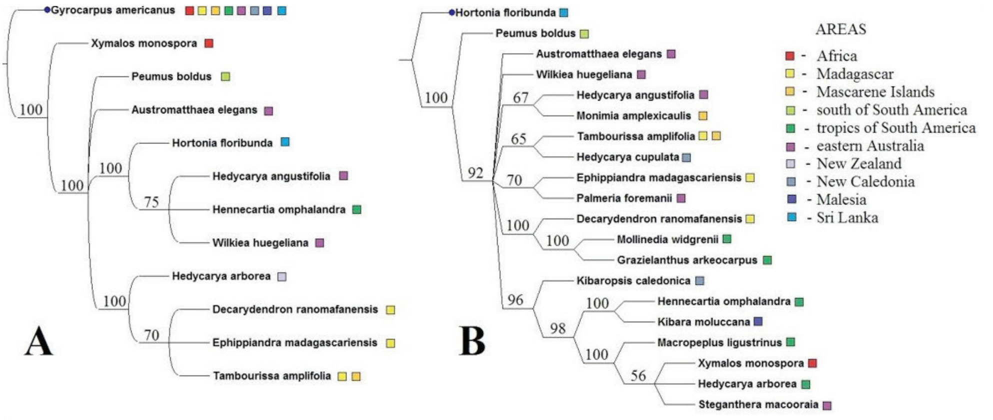

Fig. 7. Complex morphologo-molecular cladogram with bootstrap indexes indicated

the «morphological» one includes less polytomies. So, the complex cladograms (Fig. 7), which usually have less faults (Hall 2011; Wiens 2000; Wiley and Lieberman, 2011) were analyzed. The topology of the complex cladograms sufficiently differ both from the molecular ones and from each other. In spite of the first complex cladogram (Fig. 7) includes less number of taxa in comparison with the second one, it is nevertheless is used as the base for the modelling of the original scenario of distribution of Monimiaceae as well as it includes the outgroup (the genus Gyrocarpus). Bootstrap index is more than 70 in all nodes, the cladogram includes less polytomies, and the basal (original in evolution) position of the recent African genus Xymalos concords with finding in South Africa of the oldest fossil records of Monimiaceae dated by Upper Cretaceous time (100 MYA) (Renner et al. 2010).

The early stages of distribution of the family Monimiaceae were supposedly realized by the «vicarious algorithm» (Crisci et al. 2003; Heads 2012, 2013) and were dependent on the splitting of the Western Gondwana – i.e. by the split of Africa and South America about 100—110 MYA (Renner et al. 2010). Later on the territories of the Eastern Gondwana, which included Australia, Antarctic, Madagascar and India, the formation of the Monimiaceae areal proceeded as the result of long-distance dispersal (Crisci et al. 2003; Heads 2012, 2013; Renner et al. 2010), which is supported by our results.

DISCUSSION

The model of Monimiaceae distribution (Fig. 8) is based on the complex cladogram (Fig. 4) and available paleo botanical data. As well as the genus Xymalos is basal on the cladogram (Fig. 7) we suppose that Monimiaceae originated in Africa and started their distribution from there. The ancestor of recent genus Xymalos supposedly originate in the south of Africa and started distribution to the north of the continent (Fig. 8: 1). Supposedly about the same time in Upper Cretaceous Monimiaceae occupied South America (Fig. 8: 2) via Antarctica (Poole and Gottwald 2001), which brought to origin of the genus Peumus. Later, following the climate change, the areal of Monimiaceae in South America moved to the north (Fig. 8: 3), so the genera Mollinedia, Grazielanthus, Hennecartia and Macropeplus originated and became distributed on the continent.

The analysis of the fossil representatives of the family Monimiaceae from Oman allows to suppose, that to get to Australia from Africa fossil members of the family moved and distributed along the coasts of the Eastern Africa and South Asia (Fig. 8: 4), which is confirmed by occurring of

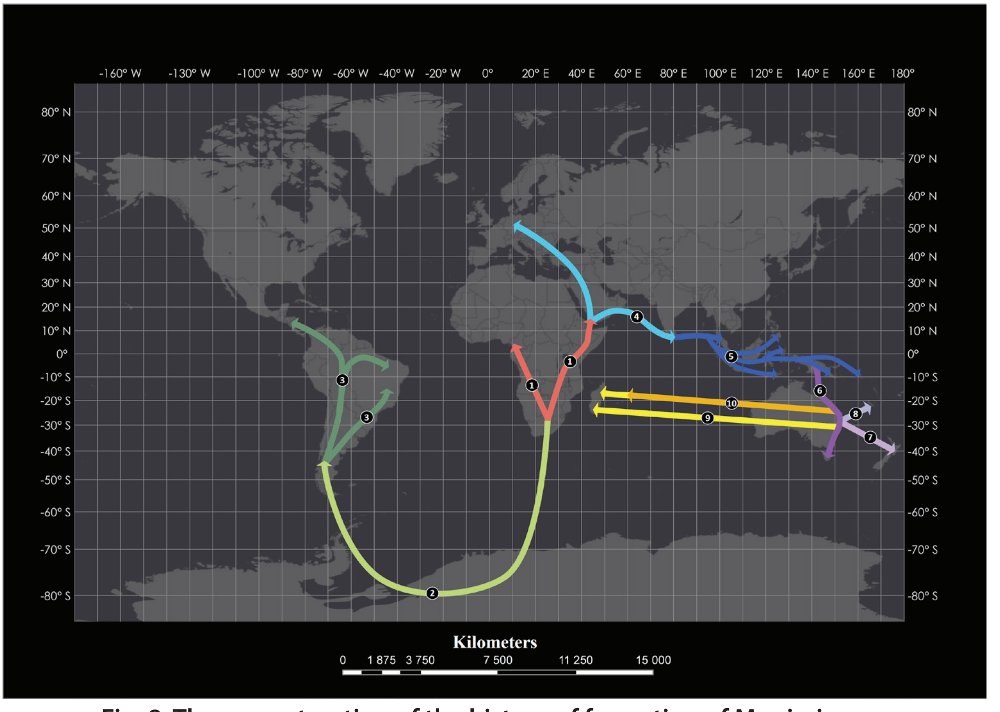

Fig. 8. The reconstruction of the history of formation of Monimiaceae current distribution

the archaic oligotypic genus Hortonia in Ceylon. The finding of the fossil records of the family in Germany indicate that yet in Upper Eocene Monimiaceae had broader distribution, and their areal included the Europe.

According to the model of phylogenetic relationships, the areal of the family Monimiaceae continued to expand to the East (Fig. 8: 5, 6) up to the recent Malesia (Kibara) and further up to Australia (Hedycarya, Palmeria, Austromatthaea, Steganthera, Wilkiea) (Whiffin and Foreman 2007). New Zealand and New Caledonia were populated with ancestors or representatives of the genus Hedycarya (Fig. 8: 7, 8). Madagascar (Decarydendron, Ephippiandra, and Tambourissa) and supposedly later Mascarene Islands (Tambourissa p.p.) were inhabited by New Caledonian or East Australian Monimiaceae (Kibaropsis, Hedycarya) (Figs. 8: 9, 10). The Monimiaceae in Australia could have a broader distribution before the period of aridization of the climate there and could inhabited Western Australia as well (now they are not represented there). During Early Tertiary period, the disposition of the continents allowed to agents of dissemination to transport diasporas from Australia to Madagascar. The processes of distribution of the family Monimiaceae in the Eastern Hemisphere supposedly occurred due to long-distance dispersal of the diasporas (the fruits, fruitlets, separate seeds) by birds (Money et al. 1950).

CONCLUSION

The genus Xymalos – is the basal genus in Monimiaceae and its African distribution allows to treat Africa as the ancestral part of the areal of the family. The distribution of Monimiaceae to South America occurred through Antarctica before the end of Cretaceous period (Peumus); later the areal of the family in South America expanded to the north of the continent (genera Mollinedia, Grazielanthus, Hennecartia, Macropeplus). To get to the Eastern tropics hypothetical representatives of ancient Monimiaceae made a long way along the coasts of Eastern Africa, Arabia, South Asia (the genus Hortonia stopped it distribution at Ceylon) and further to the islands of Malesia (genus

Kibara) to Australia (genera Hedycarya, Palmeria, Austromatthaea, Steganthera, Wilkiea). Monimiaceae representatives from Australia (by ancestors or representatives of the genus Hedycarya) occupied New Zealand. Madagascar (Decarydendron, Ephippiandra, and Tambourissa) and Mascarene Islands (Tambourissa) were occupied by Monimiaceae from New Caledonia (Kibaropsis, Hedycarya) and/or Australia (Eastern or Western).

ACKNOWLEDGEMENTS

The authors are grateful to our reviewers – Dr. Mikhail S. Romanov (Dept. of Tropical and Subtropical Floras, Main Botanical Garden, Russian Academy of Sciences, Moscow, RF) and Dr. Marc Jeanson (Herbier de l'Universite Montpellier II, Institut de Botanique, Montpellier, France) for extremely useful discussions and comments.

REFERENCES

Byng, J., Chase, M., Maarten, J. et al. (2016). An update of the Angiosperm Phylogeny Group classification for the orders and families of flowering plants: APG IV. Bot. J. Linnean Soc. 181, pp. 1–20.

Crisci, J., Katinas, L., Posadas, P. (2003). Historical Biogeography: An Introduction. Cambridge. MA: Harvard Univers. Press.

GenBank, (2016). The GenBank sequence database Official Website. (online) Available at: https://www.ncbi.nlm.nih.gov/genbank (Accessed 25 Apr. 2016).

The Plant List, (2016), The Plant List version 1.1 Official Website. (online) Available at: http://www.theplantlist.org/ (Accessed 21 Apr. 2016).

Hall, B. (2011). Phylogenetic Trees Made Easy: A How to Manual. 4th ed. Sunderland, MA: Sinauer.

Heads, M. (2012). Molecular Panbiogeography of the Tropics. Berkley, CA: Univers. of California.

Heads, M. (2013). Biogeography of Australasia. A Molecular Analysis. Cambridge: Cambridge Univers. Press.

Judd, W., Campbell, Ch., Kellogg, E., et al. (2016). Plant Systematics. A Phylogenetic Approach. 4th ed. Sunderland, MA: Sinauer.

Knight, C., Wilf, P. (2013). Rare leaf fossils of Monimiaceae and Atherospermataceae (Laurales) from Eocene Patagonian rainforests and their biogeographic significance. University Park, PA: Depart. of Geosciences, Pennsylvania State Univers.

Lorence, D. (1985). A monograph of the Monimiaceae (Laurales) in the Malagasy region (SW Indian Ocean). Ann. Missouri Bot. Gard., 72, pp. 142–210.

Money, L., Bailey, I. and Swamy, B. (1950). The morphology and relationships of the Monimiaceae. J. Arnold Arb., 31, pp. 372–404.

Perkins, J. and Gilg, E. (1901). Monimiaceae. Das Pflanzenreich, 4(101), pp. 1–122.

Philipson, W. (1986). Monimiaceae. Flora Malesiana. Spermatophyta: Flowering Plants, 10(2), pp. 255–326.

Philipson, W. (1993). Monimiaceae. The Families and Genera of Vascular Plants, 2, pp. 426–437.

Poole, I. and Gottwald, H. (2001). Monimiaceae sensu lato, an element of Gondwanan polar forests: evidence from the Late Cretaceous–Early Tertiary wood flora of Antarctica. Austral. Syst. Bot., 14, pp. 207–230.

Renner, S. (1998). Phylogenetic affinities of Monimiaceae based on cpDNA gene and spacer sequences. Persp. Plant Ecol., Evol. & Systematics., 1, pp. 61–77.

Renner, S. and Chanderbali, A. (2000). What is the relationship among Hernandiaceae, Lauraceae, and Monimiaceae? Intern. J. Plant Sci., 161, pp. 109–119.

Renner, S., Strijk, J., Strasberg, D. and The´baud, C. (2010). Biogeography of the Monimiaceae (Laurales): a role for East Gondwana and long-distance dispersal, but not West Gondwana. J. Biogeo. 37, pp. 1227–1238.

Romanov, M., Endress, P., Bobrov, A., et al. (2007). Fruit structure and systematics of Monimiaceae s. s. (Laurales). Bot. J. Linnean Soc., 153, pp. 265–285.

Stevens, P. (2001). Angiosperm Phylogeny Website. Availible at: http://www.mobot.org/MOBOT/research/APweb/ (Accessed 20 Apr. 2016).

Takhtajan, A. (2009). Flowering Plants. 2nd ed. Leipzig.: Springer.

Whiffin, T. and Foreman, D. (2007). Monimiaceae. // Flora of Australia, 2, pp. 65–91.

Wiens, J. (2000). Phylogenetic Analysis of Morphological Data. Washington, DC: Smithsonian Inst.

Wiley, E. and Lieberman, B. (2011). Phylogenetics: Theory and Practice of Phylogenetic Systematics. 2nd ed. Hoboken, NJ.: Wiley-Blackwell.

Received on November 20th, 2017 Accepted on November 22nd, 2017

Alexey V. Bobrov, Doctor of Sciences (Biology), Professor, Department of Biogeography, Faculty of Geography, M. V. Lomonosov Moscow State University. Area of scientific interests: phylogenetic systematics of higher plants, evolutionary morphology and anatomy of higher plants, reproductive biology of seed plants, carpology, palaeobotany, plant geography. The author of more than 200 publications. The organizer of more than 30 expeditions to the tropics and subtropics of the Old and New World.

Anton A. Iurmanov, 2-nd year magister student at the Department of Biogeography, Faculty of Geography, M. V. Lomonosov Moscow State University. Area of scientific interests: phylogenetic systematics of higher plants, palaeobotany, geobotany. Explorer at the N. V. Tsitsin Main Botanical Garden of the Russian Academy of Sciences. He conducted expeditions in Cameroon, Gabon, Laos, Vietnam, China, Indonesia, Cuba, New Caledonia. Organizer of field works of the Russian Geographical Society and the Expedition Centre of the Ministry of Defence of the Russian Federation.

David H. Lorence – Director of Science and Conservation in the National Tropical Botanical Garden (USA, Hawaii), PhD. Research specialties are systematic studies of tropical plants, floristics, and invasive plant species. His systematic research focuses on Pacific and Neotropical members of the large and diverse Rubiaceae family, which includes coffee, quinine, and gardenias. He also studies Pacific island pteridophytes and the Monimiaceae family of the Malagasy region. The organizer of more than 20 expeditions to Madagascar, Comores, and Neotropics.

Tatyana V. Kotova[1], Svetlana M. Malkhazova[1], Vladimir S.Tikunov[1]*, Temenoujka Bandrova[2]
[1]Lomonosov Moscow State University, Faculty of Geography, Moscow, 119991, Russian Federation
[2]University of Architecture, Civil Engineering and Geodesy, 1, Chr. Smirnenski Blvd. 1046, Sofia, Bulgaria
*** Corresponding author:** tikunov@geogr.msu.su

VISUALIZATION OF PUBLIC HEALTH DYNAMICS

ABSTRACT. Public health dynamics is one of the main methodological approaches to study spatiotemporal patterns of the population diseases spreading and to create nosogeographic maps. It is one of validity terms of geographic public health assessment and forecast. Dynamics maps usually show emergence, development, past stages, changes, and movement of analyzed phenomena. Analysis of medical-geographic maps showed that the choice of methods and techniques for elaborating dynamic aspects is limited. The results of comprehensive medical-geographic atlas mapping obtained in the Department of Biogeography and Laboratory of Integrated Mapping (Faculty of Geography, M.V. Lomonosov Moscow State University, Russia) have significantly improved this situation and demonstrated the benefits of cartographic approaches and graphic methods of visualization of public health dynamics. However, these benefits as an integral problem has not been fully realized yet and research in this direction should continue.

KEY WORDS: graphic presentation of dynamics, methods, techniques

CITATION: Tatyana V. Kotova, Svetlana M. Malkhazova, Vladimir S. Tikunov, Temenoujka Bandrova (2017) Visualization of Public health dinamics. Geography, Environment, Sustainability, Vol.10, No 4, p. 27-42
DOI-10.24057/2071-9388-2017-10-4-27-42

INTRODUCTION

The core of medical-geographic research is the study of diseases spatiotemporal patterns, their accurate cartographic presentation (nosogeographic maps), and analysis for development of public health protection measures (Malkhazova 2012). Assessment of morbidity dynamics is one of the important methodological requirements of such cartographic models and one the validity terms of medical-geographic assessment of morbidity and forecast. Maps on dynamics usually show emergence, development, past stages, and spatiotemporal changes of analyzed phenomena (the state borders shown on the years of compiling relevant maps). Their content depends on the purpose and the detail of research, as well as on character (quality) of the original information base – the duration and completeness of the time series, the comparability of the available data, the availability of spatial referencing, etc.

It is clear that dynamics is best visualized primarily through animations and multimedia technology; however, this paper focuses on the potential of non-animated maps. Analysis of published nosogeographic maps compiled as individual products or as part of integrated or sectoral medical-geographic atlases showed that the methods of dynamics presentation are somewhat limited. The methods include mainly graphs and charts that complement the essentially static maps. The purpose of the paper presented herein is to broaden the dynamic aspect of cartographic methods in research and mapping of public health issues. The paper presents the results obtained in the course of compilation of integrated medical-geographic atlases in the Department of Biogeography and Laboratory of Integrated Mapping (Faculty of Geography, Lomonosov Moscow State University).

MATERIALS

The material includes previously published medical-geographic products (Malkhazova et al. 2011), interdisciplinary theoretical works in the field of thematic cartography, and mathematical-cartographic modeling (Tikunov 1997a; Tikunov 1997b; Prokhorov and Tikunov 2001), as well as a number of medical-demographic and medical-geographic maps and atlases developed by the authors and other researchers (Malkhazova 2007a; Malkhazova 2007b; Vatlina 2012; Malkhazova 2012; Malkhazova et al. 2014), created in the Department of Biogeography. Analysis of cartographic publications showed that the sources of background information for the maps on dynamics vary depending on the territorial level (local, regional, national, and global) and include field studies, literature, and statistical data. Statistical sources best meet the requirements for the initial information because they are readily available, comparable, and collected using standardized methods. They also contain reference for administrative units at different spatial levels and cover long periods, thus allowing selecting time-intervals for analysis with consideration of specific natural and socio-economic changes. In some cases, at the global and national level mapping, literature and statistics represent the only acceptable sources of information.

The work on a medical-geographic atlas of Russia "Natural focal diseases" has clearly shown the need to strengthen the dynamic component, to create experimental cartographic models, and to conduct their subsequent analysis and assessment of the cognitive potential and feasibility of the use in medical-geographic studies. The data on public health for the world and the Russian regions are comprehensively provided on the website of the World Data Centre for Geography (icsu-wds.ru).

TYPES OF MAPS ON DYNAMICS

Visualization of medical-geographic data is based on the traditional nosogeographic methods; modern virtual-reality images, cartographic animation images, non-Euclidean matrix images, and multimedia technique have also been incorporated recently (Kapralov et al. 2010). However, analysis of nosogeographic maps created as individual products or as part of integrated or sectoral medical-geographic atlases has shown that the choice of methods of dynamics rendering is very limited. The most widely used methods are graphs and diagrams supplementing statistical, in essence, maps.

A simple, intuitive, and widely used method that does not require detailed explanations is *comparison of multi-temporal maps*. The maps on public health dynamics represent the most vivid example. Thus, maps that show public health of the Russian regions in comparison with other countries for 1990-2013 are the examples of assessment maps of public health dynamics (Tikunov and Chereshnya 2016). Today, health is an indicator of progress and social and economic development. Various methods for measuring public health exist. Public health demonstrates various trends that are described well by an integral index – the Public Health Index (PHI) – which we have proposed and used; this index integrates the objective indicators of public health: infant mortality rate and life expectancy at birth for men and women. We consider these are the most important indicators of public health (Prokhorov and Tikunov 2001), and this notion has been validated by subsequent research. These indicators have several important advantages: the data for almost all countries are available, they do not require expert assessment, and they are reliable. We have calculated PHI for Russia, which allowed us to obtain the national dynamics of public health over a 24 year period Å| from the end of the Soviet regime and the beginning of the transition to a new model of socio-economic development (1992) until the end of 2013. This index clearly illustrates changes in public health. Therefore, for the calculations we used an array of data for 266 countries and regions of Russia, considered as a single 24 year-long data set, 6384 territorial units in total with the abovementioned three parameters. The initial data can be found as file INITDATA on the website of the World Data Centre for Geography (icsu-wds.ru).

For the calculation, we used the evaluative algorithm developed earlier (Tikunov 1985; Tikunov 1997a; Tikunov 1997b). It includes normalization of the initial indicators by the formula:

$$\hat{X}_{ij} = \frac{\left| x_{ij} - \overset{0}{x}_j \right|}{\left| \max/\min^{x - \overset{0}{x}_j} \right|}$$

i=1, 2, 3,…, n; j=1, 2, 3,…, m

where $\overset{o}{x}$ is the worst value (for each indicator, in terms of their impact on the health of the population in the countries and regions of Russia [the maximum infant mortality rate, lowest life expectancy]; these values can be found on the website in file X0)$_{max/min}$ $\overset{o}{x}$; are the values most different from the $\overset{o}{x}$ values of parameters; n is the number of territorial units (6384 for the entire period); *m* is the number of indicators used for the calculations.

Ranking is carried out by comparing all territorial units on a conditional basis, characterized by the values of $\overset{o}{x}$. If there are reasonable "weights" for each indicator (for example, 0,5 for life expectancy for men and women and 1 for infant mortality), they also can be included in the formula of normalization, but in our calculations "weights" were the same.

If the normalized values $\hat{x}_{ij}$ are considered as reduced to the comparable form to obtain PHI, they can be simply summed.

$$\hat{S}_i = \sum_{j=1}^{m} \frac{\left| x_{ij} - \overset{0}{x}_j \right|}{\left| \max/\min^{x - \overset{0}{x}_j} \right|}$$

The obtained values $\hat{S}$ characterize the estimated position of the countries and regions of Russia and are presented on the website under the name RAN1MRE as a simplified version of the calculations.

The algorithm can be more strict despite the fact that ranking is carried out by comparing all territorial units on a conditional basis, characterized by the values of $\overset{o}{x}$. However, in this case, it is done using the Euclidean distance as a measure of proximity of all territorial units to the conditional basis (the worst-case values $\overset{o}{x}$ throughout a range of indicators). Then, we processed the array using principal component analysis for the purpose of orthogonalization and a "convolution" system of indicators. The algorithm with various modifications is described in (Tikunov 1997a; Tikunov 1997b). The results of the calculations can be found on the website under the name RAN2MRE and are also presented in Fig. 1 (a and b), Fig. 2, and Fig. 3.

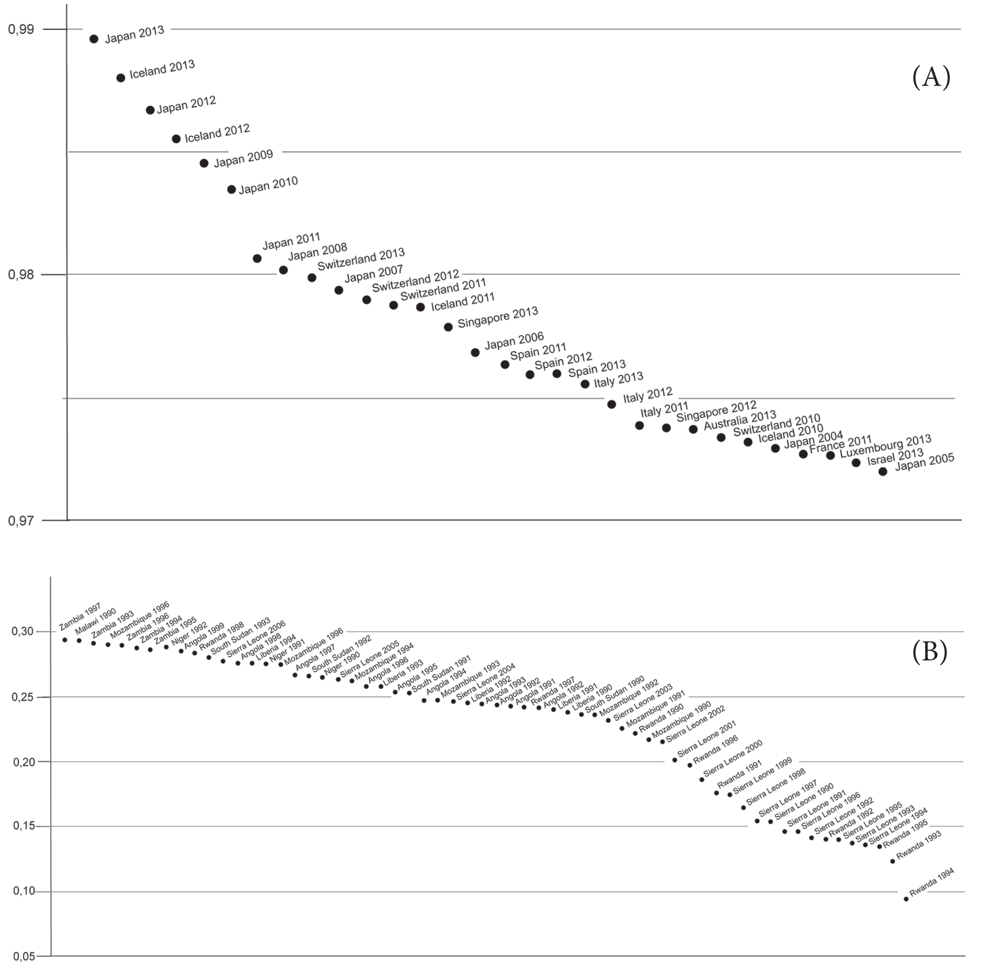

Fig. 1 a,b. Fragments of the calculation results (the upper and lowest parts of the PHI ranked series)

According to our calculations, there are no significant differences between the simplified and complete algorithms, which, among other things, have leveled out in the resulting maps with the step scale. Thus, Table 1 shows fragments of the calculation results (using the simplified algorithm) related to the upper and lowest parts of the PHI ranked series.

The PHI graphs for some countries and groups of Russian regions are presented in Fig. 3. Fig. 4 and Fig. 5 show the maps for selected years.

Fig. 2 shows a graph of PHI for the world, the European Union, and selected countries. As can be seen from the graph, growth of the index is a worldwide trend. The rate of growth is much higher in developing countries. Russia stands out among the general trend. Events of the 1990s have affected the level of public health and sustainable growth was observed only since 2001. Detailed changes in the level of public health of the Russian Federation are shown in Fig. 3.

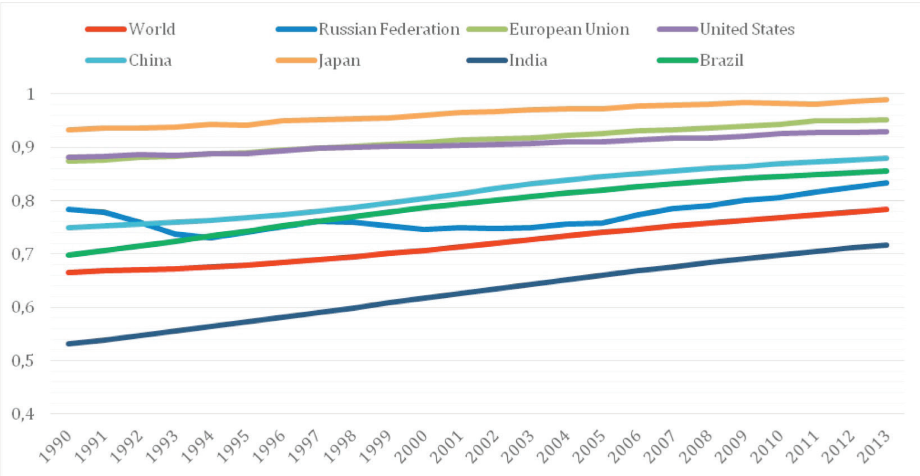

Fig. 2. PHI in selected countries

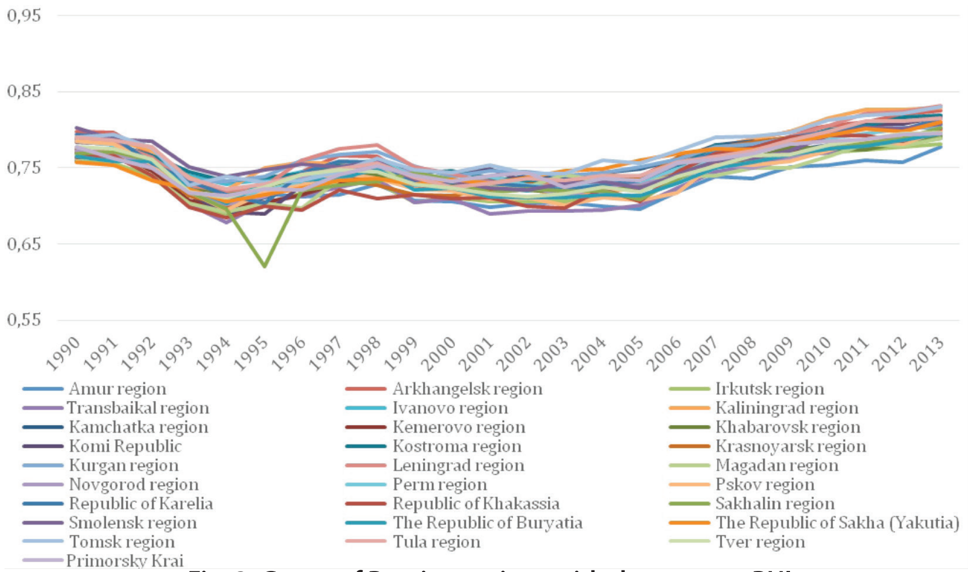

Fig. 3. Group of Russian regions with the average PHI

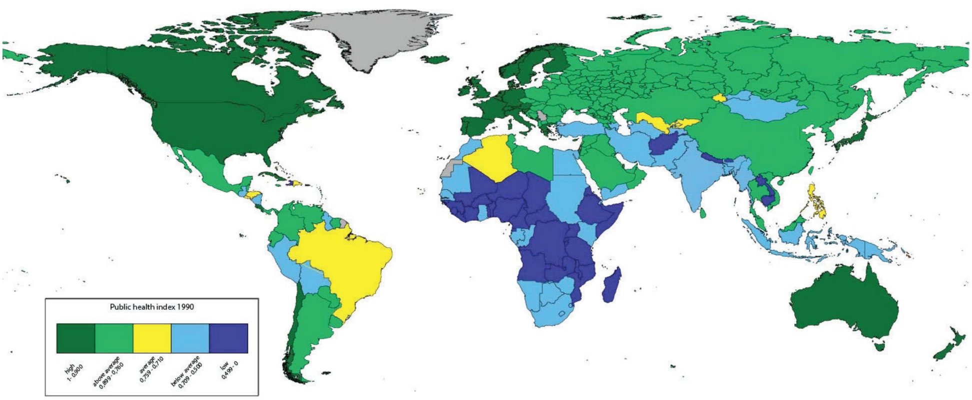

Fig. 4. World PHI in 1990

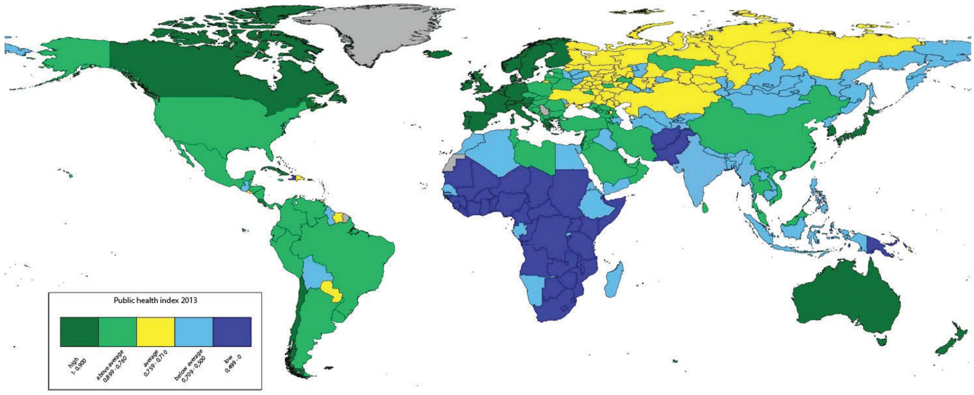

Fig. 5. World PHI in 1990

Fig. 4 and Fig. 5 illustrate spatial changes in PHI. Regions of the world that do not follow the worldwide trend of sustainable growth of public health include the former Soviet republics, and African countries. More detailed analysis of PHI is provided in other work of the authors (Tikunov and Chereshnya 2015; Tikunov and Chereshnya 2016).

Examples of maps that are directly related to morbidity dynamics based on the same method of graphic visualization are maps "Diseases of the nervous system," from "Medical-demographic atlas of the Kaliningrad Region," scales 1: 2 400 000 and 1: 600 000, which reflect the situation for 1990 and 2005, respectively (Malkhazova 2007a). These maps show the number of registered cases per 1000 adults using the cartogram method (based on the administrative territorial units). Map-users arrive at conclusions through visual comparison of the maps. This method is disease-specific and utilizes integrated indices (for individual groups of pathology classes) for different dates. Temporal reference represents an important descriptive indicator linking thematic attributes with a certain temporal span.

Superposition of multi-temporal images, similarly to the previous method, is a quite simple and clear method; however, it requires a greater effort in the selection of graphic techniques used to achieve clarity. It is especially widely used in cases where it is necessary to trace infectious diseases that, as a rule, actively emerge and spread. Fig. 6 reflects dynamics of expansion of nosologic area of West Nile fever in the territory of the Russian Federation over 15 years, a dangerous disease, previously not relevant to this area.

The dynamics of the Crimean hemorrhagic fever and plague are shown in a similar way in "Environmental atlas of the Rostov Region" (Zakrutkin and Rishkov 2000). Maps "Crimean hemorrhagic fever" and "Plague" reflect morbidity of these diseases in 1912-1938, 1963-1971, and 2000.

Fig. 7 shows maps related to the health care on the territory of Bulgaria. The first map depicts the spatial dynamics of the number of hospital beds per 1,000 people. The choropleth maps method enables the user to get an idea of the phenomena distributed on a regional territories. In addition, a chart showing the average number of beds and patients in one hospital for 3 selected years 1998, 2000 and 2003 is also provided. The impression is given of the time dynamics of the depicted phenomenon. The second map of analogous representation methods shows spatial and temporal dynamics of the phenomenon depicted: the number of patients per doctor by choropleth map and the number of patients per doctor, nurse and dentist for the three comparative years.

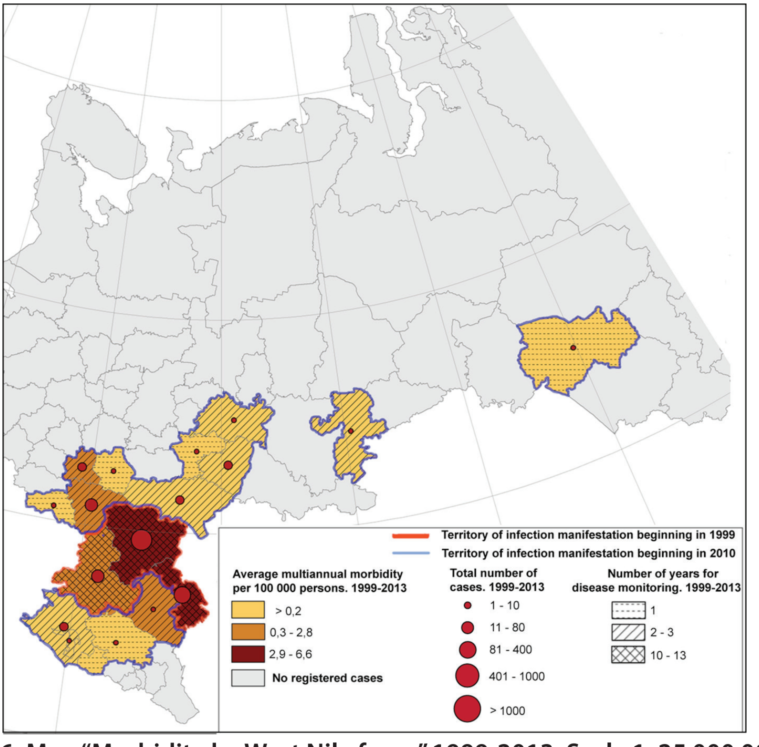

Fig. 6. Map "Morbidity by West Nile fever." 1999-2013. Scale 1: 25 000 000

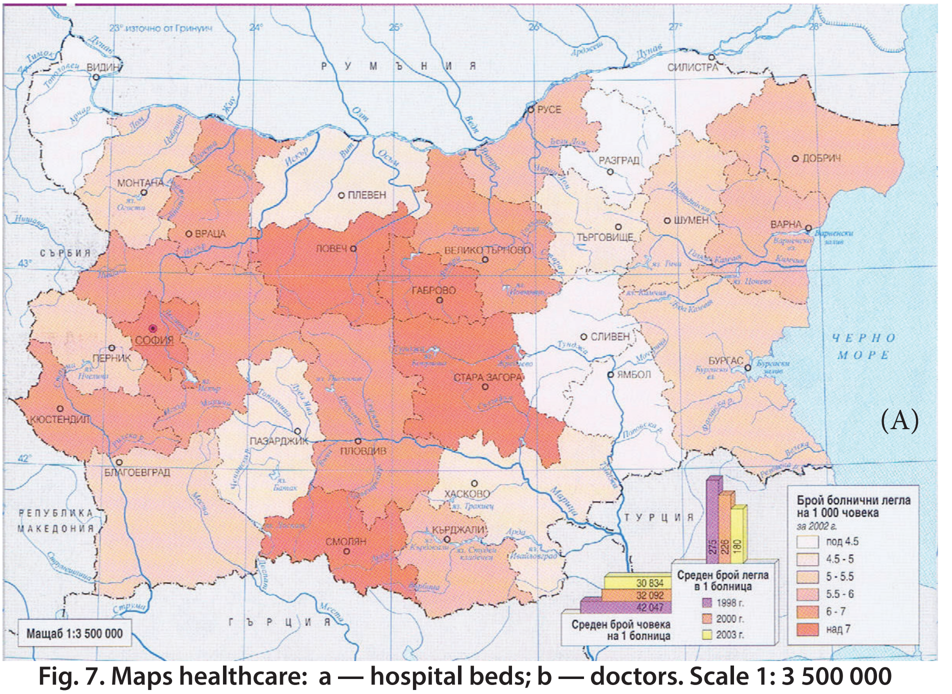

Fig. 7. Maps healthcare: a — hospital beds; b — doctors. Scale 1: 3 500 000 (Bandrova 2008)

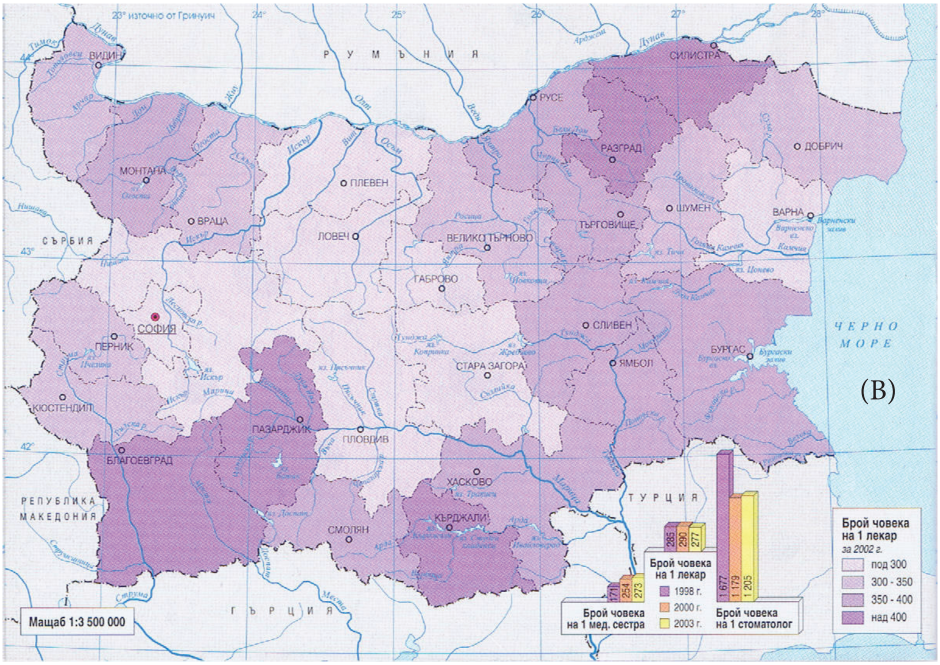

Fig. 7. Maps healthcare: a — hospital beds; b — doctors. Scale 1: 3 500 000 (Bandrova 2008)

Both cases show the possibilities of 2D maps to represent spatial and temporal dynamics of the phenomena.

Integration of indicators and characteristics is a quite simple, but a very informative method, which gives a comprehensive temporal description of nosogeographic territorial units.

Map "Nosologic profiles," scale: 1:20 000 000, was prepared for a medical-geographic atlas of Russia "Natural focal diseases" (Kotova et al. 2012). The overall picture of the natural focal diseases registered on the territory of the subjects of the Russian Federation over 11 years (Fig. 8) is represented by a matrix: the records contain information on the cases of natural focal diseases and the fields show the years when the cases were registered (1996–2006). Though the map does not contain quantitative data, it is still very informative. It reflects the annual change of the spectrum of natural focal diseases observed in the territory of the subjects of the Russian Federation and is very meaningful for analysis of the distribution of different groups and classes of diseases by various years and at the level of the subjects of the Russian Federation and for the country as a whole.

Combination of various indicators on a single map can be quite productive, which renders the manifestation of the multidimensional nature of phenomena dynamics. For example, map "Tuberculosis morbidity and mortality of the population" in "Medical-environmental atlas of the Moscow Region," (Semenov 2004) shows cases per 100 000 persons, which is another presentation of one more aspect of characteristics of dynamics.

Numerous parameters of dynamics statistical analysis, rather adequately described in the literature (Tikunov 1997a; Tikunov 1997b; Chistobaev and Semenova 2013), can be used for morbidity mapping. Traditional medical-geographic mapping uses the most important parameters that reflect patterns of various levels and relationships with other factors.

Fig. 8. Fragments of map "Nosologic profiles" and legend. Scale 1: 20 000 000

Typically, the visualization of the results of data dynamics statistical analysis is performed using statistical rendering methods, i.e., cartograms and cartodiagrams. Fig. 9 presents a map of variation in the number of cases relative to the multiannual average value. Linear diagrams for the subjects of the Russian Federation reflect positive and negative deviation about the multiannual average.

One of the objectives of such statistical research is to identify the main trends, which is important for compilation of forecast maps. The identified trends may be supplemented by either quantitative indicators or by only a verbal description. Maps "Trends in general morbidity of the population in 1997-2011," "Trends of adult morbidity in 1997-2010," and "Forecast of the general morbidity of the population," with characteristics of the average rate of increase (decrease) of the number of cases in % by cities and districts, in "Medical-demographic atlas of the Republic of Dagestan" (2013) represent examples of the first type. Examples of the second type include the maps in "Medical-demographic atlas of the Smolensk Region." Maps "Dynamics of adult morbidity" show two trends – decline and growth of morbidity in 1999 – 2007 by districts.

Maps on *morbidity dynamics typology* were developed with the help of mathematical-cartographic modeling techniques (Tikunov 1997a; Tikunov 1997b). The main criterion for the typology model is the uniformity of territorial units, broken into groups (taxa) derived from a set of initial features-indicators that characterize the disease for the selected time period. This method assumes normalization, linearization, and orthogonalization of time series and their subsequent classification. Since the average multiannual relative morbidity incidences for each territorial unit differ, their time series are normalized for comparison of the levels of morbidity variability. In this case, specific values of the time series for each subject of the Russian Federation were divided by their arithmetic mean values calculated with these series.

The legends were based on the arithmetic mean values of the relative morbidity for each year calculated within each taxon and shown as charts. Such charts of average morbidity level out individual fluctuations in the dynamic series and characterize patterns of morbidity variability for the entire monotypic groups of the subjects of the Russian Federation. The advantage of these maps is the ability to explore the patterns of variation of incidence by grouping the territorial units (the subjects of the Russian Federation) in the taxa with similar rhythms of morbidity fluctuations. This typology reveals territorial patterns of dynamics and explores not the individual series but their groups that are less subjected to random fluctuations. Based on the analysis of relative morbidity for 1997-2010, typological classification of disease dynamics and identification of the key spatial and temporal patterns in the distribution of this parameter for diseases relevant to the territory of the Russian Federation (tick-borne encephalitis, tick-borne borreliosis, hemorrhagic fever with renal syndrome, diphyllobothriases, opisthorchiasis) was conducted.

A map on morbidity dynamics for tick-borne encephalitis serves as an example of the final result (Fig. 10). It includes five taxa that can be broken conditionally (based on the calculated index and the semantic analysis of the results) into three types and five subtypes, respectively. The first type includes two taxa (I and II) with a clear decrease in the incidence over the observed period; the second type (IV taxon) exhibits a general downward trend but with significant variations in morbidity; and the third type (III and V taxa) approaches the form of a plateau with very small differences from year to year. Each subtype is characterized by specific morbidity dynamics and they are arranged by the degree of growth of this parameter. The charts serve as the legend of this map.

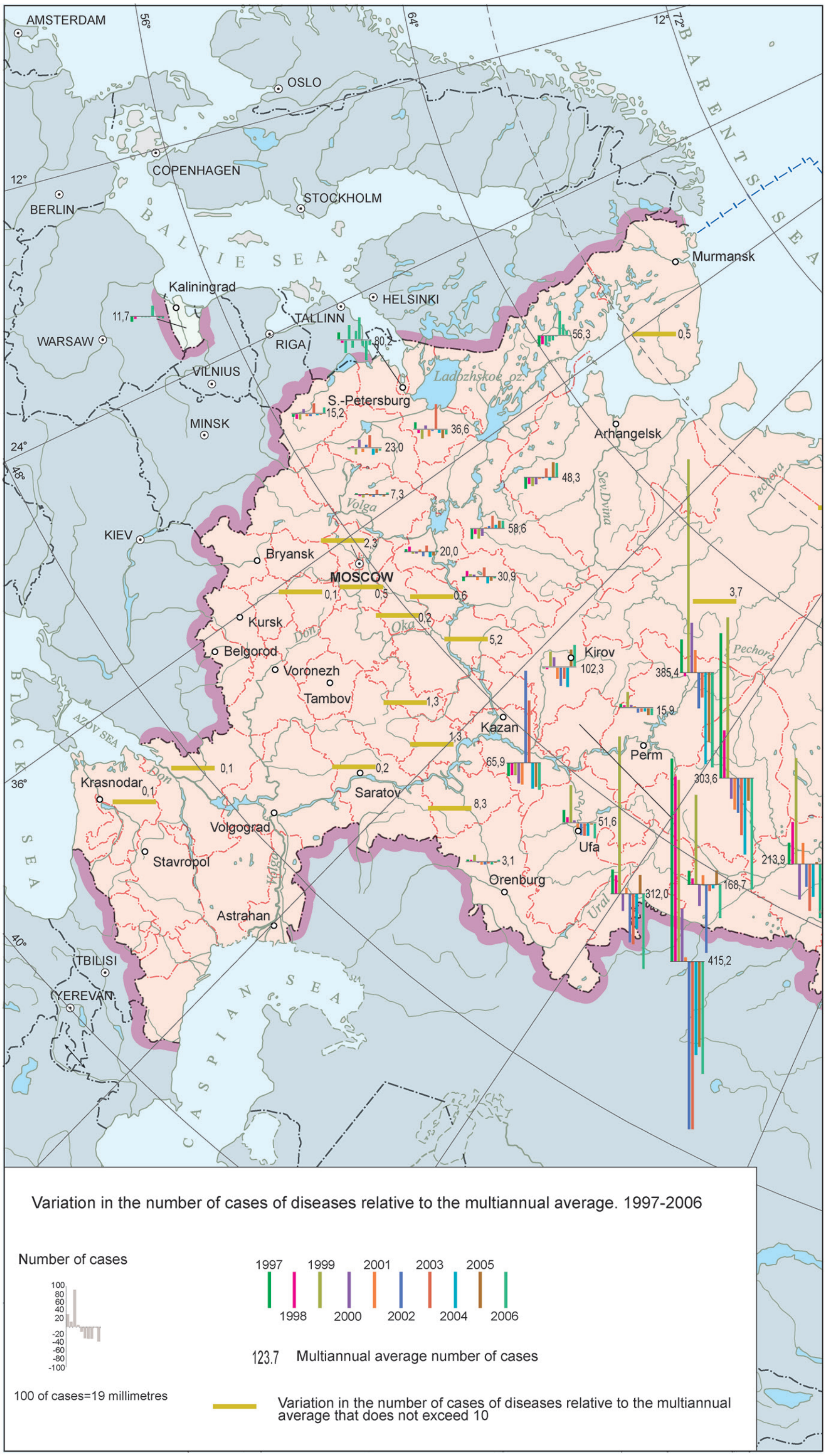

Fig. 9.Fragment of map "General morbidity of population dynamics." 1997-2006. Scale 1: 20 000 000

Fig. 10. Map "Typology of morbidity from tick-borne encephalitis. 1997-2010". Scale 1: 30 000 000

As follows from the analysis of the map, the first type of morbidity dynamics is characteristic of six subjects of the Russian Federation. The Republic of Bashkortostan, the Khanty-Mansi Autonomous Area — Yugra, the Omsk and Chita Regions, and the Khabarovsk Territory belong to the second type. Dynamics of the third and fifth types is typical of the northern regions of Russia and the central and southern regions of the European part of Russia.

Ring maps are based on diagrams that reflect the distribution of morbidity by years. They are particularly well-suited for the visualization of the relationships between spatial data and their chronology (change in time) (Huang et al. 2008). The types of sources can vary relative, absolute, or estimated morbidity parameters. Initially implemented in the GIS environment, this simple and innovative method may well be used in traditional mapping.

Fig. 11 shows a map on morbidity trend over a 17-year period. In this map, the expanded graphic representation of the time-span allows one to treat time as the "notion parameter" and not just as an attribute parameter as in the first case. The use of this model is much more beneficial at the regional level with a relatively small number of administrative units. Visual and informative aspects of the model are achieved by the rational arrangement of the diagrams that may be tied to the territorial units with the help of references.

The spatial distribution of morbidity may be shown with the help of "gravitational" and diffusive models and the Monte-Carlo method (Tikunov 1997b). In this case, modeling of disease spatial distribution is conducted for each year separately and the results are combined in animations that allow one to visualize the process in time. To date, a large number of cartographic visualization methods have been developed; among them we should note several applicable to research on morbidity dynamics, namely, animated two-dimensional maps on dynamics, animated two-dimensional maps on change, classical two-dimensional maps that use animation effect, animated linear, areal, and volume anamorphoses, animated dynamic three-dimensional presentation, and animation in virtual reality (Kapralov et al. 2010; Gusein-Zade and Tikunov 2015).

CONCLUSION

Research and mapping of dynamics of medical-geographic phenomena is an urgent practical task. Analysis of medical-geographic maps has identified limitations of the methods and techniques used for visualization of dynamic aspects. We have

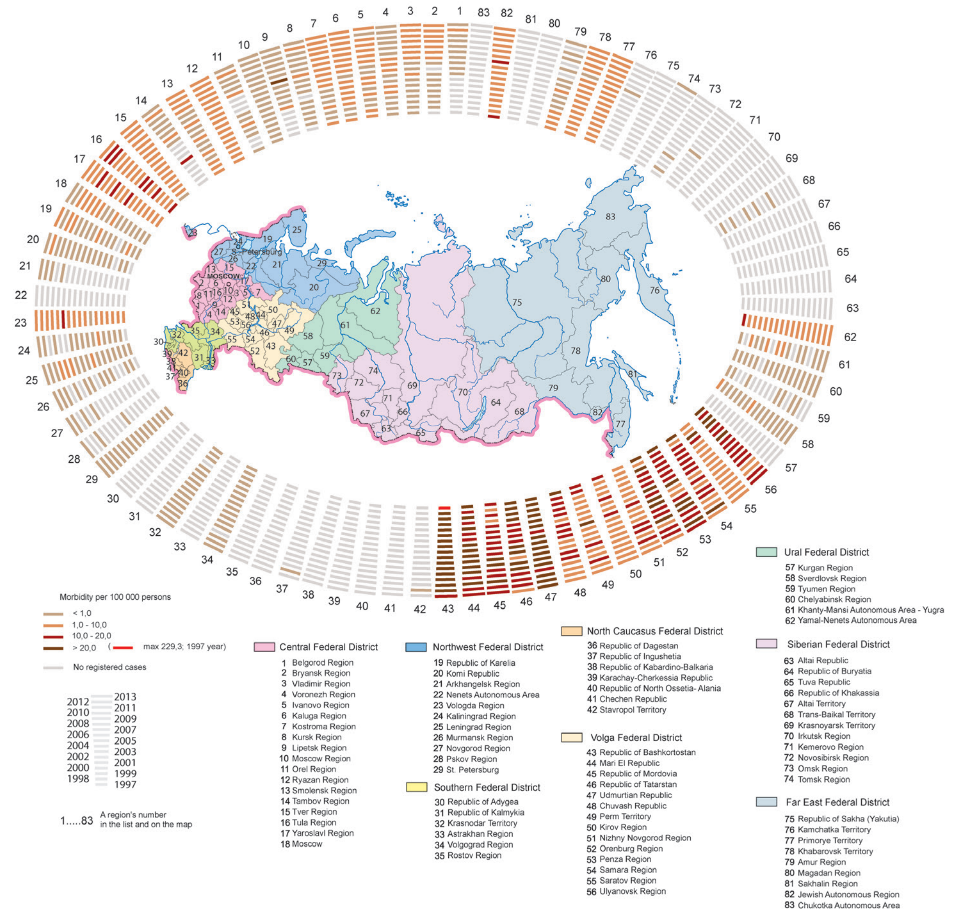

Fig. 11. Map "Morbidity from hemorrhagic fever with renal syndrome." Scale 1: 60 000 000

summarized the methods and techniques of mapping dynamic processes using public health and morbidity as examples. We also introduced other methods based on the results of preparation of integrated medical-geographic atlases. We have demonstrated the potential of cartographic presentation of spatiotemporal patterns of morbidity distribution and graphic techniques of their visualization.

Various parameters of morbidity have been used in map compilation: absolute, relative, estimated, statistical, etc. Their selection and use in thematic layers (analytic, integrated, and synthetic maps), combination, the use of either qualitative or both qualitative and quantitative parameters, and development of graphic methods of presentation on maps are determined by the goals and objectives of medical-geographic mapping, availability of informational base, mapping concepts, etc. The potential of morbidity dynamics mapping as an integral problem has not been fully realized and research in this direction should continue.

ACKNOWLEDGEMENTS

Part of this research (methodology and mathematical modeling) was funded under a grant of the Russian Science Foundation (project № 18-17-00074); part of this research was funded under the Russian Fund of Basic Research grant №16-05 00827.

REFERENCES

Bandrova, T. (2008). Atlas Geography and Economics, DataMap-Europe Ltd., Sofia, ISBN 978-954-8717-97-7, 80 p.

Chistobaev, A. and Semenova, Z. (2013). Statistical methods in medical-geographic studies. J. Geographic Bulletin: 1 (24). pp. 18-24. (In Russian)

Gabibova, P. (ed.) (2013). Medical-demographic atlas of the Republic of Dagestan (handwritten manuscript). Makhachkala: ALEF; 100 p. (In Russian)

Gusein-Zade, S. and Tikunov, V. (2015). Visualization in non-Euclidean metrics. Hong Kong: The Chinese University of Hong Kong, 213 p.

Huang, G., Govoni, S., Choi, J., Hartley, D., Wilson, J. (2008). Geovisualizing data with ring maps. ArcUser 11(1): pp. 54-55.

Kapralov, E., Koshkarev, A., Tikunov, V., et al. (2010). Geoinformatics. Vol. 1: Training manual for university students. 3rd ed. Moscow: Academiya; 400 p. (In Russian)

Kotova, T., Malkhazova, S., Orlov, D., Shartova, N. (2012). Atlas of natural focal diseases: mapping study for the territory of Russia. J. Proceedings of the Russian Geographic Society. 1; 144: 16-26. (In Russian)

Malkhazova, S. (ed.) (2007a). Medical-demographic atlas of the Kaliningrad Region. Kaliningrad. (In Russian)

Malkhazova, S. (ed.) (2007b). Medical-demographic atlas of the Moscow Region. Moscow: Moscow State University Press. (In Russian)

Malkhazova, S. (ed.) (2015). Medical-geographic atlas of Russia "Natural focal diseases". Moscow: Faculty of Geography, Lomonosov Moscow State University " (In Russian)

Malkhazova, S. (2012). Medical-geographic mapping: current state and prospects of development. Questions of Geography. Coll. 134: Current Biogeography. Moscow: Codex Publishing House. pp. 110-132. (In Russian)

Malkhazova, S., Kotova, T., Mironova, V., Shartova, N. (2011). Medical-geographic atlas of Russia "Natural focal diseases; concept and initial results". Vestnik of Moscow University. ser. 5. Geography; 4:16-23. (In Russian)

Malkhazova, S., Mironova, V., Kotova, T., Shartova, N., Orlov, D. (2014). Natural focal diseases: mapping experience in Russia. Int. J. Health Geogr. DOI: 10. 1186 / 1476-072X-13-21.

Prokhorov, B., Tikunov, V. (2001). Geographic aspects of the population health in the regions of Russia in comparison with other countries of the world. Vestnik of Moscow University, ser. 5. Geography. 5: 22-31. (In Russian)

Semenov, V. (ed.) (2004). Medical-environmental atlas of the Moscow Region. Moscow (In Russian)

Tikunov, V., Chereshnya, O. (2015). Public Health Index in Russian Federation from 1990 to 2012. Social Indicators Research, Springer Netherlands: 1-12.

Tikunov, V. and Chereshnya, O. (2016). The Public Health Index in the Russian Federation from 1990 to 2013 in comparison with other countries. Geography, Environment, Sustainability, 1: 94-108.

Tikunov, V. (1985). Modeling in socio-economic mapping. Moscow: Moscow University Press; 280 p. (In Russian)

Tikunov, V. (1997a). Classifications in geography: renaissance or fading? (The experience of formal classifications). Moscow, Smolensk: Publishing House of Smolensk University; 367 p. (In Russian)

Tikunov, V. (1997b). Modeling in cartography. Moscow: Moscow University Press; 405 p. (In Russian).

Vatlina, T. (2012). Medical-demographic atlas of the Smolensk Region. Smolensk: Smolensk State University Press (in Russian)

Zakrutkin, V. and Rishkov, M. (ed.) (2000). Ekologicheskiy atlas Rostovskoy oblasti. Rostov-on-Don; 120 p. (In Russian).

Received on October 24th, 2017 Accepted on November 22nd, 2017

Tatyana V. Kotova graduated from the Department of Geodesy and Cartography (now the Department of Cartography and Geoinformatics) of the Faculty of Geography, Lomonosov Moscow State University, in 1961, and has been with the Faculty of Geography since 1964. She received her Ph.D. in geographical studies in 1976. At present she is leading researcher of the Laboratory of Integrated Mapping (Faculty of Geography, Moscow State University). The main area of research interests is integrated thematic, biogeographic, and ecological mapping. She published over 180 papers and participated in creation of complex cartographic products as a managing editor, an editor, or an author of individual chapters (World Atlas of Resources and Environment, 1998; Atlas of the Khanty-Mansiysk Autonomous Region Ugra 2004, 2006; Atlas of the Kuril Islands, 2009; The National Atlas of Russia, 2007; 2009; etc.

Svetlana M. Malkhazova, has a degree of Doctor of Geographical Sciences. She is Professor, Head of the Department of Biogeography, Faculty of Geography, Lomonosov Moscow State University. The main research interests relate to the problems of biogeography, ecology, and medical geography. She is the author of over 250 scientific publications, including 10 books, several textbooks, and medical and environmental atlases.

Vladimir S. Tikunov is Professor, Head of the Integrated Mapping Laboratory, Geography Faculty of M.V. Lomonosov Moscow State University, and Director of the Center of the World Data System for Geography. He has led a number of Russian and international projects. His work has been used in many thematic maps and atlases: National Atlas of Russia (editor-in chief of Vol. 3), Environmental Atlas of Russia, Atlas of Socio-Economic Development of Russia, Atlas of the Khanty-Mansi Autonomous District – Yugra, etc. He is a recipient of the D.N.Anuchin Award for his work in mathematical cartographic modeling. Heis also a recipient of the Award in Science and Technology of the Russian Federation Government for the development of environmental and natural resources atlases of Russia.

Temenoujka Bandrova is Professor, President of the Bulgarian Cartographic Association and head of the Laboratory on Cartography at the University of Architecture, Civil Engineering and Geodesy, Sofia. She is Co-chair of the ICA Commission of Cartography and Children (2007-2011), a member of the Council board and a chair of Young Scientific Commission of International Society of Digital Earth (ISDE), a member of Commissions on Map Projections, on Cartography in Early Warning and Crises Management –International Cartographic Association (ICA); of Editor's group of the International Journal of Digital Earth, Cartographia and Geoinformatika, Croatia. She is Project manager in DataMap Ltd.where her school atlases and maps are published. She is an author of 30 school atlases and more than 80 wall maps in geography and history, approved by the Ministry of Education and Sciences for Bulgarian schools. She published more than 100 articles, reports, papers, book chapters and edited books published by Springer and ESRI Press. She is the organizer of series of 6 International Conferences on Cartography and GIS.

Sergey Chalov[1]*, Valentin Golosov, Anatolii Tsyplenkov[2], Philipp Theuring[3], Reza Zakerinejad[4], Michael Märker[5], Mikhail Samokhin[1]
[1]*Faculty of Geography, Department of Land Hydrology, M.V.Lomonosov Moscow State University, Moscow, Russia; Leninskie gory, 1, 119991
[2]Faculty of Geography, Makaveev laboratory of soil erosion and fluvial process M.V.Lomonosov Moscow State University, Moscow, Russia; Leninskie gory, 1, 119991
[3]SEBA Hydrometrie Gmbh, Kaufbeuren, Germany; Gewerbestrasse 61A, D-87600
[4]Faculty of the Geography, Isfahan University of Technology, Iran, Isfahan
[5]Department of Earth and Environmental Sciences, Pavia University, Pavia, Italy; via Ferrata, 1, 27100
*** Corresponding author:** srchalov@geogr.msu.ru

A TOOLBOX FOR SEDIMENT BUDGET RESEARCH IN SMALL CATCHMENTS

ABSTRACT. Sediment monitoring and assessment remain one of the most challenging tasks in fluvial geomorphology and water quality studies. As a response to various environmental and human disturbance effects, the main sources and pathways of the sediments transported within catchments, especially most pristine small one, may change. The paper discusses state-of-the-art in the sediment budget research for small catchments. We identified nine independent approaches in the sediment transport assessment and applied them in 11 catchments across Eurasia in the framework of an FP – 7 Marie Curie – International Research Staff Exchange Scheme in 2012-2016. These methods were classified as: i) Field-based methods (In-situ monitoring of sediment transport;– Soil morphological methods and dating techniques; Sediment source fingerprinting; Sediment-water discharge relationships), ii) GIS and remote sensing approaches (Riverbed monitoring based on remote sensing/historical maps; parametrization of the channel sediment connectivity; Sediment transport remote sensing modeling), and iii) Numerical approaches (Soil erosion modeling and gully erosion (stochastic and empirical models); channel hydrodynamic modeling). We present the background theory and application examples of all selected methods. Linking field-based methods and datasets with numerical approaches, process measurements as well as monitoring can provide enhanced insights into sediment transfer and related water quality impacts. Adopting such integrated and multi-scale approaches in a sediment budget framework might contribute to improved understanding of hydrological and geomorphological responses.

KEY WORDS: sediment budget, suspended sediment, erosion processes, erosion modeling

CITATION: Sergey Chalov, Valentin Golosov, Anatolii Tsyplenkov, Philipp Theuring, Reza Zakerinejad, Michael Märker, Mikhail Samokhin (2017) A toolbox for sediment budget research in small catchments. Geography, Environment, Sustainability,
Vol.10, No 4, p. 43-68
DOI-10.24057/2071-9388-2017-10-4-43-68

INTRODUCTION

Sediment monitoring and redistribution assessment for the different parts of fluvial systems remain one of the most challenging tasks in fluvial geomorphology and water quality studies. As a response to various environmental and human disturbances, the main sources and pathways of sediments transported through a catchment, especially small ones which are regarded to be the most pristine, may change. Sediment transport in and to river channels is strongly influenced by climatic conditions, particularly when heavy precipitation and warmer climate triggers fluvial processes.

Even though the importance of sediment budgets as a universal conservation law modification has been widely accepted (Alexeevsky et al. 2013), there are still no generally applicable procedures to establish a comprehensive sediment budget for a catchment (Walling and Collins 2008). Ongoing work by the authors has focused on the developing and testing of various methods and integrating them in a general approach («integrated») (Walling et al. 2001). This «integrated» approach combines some complementary techniques. They have been properly analyzed and classified according to the available tools, spatial resolution, and methodological steps, as well as in respect to an acceptable range of results.

The recent studies were carried out within an EU FP-7 project entitled: «Fluvial processes and sediment dynamics of slope channel systems: Impacts of socio economic-and climate change on river system characteristics and related services, (FLUMEN)». The project was aimed at setting up empirical experiments and modeling tests in various catchments and environments distributed over Eurasia to understand the contemporary landform evolution and sediment redistribution within river basins up to the sediment transport from the land to the ocean (in relation to mountain areas). Therefore, we identified commonly used techniques based on a detailed literature review. Moreover, we applied some of these methods and present the results achieved in the case study catchments. Generally, we provide a comprehensive classification of the available methods and techniques namely the sediment budget toolbox.

METHODS AND FLUMEN CASE STUDY CATCHMENTS

This paper intends to give an overview of complementary and comparative tools and techniques that can be used as a toolbox for future studies in various environments of Eurasia. We aimed at identifying applicable techniques that can be jointly used as a toolbox in different environmental situations. We selected the following catchments representing different environmental characteristics: i) Mongolian steppes (Kharaa), ii) volcano region at Kamchatka peninsula (Sukhaya Elizovskaya), iii) tundra of Koryak Mountains at Kamchatka (Vetvey), iv) periglacial environment on the Scandinavian peninsula (Tarfalajokk) and v) North Caucasus mountains (Dzhankuat), vi) Ukrainian Carpathian flysch mountains (Black Tisza), vii) dry and wet subtropics (San-Leonardo) and viii) Tsanik rivers, ix) arid Zagros mountains in Iran (Mazayjan), x) Sakhalin island (Langeri) and xi) Intra-Apennine Central Italy (Mugello) (Fig. 1). Implications of applying different available tools to understand the sediment budgets of a particular catchment are explored using data from these 11 catchments across Eurasia. All available tools can be split into three main groups according to the data types:
i) field-based and monitoring methods;

ii) geographic information system (GIS) and remote sensing analysis
iii) numerical approaches (catchment and in-channel modelling)
Among them, the following 11 tools will be discussed in detail (Table 1):
(i) Field based methods
1 – In-situ monitoring of sediment transport;
2 – Soil morphological method and dating techniques;
3 – Sediment source fingerprinting;
4 – Sediment-water discharge relationships;
(ii) GIS and remote sensing analysis
5 – Riverbed monitoring based on remote sensing/historical maps;
6 – parametrization of channel sediment connectivity;
7 – Sediment transport remote sensing modeling;
(iii) Numerical approaches
8 – Soil erosion modeling and gully erosion (stochastic and empirical) models;
9 – channel hydrodynamic modeling.

Field-based and monitoring methods

In-situ monitoring of sediment transport

In-situ sediment monitoring remains the main method to characterize erosion within catchments as well as sediment transport in

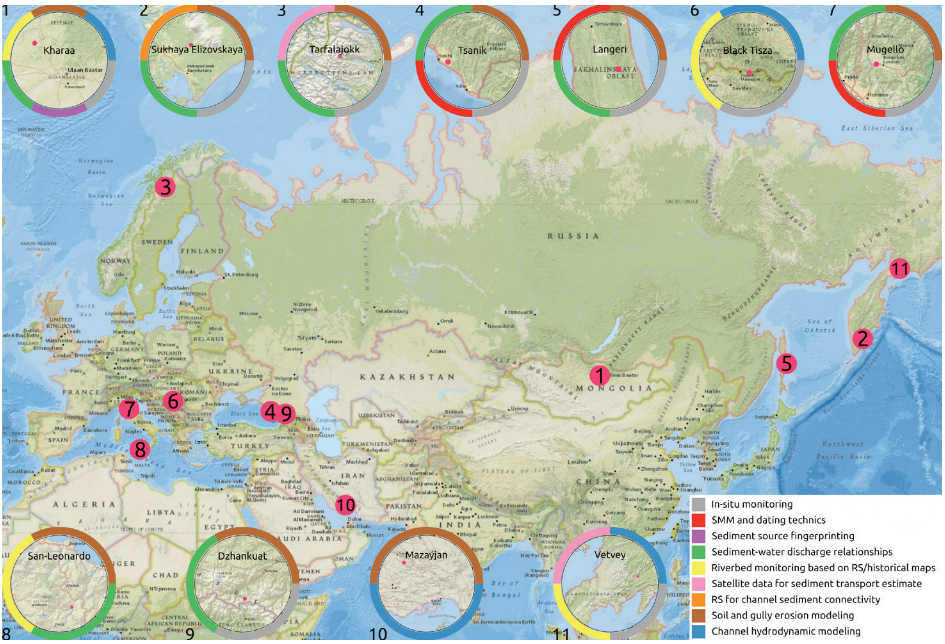

Fig. 1. Map of case study sites and used methods

the river network. The recent technologies have been drastically improved and this leads to the relatively wide range of direct and surrogate technologies for In-situ monitoring of sediment transport. Various approaches have been tested in the case study catchments (Kharaa, Sukhaya Elizovskaya, Vetvey, Tarfalajokk, Tsanik, Langeri, Black Tisza, Mugello and Dzhankuat river basins). Based on this, we developed a classification of approaches of sediment load (suspended and bed) monitoring including acceptance criteria for Suspended-Sediment Concentrations (SSC) (following (Gray and Gartner 2010)), accuracy and monitoring strategy (Table 2).

Suspended load monitoring is based both on traditional gravimetric analyses as well as advanced technological capabilities where bulk optic (turbidity), laser optic and acoustic backscatter principles are widely used and applied in the present study (Table 2). In all cases, the usefulness of the surrogate information obtained depends heavily on the existence of a close relationship between fluctuations in SSC and surrogate parameters and the calibration procedure that relates SSC to the used variable. Turbidity is an expression of the optical properties of a sample that causes light rays to be scattered and absorbed

Table 1. Case studies and used methods

River	Area	Watershed area, km²	Methods applied (according to the text)								
			1	2	3	4	5	6	7	8	9
Kharaa	Mongolia. Selenga River basin	11 345	+	-	+	+	+	-	-	+	+
Sukhaya Elizovskaya	Russia, Southern Kamchatka, Avacha riv. Basin	174	+	-	-	+	-	+	-	+	-
Tarfalajokk	Sweden, Scandinavian mountains, Kebnekaise massif	6.7	+	-	-	+	-	-	+	+	-
Tsanik	Russia, Black sea coast, Sochi	12.1	+	+	-	+	-	-	-	+	-
Langeri	Russia, Sakhalin island	1 343	+	+	-	+	-	-	-	+	-
Black Tisza	Ukrainian Carpathia	965	+	-	-	-	+	-	-	-	+
Mugello	Italy, Florenze	375	+	+	-	+	-	-	-	+	-
San-Leonardo	Italy, Sicily	253	-	-	-	+	+	-	-	+	-
Dzhankuat	Russia, Northern Caucasus, Terek riv. basin	9.1	+	-	-	+	-	-	-	+	-
Mazayjan	Iran, Zagros Mountains	900	-	-	-	-	-	-	-	+	+
Vetvey	Russia, Norten Kamchatka, Koryak Plateau	181	+	-	-	-	+	-	+	-	+

rather than transmitted in straight lines through the sample. Turbidity is a measurement unit for quantifying the degree to which light is penetrating through a water column that in turn is scattered by the suspended organic (including algae) and inorganic particles. Laser diffraction instruments exploit the principles of small-angle forward scattering. Pressure differential instruments measure mass density in a water column, thus integrating substantially more streamflow than a point measurement. Acoustic Doppler profilers use acoustic backscatter to measure suspended sediment concentrations in much higher stream orders than do instruments that rely on point measurements.

Bed load still remains one of the most poorly explored components in the fluvial system. Monitoring approaches consist of direct and surrogate measurements. In our study, different types of bedload samplers were used to characterize bed load in small mountain streams (Table 2): Box or basket samplers, pan or tray samplers, pressure-difference samplers, and trough pit samplers. Box samplers intercepted particles due to a reduction in flow velocity (Gray et al. 2010). Pan or tray samplers retain the sediment that drops into one or more slots after the sediment has rolled, slid, or skipped up an entrance ramp. Pressure-difference samplers are designed so that a sampler's entrance velocity is about the same as the stream velocity. Additionally, acoustic Doppler current profiles (ADCP) were used to estimate apparent bed velocities and ultimately to infer bedload-transport rate according to a method described by (Guillermo et al. 2017).

Soil morphological methods and data techniques

Quantitative assessment of soil losses and sediment deposition can be evaluated based on a comparison of soil profiles of undisturbed soil, that formed under given climate conditions with soil profiles after the beginning of cultivation. Erosion and deposition processes lead to soil profile transformations and detailed descriptions of soil profiles allow to quantitatively evaluate the soil losses or gains. Depending on the soil type the decrease of thickness in the A_{plough}, A_1, AB and/or B horizons in cultivated areas can be used to estimate the total soil loss or gain for the entire period of cultivation for different positions along the slope (Belyaev et al. 2005; Larionov et al. 1973; Olson et al. 2008; Rommens et al. 2005). The accuracy of the method, also called as soil morphological method (SMM), can also be refined by choosing different geomorphic locations for the survey pits (Kiryukhina and Serkova 2000; Rommens et al. 2005).

Limitations of this approach are often associated with variations in natural soil horizon thickness in particular for mountain conditions because of microclimatic and lithology differences. However, it has been shown that in case of severe soil losses this variation is less than that due to erosion (Belyaev et al. 2005; Larionov et al. 1973; Rommens et al. 2005). Besides, it is necessary to know the total duration of cultivation for a particular site in order to correctly calculate the mean annual soil loss or sediment gain for the entire period of cultivation. In case of areas with a relatively short history of intensive cultivation, like the Great Plains in the USA, the southern part of the Russian Plain or Australia information might be available in form of archive data. It is more difficult to identify the period of cultivation for a site with a longer history of anthropogenic influence. In this case, some archeological methods and dating techniques are helpful. The buried soil method is widely used for the evaluation of total deposition for a given agriculture period, in particular in case of dry valley bottoms or river floodplains (Alexandrovskiy et al. 2004; Knox 2001). The applicability of this method considerably increases during last decades because of serious progress in dating techniques (Notebaert and Verstraeten 2010).

Most sediment dating techniques were initially elaborated for the evaluation of sedimentation rates in lakes, reservoirs and sea bottoms (Appleby 2008). However, they are also applied for the evaluation of contemporary sedimentation rates of other terrestrial sediment sinks (cones, dry valley bottoms, river floodplains).

There is a range of dating techniques available, but the most widely used can be split into two groups: i) application of fallout radionuclides and ii) substances contained in the sediments (Table 3). Radionuclides, such as Lead-210 (210Pb, t½=22.3 y) and Cesium-137 (137Cs, t½=30.2 y), are the most widely-used and reliable methods employed to calculate short-term (years to decades) sediment deposition and accumulation rates in fluvial environments (Appleby and Oldfieldz 1983; Belyaev et al. 2011; Belyaev et al. 2013; Du and Walling 2012; Golosov 2009; Golosov et al. 2010; He and Walling 2003; Mizugaki et al. 2006; Owens and Walling 2002; Ritchie et al. 2004; Ritchie and McHenry 1990; Walling 1999). Generally, 210Pb dates are confirmed using 137Cs profiles, when the 137Cs profiles are sufficiently intact (Appleby and Oldfieldz 1983; Du and Walling 2012).

Recently it is possible to use bomb-derived 137Cs as a tracer for the identification of sedimentation rates since 1963 (maximum fallout) and in some cases between 1959-1963, because in particular in 1958-59 a second maximum of bomb-derived 137Cs fallout was observed. In addition, for the most parts of Europe it is possible to use Chernobyl-derived 137Cs for dating (Golosov 2000; Leenaers 1991; Walling et al. 1998). So, recently in case of using both bomb-derived and Chernobyl-derived 137Cs it is possible to evaluate e.g. overbank sedimentation dynamics for relatively homogeneous time intervals (1963-1986 and 1986-sampling time) (Du and Walling 2012; Golosov et al. 2010). However, in areas with very high Chernobyl contamination levels usually it is not possible to identify any bomb-derived peak. Also, the 1986 peak can not

Table 2. Sediment monitoring approaches applied for different fluvial systems of the FLUMEN project

Approach	Suggested acceptance criteria and measurement requirements	Suggested monitoring strategy	Advantage	Disadvantage	Examples of application (Reference)	Example of application among case studies (according to Table 1)
Suspended load (SSC)						
Gravimetric analyses	The mass of the filtered sediment should be comparable with filter mass	Used for calibration of surrogate technologies	Direct parameter of SSC	routine collection and analysis of water samples	(Minella et al. 2014; Piper et al. 2006)	Kharaa, Sukhaya Elizovskaya, Tarfalajokk, Tsanik, Langeri, Black Tisza, Mugello, San-Leonardo, Dzhankuat
Bulk optic (turbidity), backscatter	SSC acceptance criteria range from ±50% uncertain-ty at lowest SSCs to ±15% uncertainty for SSC's exceeding 1 g/L.	affordable time series data		existence of a close relationship with fluctuations in SSC which are differed between rivers and in time	(Göransson et al. 2013; Gray and Gartner 2010)	Kharaa, Sukhaya Elizovskaya, Tarfalajokk, Tsanik, Langeri, Black Tisza, Mugello, San-Leonardo, Dzhankuat
Laser optic		affordable time series data	Obtaining both suspended concentrations and grain sizes		(Gray and Gartner 2010)	Sukhaya Elizovskaya, Tarfalajokk

Acoustic backscatter		SSC distribution at the reaches of high probability of local (profile) spatial variability	Provide a profile (vertical and horizontal) of the	Applicable only for large rivers, requires existence of a close relationship with fluctuations in SSC	(Chanson et al. 2008)	Kharaa
Bedload						
Box or basket samplers			Easy field installation	Influenced by flow fields		Sukhaya Elizovskaya, Dzhankuat
pan or tray sampler			Easy field installation	Influenced by flow fields		Sukhaya Elizovskaya
pressure-difference samplers			Easy field installation	Influenced by flow fields		Kharaa, Sukhaya Elizovskaya, Tarfalajokk, Tsanik, Langeri, Dzhankuat
ADCP	apparent velocity of particles at the bedload layer as resulting by comparing the ADCP's velocity from its capability to acoustically track the bottom and from accurate GPS recording			Dependence on instrument frequency, acoustic pulse length used and site-specific properties, such as riverbed composition and bedforms presence	(Guillermo et al. 2017).	Kharaa

Table 3. Dating techniques used for evaluation of sedimentation rates in different fluvial sinks

Dating technique	Decay	Age range	Advantage	Disadvantage
fallout radionuclides				
^{7}Be (0.14 yr)	63 days	<0.6 yr	Event base, easy to measure	Need to measure reference systematically, to be collected very soon after deposition event
Fukushima-derived ^{137}Cs	30.2 years	Peak March 2011	Clear peak with fix time	Local scale, can be applied only in Japan
Chernobyl-derived ^{137}Cs	30.2 years	Peak May 1986	Clear peak with fix time	Regional scale, can be applied in parts of Europe
Bomb-derived ^{137}Cs	30.2 years	Peaks 1958/59 and 1963/64	One clear peak, distribute across the Earth	Now low value in Southern Hemisphere, difficult to identify
^{241}Am	432.6 years	Peaks 1963/64	Allows to identify bomb-derived ^{137}Cs peaks from others	Precision has still to be improved, expensive
^{238}Pu	87.74 years		Can be used instead bomb-derived ^{137}Cs	It still need to improve the precision, expensive
$^{239+240}Pu$	$2.411 \cdot 10^{4}$ and 6 564 years	Peaks 1963/64		
$^{210}Pb_{ex}$	22.3 year	1-130 years	Useful for identification of deposition rate dynamics for the last 130 year in case of application with other FRN	Improvement of measurement accuracy is still needed
material in deposits				
^{14}C	5.7 kyr	100 yr–50 kyr	Relatively simple to collect	insufficient accuracy for the assessment of contemporary sedimentation rates, expensive
Optically simulated luminescence	-	50 yr–100 kyr	Detail dating of sedimentation rates for few time intervals	It is necessary to have quarzitic sand deposits, expensive
Fly ash	-	100-150 years	Cheap analytical equipment	labor-intensive and time-consuming method of analysis

be determined in case of very low fallout of Chernobyl-derived 137Cs even in the North of the European part of the Russian Plain.

The application of the SMM in the Langeri river for floodplain in the downstream part of the basin allows to evaluate the mean annual net accumulation for the last 50 years in the range of 2.3±0.6 mm/year (≈200 t/year), that are in fitting well with assessments of sediment budget using other methods (Chalov and Tsyplenkov 2016).

SEDIMENT SOURCE FINGERPRINTING

Another tracing technique capable of providing useful information to assess catchment sediment budgets is the fingerprinting approach. Sediment source fingerprinting can generate valuable information on the relative importance of individual potential sources contributing to the downstream suspended sediment flux of a river. Such information is clearly of considerable value both providing information on the linkages between upstream sediment sources and downstream sediment yield. It allows sediment budgeting and a more precise sediment control as well as related measures and thus optimizing the effectiveness of such work in reducing downstream sediment fluxes. Moreover, the source fingerprinting technique has been successfully deployed to investigate spatial sediment sources, classified in terms of discrete geological zones (Collins et al. 1998) or tributary sub-catchments (Collins et al. 1996). Information on individual source types e.g. surface soils characterized by different land use and eroding channel banks (Collins et al. 1997; Motha et al. 2004; Walling 1999) are valuable especially in a management context. The fingerprinting approach is based on the link between geochemical properties of sediment and those of its sources. The assumption is that the potential sediment sources can reliably distinguish by their geochemical properties «fingerprints». Thus, the provenance of the sediments can be established by comparing its properties with those of the sources, using a numerical mixing model coupled with uncertainty analysis.

This method was successfully adopted to the Kharaa river basin, where the identification of the contributing sources showed a dominance of riverbank erosion to the total suspended sediments at the outlet. Riverbank erosion contributed 74.5% to the total load, whereas only 21.7% originated from surface erosion and 3.8% from gully erosion (Theuring et al. 2013). By the way, in the upper parts of the catchment in average 63.8 % of the SS originated from riverbank erosion and 36.2% from surface erosion. However, in spring 2011, when snowmelt occurred in combination with strong precipitation, surface erosion contributed with 53.9% (Theuring et al. 2013). This indicates that an elevated contribution of suspended sediments from surface erosion to the sediment load was mainly associated with increased precipitation.

Sediment – water discharge relationship

In natural river systems, sediment transport hysteresis can be observed to varying extents (Fan et al. 2012; Lawler et al. 2006); thus, sediment discharge is variable for similar or equivalent water discharges. Furthermore, sediment concentration (SC) – water discharge (Q) hysteresis loops can vary from clockwise to anti-clockwise. Clockwise hysteresis loops occur when the SC peak arrives before the Q peak. The SC is then generally greater during the rising limb of a flow hydrograph than during the falling limb. Clockwise hysteresis loops are often related to the depletion of readily available sediment sources and the associated dilution of suspended sediment concentrations (Bača 2008). High SC-Q skewness can occur when the bed load constitutes a considerable portion (>30%) of the total sediment load (Alexeevsky 1998), such as in the presence of large in-channel sediment sources (e.g., submerged bars). Anti-clockwise hysteresis loops occur when the sediment delivery to the river channel is limited at the beginning of an event. These loops can, for instance, be associated with catchment processes that delay the sediment delivery from the upper portions of a river basin (Hughes et al. 2012). For instance, anti-clockwise loops can be a result of the delivery of fine-grained material from disturbed floodplains, including mining sites (Chalov 2014).

The SC–Q relations in rivers are typically governed by multiple and relatively complex processes (Hudson 2003; Lawler et al. 2006; Lefrançois et al. 2007), such as hillslope erosion within catchment areas (Nadal-Romero et al. 2008; Runkui et al. 2010), sediment wave dispersion (Bull 1997), upstream floodplain sedimentation (Asselman and van Wijngaarden 2002) or an abrupt erosion of river banks (Lefrançois et al. 2007). In many cases, the net effect of such varied processes is quantified empirically based on historical observation data. Commonly, these relations take the power law form:

$$SC = aQb \qquad (1)$$

where a and b are regression coefficients (Asselman 2000). However, the above-mentioned hysteresis effects cause scatter in the empirical datasets, which must be understood and considered to enable dependable predictions for river system management. A primary challenge is therefore to identify key governing processes and their relative contribution to such hysteresis, particularly at large-catchment scales, where many of the processes are less well investigated or understood than at smaller scales (Alexeevsky 1998; Williams 1989).

The SC–Q relations built for the Sukhaya Elizovskaya river show different types according to the location of the gauging station. For example, in the upper stream where the river characterizes by incised channels with rifles and waterfalls the SC-Q relation type is taking the form of a simple linear regression. However, in the middle reach where channel type changes to wandering the SC-Q relation changes to figure-to-eight hysteresis pattern. Downstream, in the lower part of the basin due to the flattening of a longitudinal profile (Chalov et al. 2017) the channel as such disappears and the water flows in a laminar way like a sheet erosion. In this area, the SC-Q relation has an anti-clockwise pattern with a rapid rise event, with a slight sediment lag resulting in a narrow anti-clockwise loop.

GIS ANALYSIS, REMOTE SENSING AND HISTORICAL MAP ANALYSIS

Channel planform dynamics based on remote sensing/historical maps

A widely accepted approach for assessing the role of in-channel processes in sediment transport is related to the evaluation of channel planform dynamics based on remote sensing/historical maps. The approach based on a detailed reconstruction of channel changes requires a significant number of measurements of one or more channel features (e.g., channel width, bed elevation, sinuosity, braiding intensity) over a specific time period. The number of measurements generally depends on available data (e.g., aerial photos, topographic data, data from gauging stations) and defines the quality of reconstruction, which is the temporal detail of the evolutionary trajectory.

To identify the main morphological changes of Black Tisza River and also to assess the most unstable river reaches, remote sensing data and detailed topographical maps were used for a time period that covers more than 100 years. The research time frame goes back to 1869, when during the third military survey detailed maps on a scale of 1:75 000 were obtained. These maps are indicating the closest natural conditions of the river without a significant anthropic intervention. Other maps used were the result of geodetic surveys during the Soviet Union period: scale 1:100 000 (edition 1976), scale 1:10 000 (edition 1992) and satellite data from 2013. Using ArcGIS analysis, main hydrographic, geomorphologic and morphometric characteristics of Black Tisza and its tributaries were obtained based on ASTER Global Digital Elevation Model (DEM) (NASA LP DAAC 2015). The resolution of the DEM (30 x 30 m/pixel) was not detailed enough to identify the precise location of the main channel that is why it was not taken into account for the channel morphologic dynamics.

A comparison of WorldView 2 and Landsat 7ETM+ satellite images in the downstream part of Langeri river for 2012 (WorldView 2, 2012-06-16) and 2015 (Landsat 7ETM+, 2015-07-20) years made it possible to assess channel planform dynamics. As a result, we got total

Fig. 2. Landform dynamics of the Langeri River in 2012-2015

erosion area that amounts to 0.145 km^2 for a period from 16.06.2012 to 20.07.2015. This corresponds to a streambank erosion rate of 1 593 060 kg/year.

Parametrization of in-channel sediment connectivity

The mentioned approach (6) is closely related to the understanding of structural and functional sediment connectivity in a long time span for the migrating river channels via remote sensing applications. The methodology consists of and represents the identification of flood periods as well as data processing (e.g. (Kidová et al. 2016)) and is based on different steps. First of all, it is a discrimination of bank-attached and mid channel gravel bar areas as potential sediment sources and stores in GIS. Secondly — we estimated the potential connection links between bars based on the Euclidean distance in GIS and the calculation of probabilities. Then we identified the type of connectivity based on an estimation of balance between accreted and eroded areas of bars or floodplains followed by a process-based interpretation of structural connectivity for different flood periods as well as for single channel reaches.

In case of braided and anabranching channels the identification of the main processes that are conditioning different forms of the sediment connectivity is based on the assessment of the balance between accreted (ΔS_2) and eroded (ΔS_3) areas by overlaying the braidplain components polygons in two consecutive time horizons t–1 and t.

$$K_1 = \frac{\Delta S_1}{S_{t-1}} \quad (2)$$

$$K_2 = \frac{\Delta S_2}{S_{t-1}} \quad (3)$$

$$K_3 = \frac{\Delta S_3}{S_t} \quad (4)$$

where $K_{1\text{-}3}$ – and additionally ΔS^1 represent unchanged area within floodplain polygons (Fig. 3).

The application of the approach revealed spatial discrepancies of the connectivity patterns in different river systems. Such methodology was applied to the Sukhaya Elizovskaya river which has an anabranching channel in the upper reach (Fig. 3). Rapid filling and release of the shallow underground aquafers of the lahar deposits induce such

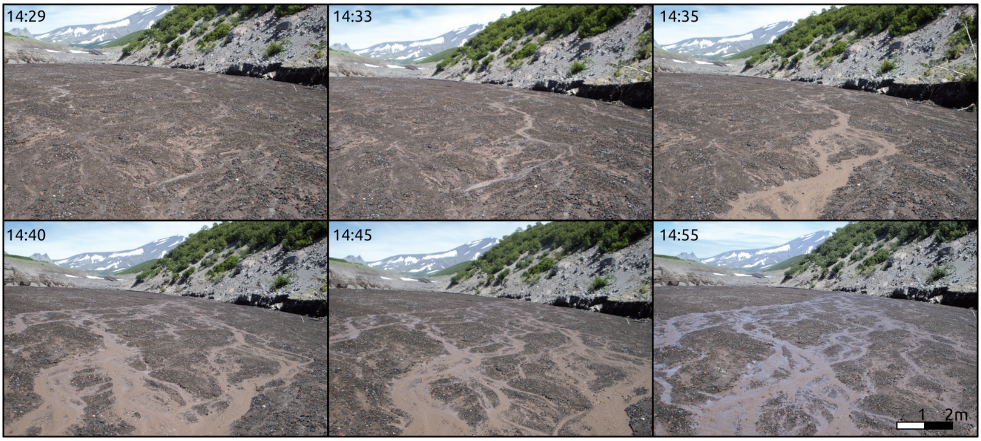

Fig. 3. Short-term planform changes of the Sukhaya Elizovskaya river

branches (Chalov et al. 2017). This short-term changes in water and consequently sediment discharges are common within river sections of lahar valleys (Mouri et al. 2014). They represent most unstable and highly dynamic types of channel planforms.

Sediment transports remote sensing modeling

Using of satellite images for SSC assessment presents a new way to study flow and sediment dynamics. Only a few works have been done yet about the application of the remote sensing for SSC in streams. Most of them deal with reservoirs, estuaries and seas. Experiments in the estuary of the Pearl River (China) (Chen et al. 2009) found negative regression model between water turbidity and reflectance at 570 nm (maximum correlation spectral band between 350 and 2500 nm) $R_{570.}$ The best fit relationship was

$$T = -439.52 \times R_{570} + 22.9 \qquad (5)$$

where T, R_{570} are the degree of turbidity (in Nephelometric Turbidity Unit, NTU), surface water reflectance at 570 nm, respectively. It resulted from an increase of organic matters in the suspended solids. The best model for water turbidity in the Guadalquivir River explained 78% of variance in ground-truth data and included as predictors band 3 (630–690 nm), band 5 (1550–1750 nm) and the ratio between band 1 (450–520 nm) and band 4 (760–900 nm) (Bustamante et al. 2009). For the Tawa Reservoir (Choubey 1997) simple linear regression analyses shows that LISS-I band 3 (0.62±0.68 mm) is the best for correlations of turbidity and radiance values:

$$T = -078 \times band3 + 5.73 \qquad (6)$$

Multiple regression equations have higher correlations (r = 0.91):

$$T = -42.82 + 1.79 \times (band1 + 2 + 3) + 3.67(band1 + band3) \qquad (7)$$

In our experiments in the rivers of the Vetvey basin it was found that even raw data DN (pixel values in bands measured in digital number, dn) could be used to estimate SSC. That suits necessity to expand data on unstudied rivers, which are taken by the same image with rivers covered by field measurements. According to differences in SSC=f(DN) variables we classified streams with low (light color) and high (dark color) human impact. Even low-quality images are a useful instrument for stream monitoring providing the information on larger areas. The general range of digital numbers for clear streams was found from 1 to 120 dn, for streams polluted by mining activity – >120 dn.

We estimated the limits of the streams that could be studied through remote sensing application. 5.8 m resolution of the ISR-P6 images provides necessary information to study streams with a width not less than 10 m (5 pixels per channel width). For the narrow creeks (1-2 pixels per channel width) a quantitative calculation of SSC is impossible because of reflectance intensity transformation caused by the morphology of shallow streams. The problems to make

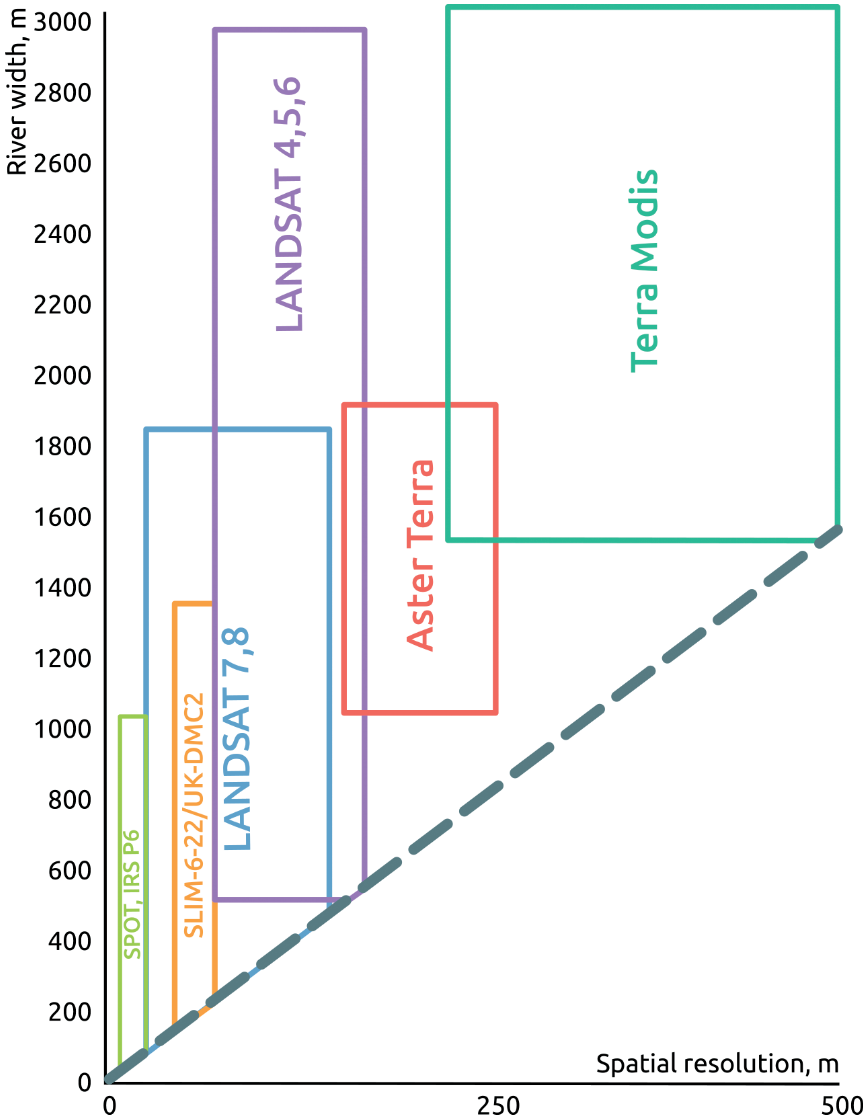

Fig. 4. Spatial limits of RS application in sediment concentration analyses

a calculation of water turbidity occur also at shallow braided reaches especially those characterized by alluvial fans. The suspended load monitoring of small rivers should be provided by higher resolution remote sensing.

NUMERICAL APPROACHES (CATCHMENT AND IN-CHANNEL MODELING)

Soil and gully erosion modeling

In the last decades, significant progress has been made to understand water erosion in general and gully erosion in particular in terms of the controlling factors and associated processes. However, many research questions remain, concerning the most predominant type of water erosion and/or the role of the human impacts and climate change on soil loss in different landscapes or modeling units. Hence, the prediction of areas with higher susceptibility to specific types of water erosion, and in particular gully erosion, is crucial and a key information for a proper land use management in many parts of the world. However, the quantitative and qualitative assessment of gully features has been widely neglected and thus, the estimation of erosion and quantification of sediment production is always limited (Kumar and Kushwaha 2013).

Although there are many models for evaluating water erosion rates (Flanagan and Nearing 1995; Merritt et al. 2003; Poesen et al. 2003), most of these models are physical based that need detailed input data and are difficult to apply on large areas. The application of different soil erosion models and soil conservation methods varies in their context, purpose, and degree of detail and therefore, the most suitable model depends on the proposed use, and the characteristics of the basin being considered. The numerical models for the assessment of water erosion can be classified in physically based models, stochastic models and empirical models. According to the different model approaches, users have to select specifically the relevant input data and processing techniques, depending on their expertise, local conditions and data availability (Conoscenti et al. 2008; Karydas et al. 2013).
In the Mazayjan catchment of Central Zagros Mountains we applied different approaches to identify and quantify especially gully erosion processes and their contribution to the general sediment budget. Using the Erosion Response Units (ERU) concept (Märker et al. 2001) we generated a susceptible map for the entire Mazayjan catchment area based on a detailed terrain analysis and a stochastic approach. We used the Maxent model (stochastic mechanics) (Zakerinejad and Märker 2014) to identify gully susceptible areas that later on were used in the quantitative approach. For this study 12 topographic indices that included: elevation, slope, aspect, analytical hillshading, plan and profile curvature, curvature classification, convergence index, altitude above channel network, catchment area, stream power index, length-slope factor have been used to predict gully erosion applying the Maxent model. As depended variable gully areas mapped in Google Earth were used. The approach allows the assessment of the potential spatial distribution of gullies in the Mazayjan catchment. We applied a combined approach using the USPED (Mitasova et al. 1996) model together with a SPI (Stream Power Index) index based approach to assess the gully areas in the Mazayjan catchment in the southwest of the Zagros Mountains in Iran. We show that sediment production and transport by gully erosion is not considered in traditional «sheet erosion» models like RUSLE, USPED or WEPP. However the proposed approach allows for a detailed quantification of sediments produced by gully systems.

For the Tsanik and San-Leonardo river basins the erosion rates have been computed through an indirect assessment based on the application of the Revised Universal Soil Loss Equation (RUSLE) (Renard et al. 1997). In both basins the most eroded land use/land cover type are agricultural lands. During wet years the San-Leonardo erosion rates are twice as high as the Tsanik basin but in dry years these difference is lower or inverse – The Tsanik basin erosion rates are 9% higher. The same situation appears in forested areas - in wet years in Sicilian basin erosion rates are 1.5 times higher than in dry years where they are two times lower (Tsyplenkov et al. 2017). The spatial distribution of net annual erosion rates for the San-Leonardo and the Tsanik rivers have been carried out with a RUSLE modeling approach illustrated in Fig. 5.

HYDRODYNAMIC MODELING

According to various observations, the river channel often controls the sediment transport by acting as the main source of the material during high flow events (David et al. 2012; Petticrew et al. 2007). In most river systems, in-channel sediments are stored for a relatively short time in comparison to material accumulated, for instance on floodplains (Walling et al. 1998). On the other hand, in-channel bed storage, which is depleted after even the most extreme flow events, can also be replenished in a relatively short time (Ciszewski 2001). Thus, the exchange of sediments on a channel bed can be very dynamic under transient flow conditions. The dynamics of in-channel storage of sediments control the variability in sediment yield of a catchment. It is because bed erosion/deposition processes within a channel contribute to the evolution

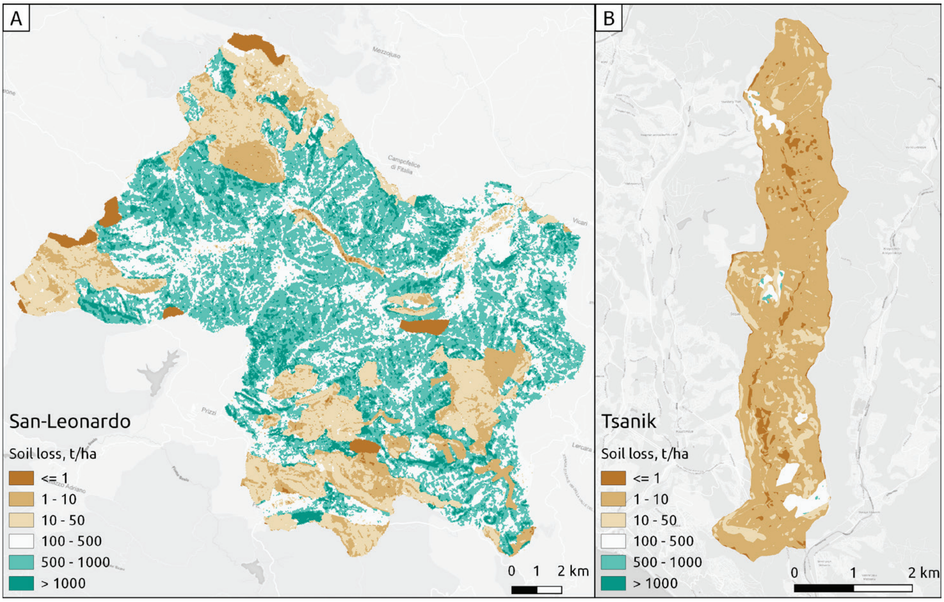

Fig. 5. Application of erosion models for San-Leonardo (A) and Tsanik (B) river basins (net annual soil losses, t/ha)

of the difference between upstream and downstream sediment loads and concentrations (Owens et al. 1999; Smith 2003).

Due to limited information available on the nature of channel changes, numerical simulation remains the main tool providing a certain amount of sediment washed due to in-channel changes or stored in river channels. Flow phenomena in natural rivers are three-dimensional, especially those at or near a meander bend, local expansion and contraction, or a hydraulic structure. Sophisticated numerical schemes have been developed to solve truly three-dimensional flow phenomena.

Most sediment transport models are one-dimensional, especially those used for long-term simulation of a long river reach. However, one-dimensional models are not suitable for simulating truly two- or three-dimensional local phenomena.

In the autumn of 2014 field surveys were conducted along the whole 51 km reach of Black Tisza River. Using modern geodetic (GPS Sokkia GRS 1 and a dumpy level Leica Sprinter 150) and hydrometric equipment (current meter), morphological parameters of the channel-floodplain zone were determined; stream velocity and water runoff measurements were conducted, as well as granulometric analysis (sorting method) of the bed-load was undergone. Hydrological data regarding the water flow was collected from the hydrometric gauging station in Yasynia village. Hydraulic modeling using one-dimensional HEC-RAS software was performed for floodplain delineation and in order to obtain streamflow characteristics during flood peak discharges.

Forecasting assessments in terms of the HEC-RAS hydraulic model for the section of the lower reach of the branched channel of one of the Vetvey tributaries, with complete cessation of placer platinum mining in 2014 taken into account, showed that vertical deformation of the longitudinal profile was responsible for the input of 300 to 1000 t/year to the river channel (Chalov et al. 2015).

Zero-dimensional modeling was performed by using «SedimentLoad» for Langeri and Vetvey rivers. This model builds a SSC longitudinal profile. Based on river morphology obtained from SRTM DEM and field measurements we found that at a distance of less than 2 km from the source (platinum deposit in Vetvey basin) occurs mass deposition with an average accumulation rate up to 3 mm/day.

DISCUSSION: COMPILING THE TOOLBOX

A range of different research methods to investigate and quantify soil erosion, sediment transport and sediment input have been applied to nine case study catchments located over various environments over Eurasia domain. A range of state-of-the-art 11 methodological approaches was tested and compared, resulting in a set of most effective methods that can be used for a reliable and cost-time effective assessment of fluvial sediment transport and sediment sources at the catchment scale (Fig. 6).

Based on the general analyses of deliverables, constraints and experience, we identified schematically the analytical framework of sediment budget tools (conceptual framework). This consists of (a) identification and mapping of catchment sediment sources on the certain sub-basins; (b) quantification of the contribution of sediment source areas by processing remote sensing and auxiliary data in a GIS framework; (c) detailed investigation and processing of the sediment transport data for the evaluation of the contribution of various sub-basins; (d) carrying out the balance calculation and developing the sediment budget. The resulting sediment budget equation consists of 3 independent estimates of catchment, in-channel and delta equations. The delivery from the catchment ΔW is related to the identification of *i* sediment sources, located within the catchment (both slope wash and gullies): $\sum A_i$ or related to the upstream in-channel sources $\sum C_i$ and compared with the sediment load at the sub-basin outlet W_H:

$$\sum A_i + \sum C_1 - W_H = \Delta W \qquad (8)$$

In-channel sediment budget is most effectively used for the downstream part of the catchments where the contribution of in-channel sources is of crucial importance. The resulting balance is related to k channel patterns units where due to sediment connectivity increase (erosion) or decrease (channel storage) sediment transport ΔW may occur (Alexeevsky et al. 2013):

$$(\sum A_i + \sum C_i)_{\Gamma\Lambda} + \sum_{j=1}^{j}(\sum A_i + \sum C_i) \pm \sum_{k=1}^{k}(\Delta W) - W_H = \Delta W \qquad (9)$$

The assessment of significant changes of sediment transport along bifurcation deltaic areas is limited by constraints in monitoring of independent channels and thus, requires additional approaches to test the sediment budget (Chalov et al. 2017). Combination of catchment, in-channel and delta approaches with respect to available tools enables to construct a conceptual framework of a catchment sediment budget toolbox, finally allowing to built a catchment-scale sediment budget model.

The proposed methodology allows the application of field data, collected and provided by the above-mention methods and techniques to assess different erosion types, sediment redistribution, sediment transport and the sediment budget. The selection of an optimal set of methods and approaches for the evaluation of contemporary sediment budgets in river basins, allow for an assessment of extreme events in terms of sediment redistribution and problems like the selection of the appropriate temporal scale to study the evaluation of sediment budgets. It offers a unique possibility to estimate total sediment budget for the catchments. In the case study of Lange River (Russia, Sakhalin island) we applied methods 1, 4 and 8 in order to reveal the contribution of various catchment and in-channel processes in a river network affected (Table 4). In this particular case, the combination of various approaches including soil inventories allows for the classification of mass fluxes based on different grain sizes. We observed a significant increase of sediment delivery from the catchment due to gold mining processing. The results indicate the deposition of around 1000 t/day of sediments during flood events in the downstream section of the river which in turn is described by 137Cs analyses of the floodplain cores with 2.3±0.6 mm/year rates.

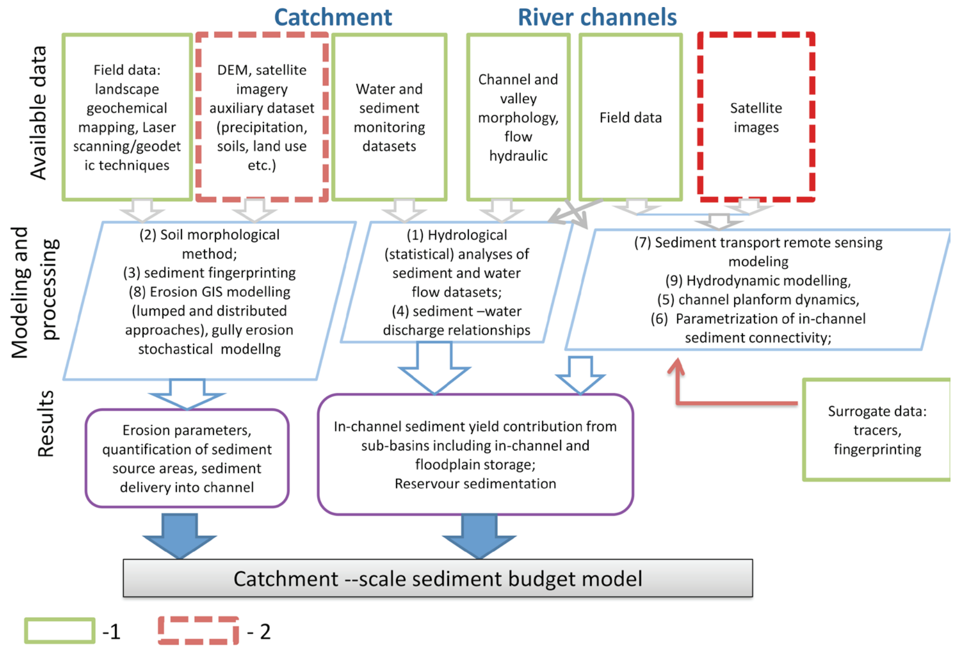

Fig. 6. Conceptual framework of catchment sediment budget toolbox (1 – field-based datasets; 2 – GIS and RS datasets)

Table 4. Integrated sediment budget assessment for Langeri River basin (for the summer period - from June to August)

Grain size class	Sediment discharge at the outlet downstream station, t	Sediment delivery from catchment, t	Sediment delivery from eroded banks, t	Sediment deposition on the floodplain, t
< 0.001 mm	4361	5881	414	43.1
0.001 – 0.5 mm	8722	865	589	61,3
> 0.5 mm	2907	1911	589	61,3
Total	14537	8657	1593	165

CONCLUSION

Between 2012 and 2016 we set up empirical experiments and modeling tests in a various catchment of different scales and environments located over Eurasia to understand i) the contemporary landform evolution and ii) sediment redistribution within the river basins up to iii) the sediment transport from the land to the ocean. The results of the investigations allowed to give an overview of complementary and comparative tools and techniques that can be used as a toolbox for future studies in various environments of Eurasia. In this paper we present the methodologies grouped according to the type of data collection: i) field methods; ii) GIS and remote sensing analysis; iii) numerical approaches. They are integrated within the general framework, that finally allows a comprehensive approach for sediment budget assessment.

ACKNOWLEDGEMENTS

This research was conducted within the projects of Russian Foundation of Basic Research № 15-05-05515 and 16-55-53116 and PEOPLE MARIE CURIE ACTIONS International Research Staff Exchange

Scheme Call: FP7-PEOPLE-2012-IRSES «Fluvial processes and sediment dynamics of slope channel systems: Impacts of socio economic-and climate change on river system characteristics and related services». We thank all participants of the field work on the case study areas mentioned in the paper.

REFERENCES

Alexandrovskiy, A., Glasko, M. , Krenke, N. and Chichagova, O. (2004). Buried soils of floodplains and paleoenvironmental changes in the Holocene. Revista Mexicana de Ciencias Geologicas, 21(1), 9–17.

Alexeevsky, N. (1998). Forming and Transport of River Sediments. Moscow: MSU Publishing House. (In Russian)

Alexeevsky, N., Chalov, R., Berkovich, K. and Chalov, S. (2013). Channel changes in largest Russian rivers: natural and anthropogenic effects. International Journal of River Basin Management, 11(2), 175–191.

Appleby, P. (2008). Three decades of dating recent sediments by fallout radionuclides: a review. The Holocene, 18(1), 83–93. https://doi.org/10.1177/0959683607085598

Appleby, P. and Oldfieldz, F. (1983). The assessment of 210Pb data from sites with varying sediment accumulation rates. Hydrobiologia, 103(1), 29–35. https://doi.org/10.1007/BF00028424

Asselman, N. and Van Wijngaarden, M. (2002). Development and application of a 1D floodplain sedimentation model for the River Rhine in The Netherlands. Journal of Hydrology, 268(1–4), 127–142. https://doi.org/10.1016/S0022-1694(02)00162-2

Asselman, N. (2000). Fitting and interpretation of sediment rating curves. Journal of Hydrology, 234(3–4), 228–248. https://doi.org/10.1016/S0022-1694(00)00253-5

Bača, P. (2008). Hysteresis effect in suspended sediment concentration in the Rybárik basin, Slovakia. Hydrological Sciences Journal, 53(1), 224–235. https://doi.org/10.1623/hysj.53.1.224

Belyaev, V., Golosov, V., Markelov, M., Evrard, O., Ivanova, N., Paramonova, T. and Shamshurina, E. (2013). Using Chernobyl-derived 137Cs to document recent sediment deposition rates on the River Plava floodplain (Central European Russia). Hydrological Processes, 27(6), 807–821. https://doi.org/10.1002/hyp.9461

Belyaev, V., Wallbrink, P., Golosov, V., Murray, A. and Sidorchuk, A. (2005). A comparison of methods for evaluating soil redistribution in the severely eroded Stavropol region, southern European Russia. Geomorphology, 65(3–4), 173–193. https://doi.org/10.1016/j.geomorph.2004.09.001

Belyaev, V., Zavadsky, A., Markelov, M., Golosov, V., Aseeva, E., Kuznetsova, Y., Ottesen, R., Bogen, J. (2011). Assessment of overbank sedimentation rates and associated pollutant transport within the Severnya Dvina river basin. Geography, Environment, Sustainability, 4(3), 68–84. https://doi.org/10.24057/2071-9388-2011-4-3-68-84

Bull, L. (1997). Relative velocities of discharge and sediment waves for the River Severn, UK. Hydrological Sciences Journal-Journal Des Sciences Hydrologiques, 42(5), 649–660. https://doi.org/10.1080/02626669709492064

Bustamante, J., Pacios, F., Díaz-Delgado, R. and Aragonés, D. (2009). Predictive models of turbidity and water depth in the Doñana marshes using Landsat TM and ETM+ images. Journal of Environmental Management, 90(7), 2219–2225. https://doi.org/10.1016/j.jenvman.2007.08.021

Chalov, S. (2014). Effects of placer mining on suspended sediment budget: case study of north of Russia's Kamchatka Peninsula. Hydrological Sciences Journal, 59(5), 1081–1094. https://doi.org/10.1080/02626667.2014.903330

Chalov, S., Bazilova, V. and Tarasov, M. (2017). Suspended Sediment Balance in Selenga Delta at the Late XX–Early XXI Century: Simulation by LANDSAT Satellite Images. Vodnie Resursi, 44(3), 1–8. https://doi.org/10.7868/S0321059617030075 (In Russian)

Chalov, S., Shkolnyi, D., Promakhova, E., Leman, V. and Romanchenko, A. (2015). Formation of the sediment yield in areas of mining of placer deposits. Geography and Natural Resources, 36(2), 124–131. https://doi.org/10.1134/S1875372815020031

Chalov, S. and Tsyplenkov, A. (2016). Integrated assessment of sediment yeild: Langeri river example (Sakhalin island). In Thirty-first plenary interuniversity coordination meeting on the problem of erosion, fluvial and estuarine processes. (pp. 172–173). Arkhangelsk. (In Russian)

Chalov, S., Tsyplenkov, A., Pietron, J., Chalova, A., Shkolnyi, D., Jarsjö, J. and Märker, M. (2017). Sediment transport in headwaters of a volcanic catchment - Kamchatka Peninsula case study. Frontiers of Earth Science, 11(3), 565–578. https://doi.org/10.1007/s11707-016-0632-x

Chanson, H., Takeuchi, M. and Trevethan, M. (2008). Using turbidity and acoustic backscatter intensity as surrogate measures of suspended sediment concentration in a small subtropical estuary. Journal of Environmental Management, 88(4), 1406–1416. https://doi.org/10.1016/j.jenvman.2007.07.009

Chen, S., Fang, L., Zhang, L. and Huang, W. (2009). Remote sensing of turbidity in seawater intrusion reaches of Pearl River Estuary – A case study in Modaomen water way, China. Estuarine, Coastal and Shelf Science, 82(1), 119–127. https://doi.org/10.1016/j.ecss.2009.01.003

Choubey, V. (1997). Monitoring turbidity with IRS-1A data. Hydrological Processes, 11(15), 1907–1915. https://doi.org/10.1002/(SICI)1099-1085(199712)11:15<1907::AID-HYP537>3.0.CO;2-2

Ciszewski, D. (2001). Flood-related changes in heavy metal concentrations within sediments of the Biała Przemsza River. Geomorphology, 40(3–4), 205–218. https://doi.org/10.1016/S0169-555X(01)00044-7

Collins, A., Walling, D. and Leeks, G. (1996). Composite fingerprinting of the spatial source of fluvial suspended sediment : a case study of the Exe and Severn river basins, United Kingdom. Géomorphologie : Relief, Processus, Environnement, 2(2), 41–53. https://doi.org/10.3406/morfo.1996.877

Collins, A., Walling, D. and Leeks, G. (1997). Source type ascription for fluvial suspended sediment based on a quantitative composite fingerprinting technique. CATENA, 29(1), 1–27. https://doi.org/10.1016/S0341-8162(96)00064-1

Collins, A., Walling, D. and Leeks, G. (1998). Use of composite fingerprints to determine the provenance of the contemporary suspended sediment load transported by rivers. Earth Surface Processes and Landforms, 23(1), 31–52. https://doi.org/10.1002/(SICI)1096-9837(199801)23:1<31::AID-ESP816>3.0.CO;2-Z

Conoscenti, C., Di Maggio, C. and Rotigliano, E. (2008). Soil erosion susceptibility assessment and validation using a geostatistical multivariate approach: a test in Southern Sicily. Natural Hazards, 46(3), 287–305. https://doi.org/10.1007/s11069-007-9188-0

David, A., Bancon-Montigny, C., Salles, C., Rodier, C. and Tournoud, M. (2012). Contamination of riverbed sediments by hazardous substances in the Mediterranean context: Influence of hydrological conditions. Journal of Hydrology, 468–469, 76–84. https://doi.org/10.1016/j.jhydrol.2012.08.015

Du, P. and Walling, D. (2012). Using 210Pb measurements to estimate sedimentation rates on river floodplains. Journal of Environmental Radioactivity, 103(1), 59–75. https://doi.org/10.1016/j.jenvrad.2011.08.006

Fan, X., Shi, C., Zhou, Y. and Shao, W. (2012). Sediment rating curves in the Ningxia-Inner Mongolia reaches of the upper Yellow River and their implications. Quaternary International, 282, 152–162. https://doi.org/10.1016/j.quaint.2012.04.044

Flanagan, D. and Nearing, M. (1995). USDA water erosion prediction project: Hillslope profile and watershed model documentation, NSERL Rep. 10. Agric. Res. Serv., West Lafayette, Indiana, (July), 1995.

Golosov, V. (2000). The use of radioisotopes in the study of erosion-accumulation processes. Geomorphologia, 2, 26–33. (In Russian)

Golosov, V. (2009). Investigations of sediment deposition on the floodplains: potentials of methods and perspectives. Geomorphologia, 4, 39–44. https://doi.org/10.15356/0435-4281-2009-4-39-44. (In Russian)

Golosov, V., Belyaev, V., Markelov, M. and Kislenko, K. (2010). Dynamics of overbank sedimentation rates on floodplains of small rivers of the Central European Russia. In Sediment Dynamics for a Changing Future (Proceedings of the ICCE symposium held at The Warsaw University of Life Sciences - SGGW, Poland, 14–18 June 2010) (pp. 129–136). Warsaw: IAHS Publ 337.

Göransson, G., Larson, M. and Bendz, D. (2013). Variation in turbidity with precipitation and flow in a regulated river system-river Göta Älv, SW Sweden. Hydrology and Earth System Sciences, 17(7), 2529–2542. https://doi.org/10.5194/hess-17-2529-2013

Gray, J. and Gartner, J. (2010). Technological advances in suspended-sediment surrogate monitoring. Water Resources Research, 46(4). https://doi.org/10.1029/2008WR007063

Gray, J., Laronne, J. and Marr, J. (2010). Bedload-surrogate monitoring technologies. U.S. Geological Survey Scientific Investigations Report, 5091, 1–37.

Guillermo, F., Nicolás, R., Guerrero, M., Amsler, L. and Vionnet, C. (2017). The ADCP's bottom track capability for bedload prediction : Evidence on method reliability from sandy river applications. Flow Measurement and Instrumentation, 54(June 2016), 124–135. https://doi.org/10.1016/j.flowmeasinst.2017.01.005

He, Q. and Walling, D. (2003). Testing distributed soil erosion and sediment delivery models using 137Cs measurements. Hydrological Processes, 17(5), 901–916. https://doi.org/10.1002/hyp.1169

Hudson, P. (2003). Event sequence and sediment exhaustion in the lower Panuco Basin, Mexico. Catena, 52(1), 57–76. https://doi.org/10.1016/S0341-8162(02)00145-5

Hughes, A., Quinn, J. and McKergow, L. (2012). Land use influences on suspended sediment yields and event sediment dynamics within two headwater catchments, Waikato, New Zealand. New Zealand Journal of Marine and Freshwater Research, 46(3), 315–333. https://doi.org/10.1080/00288330.2012.661745

Karydas, C., Petriolis, M. and Manakos, I. (2013). Evaluating Alternative Methods of Soil Erodibility Mapping in the Mediterranean Island of Crete. Agriculture, 3(3), 362–380. https://doi.org/10.3390/agriculture3030362

Kidová, A., Lehotský, M. and Rusnák, M. (2016). Geomorphic diversity in the braided-wandering Belá River, Slovak Carpathians, as a response to flood variability and environmental changes. Geomorphology, 272, 137–149. https://doi.org/10.1016/j.geomorph.2016.01.002

Kiryukhina, Z. and Serkova, Y. (2000). Podsolic soils morphometric characteristics variability and the diagnostics of soil erosion. Soil Erosion and Channel Processes, 12, 63–70.

Knox, J. (2001). Agricultural influence on landscape sensitivity in the Upper Mississippi River Valley. Catena, 42(2–4), 193–224. https://doi.org/10.1016/S0341-8162(00)00138-7

Kumar, S. and Kushwaha, S. (2013). Modelling soil erosion risk based on RUSLE-3D using GIS in a Shivalik sub-watershed. Journal of Earth System Science, 122(2), 389–398. https://doi.org/10.1007/s12040-013-0276-0

Larionov, G., Kiryukhina, Z. and Samodurova, L. (1973). Determination of slope wash rates by the method of paired soil pits descriptions. Eroziia pochv i ruslovye protsessy, 3, 162–167. (In Russian)

Lawler, D., Petts, G., Foster, I. and Harper, S. (2006). Turbidity dynamics during spring storm events in an urban headwater river system: The Upper Tame, West Midlands, UK. Science of the Total Environment, 360(1–3), 109–126. https://doi.org/10.1016/j.scitotenv.2005.08.032

Leenaers, H. (1991). Deposition and storage of solid-bound heavy metals in the floodplains of the River Geul (the Netherlands). Environmental Monitoring and Assessment, 18(2), 79–103. https://doi.org/10.1007/BF00394972

Lefrançois, J., Grimaldi, C., Gascuel-Odoux, C. and Gilliet, N. (2007). Suspended sediment and discharge relationships to identify bank degradation as a main sediment source on small agricultural catchments. Hydrological Processes, 21(21), 2923–2933. https://doi.org/10.1002/hyp.6509

Märker, M., Moretti, S. and Rodolfi, G. (2001). Assessment of water erosion processes and dynamics in semi-arid regions of Southern Africa (Kwazulu/Natal, RSA, and Swaziland) using the Erosion Response Units concept (ERU). Geografia Fisica E Dinamica Quaternaria, 24(1), 71–83.

Merritt, W., Letcher, R. and Jakeman, A. (2003). A review of erosion and sediment transport models. Environmental Modelling and Software, 18(8–9), 761–799. https://doi.org/10.1016/S1364-8152(03)00078-1

Minella, J., Walling, D. and Merten, G. (2014). Establishing a sediment budget for a small agricultural catchment in southern Brazil, to support the development of effective sediment management strategies. Journal of Hydrology, 519(PB), 2189–2201. https://doi.org/10.1016/j.jhydrol.2014.10.013

Mitasova, H., Hofierka, J., Zlocha, M. and Iverson, L. (1996). Modeling topographic potential for erosion and deposition using GIS. International Journal of Geographical Information Systems, 10(5), 629–641. https://doi.org/10.1080/02693799608902101

Mizugaki, S., Nakamura, F. and Araya, T. (2006). Using dendrogeomorphology and 137Cs and 210Pb radiochronology to estimate recent changes in sedimentation rates in Kushiro Mire, Northern Japan, resulting from land use change and river channelization. CATENA, 68(1), 25–40. https://doi.org/10.1016/j.catena.2006.03.014

Motha, J., Wallbrink, P., Hairsine, P. and Grayson, R. (2004). Unsealed roads as suspended sediment sources in an agricultural catchment in south-eastern Australia. Journal of Hydrology, 286(1–4), 1–18. https://doi.org/10.1016/j.jhydrol.2003.07.006

Mouri, G., Ros, F. and Chalov, S. (2014). Characteristics of suspended sediment and river discharge during the beginning of snowmelt in volcanically active mountainous environments. Geomorphology, 213, 266–276. https://doi.org/10.1016/j.geomorph.2014.02.001

Nadal-Romero, E., Regüés, D. and Latron, J. (2008). Relationships among rainfall, runoff, and suspended sediment in a small catchment with badlands. CATENA, 74(2), 127–136. https://doi.org/10.1016/j.catena.2008.03.014

NASA LP DAAC (2015). ASTER Level 1 Precision Terrain Corrected Registered At-Sensor Radiance V003 [Data set]. NASA EOSDIS Land Processes DAAC. https://doi.org/10.5067/aster/ast_l1t.003

Notebaert, B. and Verstraeten, G. (2010). Sensitivity of West and Central European river systems to environmental changes during the Holocene: A review. Earth-Science Reviews, 103(3–4), 163–182. https://doi.org/10.1016/j.earscirev.2010.09.009

Olson, K., Gennadiyev, A. and Golosov, V. (2008). Comparison of Fly-Ash and Radio-Cesium Tracer Methods To Assess Soil Erosion and Deposition in Illinois Landscapes (Usa). Soil Science, 173(8), 575–586. https://doi.org/10.1097/SS.0b013e318182b094

Owens, P. and Walling, D. (2002). Changes in sediment sources and floodplain deposition rates in the catchment of the River Tweed, Scotland, over the last 100 years: the impact of climate and land use change. Earth Surface Processes and Landforms, 27(4), 403–423. https://doi.org/10.1002/esp.327

Owens, P., Walling, D. and Leeks, G. (1999). Deposition and storage of fine-grained sediment within the main channel system of the River Tweed, Scotland. Earth Surface Processes and Landforms, 24(12), 1061–1076. https://doi.org/10.1002/(SICI)1096-9837(199911)24:12<1061::AID-ESP35>3.0.CO;2-Y

Petticrew, E., Krein, A. and Walling, D. (2007). Evaluating fine sediment mobilization and storage in a gravel-bed river using controlled reservoir releases. Hydrological Processes, 21(2), 198–210. https://doi.org/10.1002/hyp.6183

Piper, D., Ludington, S., Duval, J. and Taylor, H. (2006). Geochemistry of bed and suspended sediment in the Mississippi river system: Provenance versus weathering and winnowing. Science of The Total Environment, 362(1–3), 179–204. https://doi.org/10.1016/j.scitotenv.2005.05.041

Poesen, J., Nachtergaele, J., Verstraeten, G. and Valentin, C. (2003). Gully erosion and environmental change: importance and research needs. CATENA, 50(2–4), 91–133. https://doi.org/10.1016/S0341-8162(02)00143-1

Renard, K., Foster, G., Weesies, G., McCool, D. and Yoder, D. (1997). Predicting soil erosion by water: a guide to conservation planning with the Revised Universal Soil Loss Equation (RUSLE). Agricultural Handbook No. 703. https://doi.org/DC0-16-048938-5 65–100.

Ritchie, J., Finney, V., Oster, K. and Ritchie, C. (2004). Sediment deposition in the flood plain of Stemple Creek Watershed, northern California. Geomorphology, 61(3–4), 347–360. https://doi.org/10.1016/j.geomorph.2004.01.009

Ritchie, J. and McHenry, J. (1990). Application of Radioactive Fallout Cesium-137 for Measuring Soil Erosion and Sediment Accumulation Rates and Patterns: A Review. Journal of Environment Quality, 19(2), 215. https://doi.org/10.2134/jeq1990.00472425001900020006x

Rommens, T., Verstraeten, G., Lang, A., Poesen, J., Govers, G., Van Rompaey, A., Lang, A., Peeters, I. (2005). Soil erosion and sediment deposition in the Belgian oess belt during the Holocene: establishing a sediment budget for a small agricultural catchment. The Holocene, 15(7), 1032–1043. https://doi.org/10.1191/0959683605hl876ra

Runkui, L., A-xing, Z., Xianfeng, S. and Ming, C. (2010). Seasonal Dynamics of Runoff-Sediment Relationship and Its Controlling Factors in Black Soil Region of Northeast China. Journal of Resources and Ecology, 1(40971236), 345–352. https://doi.org/10.3969/j.issn.1674-764x.2010.04.007

Smith, B., Naden, P.., Leeks, G. and Wass, P. (2003). The influence of storm events on fine sediment transport, erosion and deposition within a reach of the River Swale, Yorkshire, UK. In Science of the Total Environment (Vol. 314–316, pp. 451–474). Elsevier. https://doi.org/10.1016/S0048-9697(03)00068-8

Theuring, P., Rode, M., Behrens, S., Kirchner, G. and Jha, A. (2013). Identification of fluvial sediment sources in the Kharaa River catchment, Northern Mongolia. Hydrological Processes, 27(6), 845–856. https://doi.org/10.1002/hyp.9684

Tsyplenkov, A., Golosov, V. and Kobilchenko, L. (2017). Assessment of basin component of suspended sediment yeild generated due to rainfall events at small rivers in wet and dry subtropics. Inzhenernye Izyskaniia, 9, [In print]. (In Russian)

Walling, D. (1999). Using fallout radionuclides in investigations of contemporary overbank sedimentation on the floodplains of British rivers. Geological Society, London, Special Publications, 163(1), 41–59. https://doi.org/10.1144/GSL.SP.1999.163.01.04

Walling, D. and Collins, A. (2008). The catchment sediment budget as a management tool. Environmental Science and Policy, 11(2), 136–143. https://doi.org/10.1016/j.envsci.2007.10.004

Walling, D., Collins, A., Sichingabula, H. and Leeks, G. (2001). Integrated assessment of catchment suspended sediment budgets: a Zambian example. Land Degradation and Development, 12(5), 387–415. https://doi.org/10.1002/ldr.461

Walling, D., Owens, P. and Leeks, G. (1998). The role of channel and floodplain storage in the suspended sediment budget of the River Ouse, Yorkshire, UK. Geomorphology, 22(3–4), 225–242. https://doi.org/10.1016/S0169-555X(97)00086-X

Williams, G. (1989). Sediment concentration versus water discharge during single hydrologic events in rivers. Journal of Hydrology, 111(1–4), 89–106. https://doi.org/10.1016/0022-1694(89)90254-0

Zakerinejad, R. and Märker, M. (2014). Prediction of gully erosion susceptibilities using detailed terrain analysis and maximum entropy modeling: A case study in the Mazayejan plain, southwest Iran. Geografia Fisica E Dinamica Quaternaria, 37(1), 67–76. https://doi.org/10.4461/GFDQ.2014.37.7

Received on November 20th, 2017 Accepted on November 22nd, 2017

Sergey Chalov received his M.S. and Ph.D in Fluvial Processes and Hydrology from Faculty of Geography of Lomonosov Moscow State University (LMSU) in 2004 and 2007, respectively. After received his Ph.D., he works at the Hydrology Department of Faculty of Geography. Currently, he is a Senior Researcher at Hydrology Department of Faculty of Geography of LMSU and Deputy Dean of the Faculty of Geography of LMSU for international relations. Since 2015 serves as Vice-president of the International Commission on Continental Erosion (ICCE) of International Association of Hydrological Sciences. His research interests are focused on Water resources, Fluvial processes, Environmental Hydraulics and Sedimentation with special emphasis on hydrodynamics, stream communities and biodiversity, Transboundary rivers, Sediment transport and sediment hazards.

Valentin Golosov s principal research scientist in Laboratory of Soil Erosion and Fluvial Process, Faculty of Geography Lomonosov Moscow State University (LMSU) and in Department of Landscape Ecology, Institute of Ecology and Enviromentant, Kazan Federal University. He is member of Steering Committee of International Sediment Initiative (ISI) UNESCO and World Association of Water and Soil Conservation (WASWAC), V. Golosov was President of the International Commission on Continental Erosion (ICCE) of International Association Hydrological Sciences in 2009-2013. He is member of editing board of some international scientific Journals, including Water and Soil Conservation, Journal of Agricultural Engineering and others). His research interests are focused on soil erosion, sediment and sediment-associated pollutants redistribution, sediment deposition and radioecology. V. Golosov is author of more than 200 papers published in National and International Journals and invited speaker on several International Conference and Symposium.

Anatolii Tsyplenkov is currently a PhD student at Department of Land Hydrology, Faculty of Geography Lomonosov Moscow State University (LMSU) and a junior researcher at Laboratory of Soil Erosion and Fluvial Process, Faculty of geography, LMSU. He received his MS degree in Hydrology in 2015 in the LMSU at the Department of Land Hydrology. His scientific interests are focused on sediment transport, fluvial geomorphology, soil erosion and mountain hydrology.

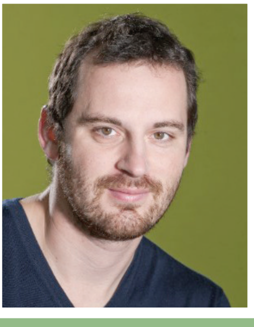

Philipp Theuring received his Master of Geography with a specialization on mass wasting slope processes from University of Jena, Germany in 2008. Following this, he worked at the Helmholtz Centre for Environmental Research in Magdeburg, Germany in a range of projects focused on the tracing of diffuse sources of fluvial sediments in Mongolia, Burkina Faso, Sweden and Russia. Since 2015 he is working as a project Manager for the development of hydrological monitoring systems at SEBA Hydrometrie in Kaufbeuren, Germany. His research interests are focused on Integrated Water Resources Management, Sediment source Tracing, Fluvial processes, Slope Processes, Transboundary rivers and Sediment transports.

Reza Zakerinejad received his M.S. and Ph.D. in Natural Resource Engineering and Physics Geography (GIS & RS) from Shiraz University in Iran and Tübingen University in Germany 2010 and 2015, respectively. After received his Ph.D., he works at the Geography department of Tübingen University until 2016 as a Postdoctoral researcher. From beginning of 2017 he got a new Postdoctoral position at the Technology University of Isfahan (IUT) in Iran. Currently, he is a senior researcher at the Faculty of Geography of the Isfahan University in Iran. His research interests are focused on soil erosion assessment, geomorphic process modelling in arid and semi-arid areas, gully erosion, land degradation, terrain analysis.

Michael Märker is Associate Professor for Physical Geography and Geomorphology at Pavia University. He obtained a PhD at Jena University, Germany in Geoinformatics and Physical Geography. Michael Märker is leading an interdisciplinary research group with major research subjects in landscape evolution, soil erosion and geomorphic processes modelling as well as digital soil mapping and soil hydrology modelling. Therefore, mainly non or minimal invasive methods and multispectral/hyperspectral remote sensing is used to assess soil, vegetation and terrain features and characteristics. Moreover, he developed and integrated innovative and integrative GIS applications for geohazard assessment and scenario analysis. Michael Märker has published more than 50 peer reviewed ISI listed papers and headed several national and international research projects.

Samokhin Mikhail A. is a researcher from Lomonosov Moscow State University. He get his phD in 2006 on Hydrology with a focus on river water level assessment and prediction. He is an expert in on-site river research technologies.

Alexander Zolotokrylin[1], Elena Cherenkova[1]*,
[1]Institute of Geography, Russian Academy of Sciences, Staromonetny per., 29, Moscow, Russia, 119017
*** Corresponding author:** cherenkova@igras.ru

SEASONAL CHANGES IN PRECIPITATION EXTREMES IN RUSSIA FOR THE LAST SEVERAL DECADES AND THEIR IMPACT ON VITAL ACTIVITIES OF THE HUMAN POPULATION

ABSTRACT. Seasonal regional features of the daily precipitation extremes were studied based on Russian meteorological stations datasets for the period of 1991-2013 compared to the 1961-1990 climate baseline conditions. Precipitation extreme changes were assessed for the most vulnerable regions of Russia with high population density, where precipitation extremes result in negative impacts on the environment and human activities. It was found that the frequency of precipitation extremes in winter and in spring for the period 1991-2013 significantly increased, by 20-40% at the average, in most parts of the case study area. Due to positive trends in daily precipitation extremes changes which was revealed for the winter and spring periods (not exceeding on average 0.2 mm/day/decade), the risks of catastrophic spring floods have been analysed, especially in the areas with a higher recurrence rate of dangerous floods, i.e. - the South Urals region and the Altai region. Strong positive trends of extreme precipitation changes were observed in the Russian Far East region. It indicates higher risk of summer rain floods in the Amur River basin. A significant impact on human activities and in particular population health is associated with revealed trends in hydrological cycle changes that are not relevant to typical meteorological and hydrological regimes. The significant increase of the frequency of extreme summer precipitation events in the Central Chernozem region of European Russia in the period of 1961-2013 was accompanied by the leptospirosis disease incidences.

KEY WORDS: precipitation extremes; climate change; flood; waterborne disease; health consequences; Russia

CITATION: Alexander Zolotokrylin, Elena Cherenkova (2017) Seasonal changes in precipitation extremes in Russia for the last several decades and their impact on vital activities of the human population. Geography, Environment, Sustainability,
Vol.10, No 4, p. 69-82
DOI-10.24057/2071-9388-2017-10-4-69-82

INTRODUCTION

Continued Global Warming affects all sides of Russian population vital activities. Its consequences may be both positive and negative. The term Vital Activity refers to the population ability to act vigorously and to rest, as well as to preserve the health in the course of creating conditions for existence and development that are closely interrelated with the environment and social realities.

A frequency and an intensity of precipitation extremes is the one among many factors, affecting on the population vital activity. Winter precipitation extremes increase snow storage and provide conditions for dangerous spring floods. Precipitation extremes in off-season and summer periods often cause catastrophic floods in some areas increasing the risks for life and for industrial and social infrastructure operation. They critically affect water supply, waste water, and storm water drain facilities. Moreover, this effect acts stronger for aging infrastructure.

Water supply and sewage systems become not able to perform their functions during heavy precipitation, and begin to pose a threat for environment and human health because they turn to sources of significant chemical and biological contamination for ecosystems, water bodies and soils due to discharges and overloads. Sometimes such a contamination can be irreversible and can affect nearby areas.

On numerous occasions, precipitation extremes lead to injuries and loss of life, i.e. can directly affect human health. Health effects may also occur after extreme events: a person may be engaged in health risk activities, both during infrastructure recovery and territory cleaning after floods.

Annual average number of destructive weather and climate events in Europe for the period from 1998 to 2007 increased by about 65% (EEA 2008). According to the same source, the total amount of losses caused by weather and climate events, for the period 1980-2007 increased from less than 7.2 billion Euros at an average for the decade (1980-1989) to about 13.7 billion Euros (1998-2007).

With regard to social consequences, according to the information from the database of emergencies CRED (EM-DAT 2009) (Center for Research on the Epidemiology of Disasters) and in terms of the Epidemiology of Disasters, it was shown that about 40 million people needed health services and satisfaction of basic needs related to survival, such as safe shelter, medical care, safe water supply and sanitary measures for the past 20 years. This number of persons exceeds eight million persons who suffered for the past two decades (1970-1990) by about 400%.

Limited data on floods resulting from several epidemiological studies showed that the highest mortality is associated with drowning, heart attacks, hypothermia, injuries and traffic accidents (Meusel et al. 2004). Studies on long-term flood impacts on health were not conducted (WHO Regional Office for Europe 2005).

Heavy rainfalls often precede waterborne disease outbreaks in Europe (Miettinen et al. 2001). However, it is not possible to extrapolate the consequences of these phenomena in terms of climate (McMichael et al. 2004).

Targeted studies on extreme precipitation and floods influences on population health were conducted in the USA (USGCRP 2016). It was proved that extreme precipitations and runoff cause waterborne disease outbreaks (Curriero et al. 2001). Therefore, a forecast of long-term trends in precipitation is important to assess the expected risks of disease outbreaks. Precipitation extremes cause disease outbreaks due to contamination of surface and underground waters. A time lag of outbreaks is about a month for contaminated surface water, and two months for groundwater.

Another study (Alderman et al. 2012) presents a detailed review of works of 2004-2011 analyzing quantitative relationships between floods and human health in the

USA. This work revealed short-term and long-term consequences of flood influence on human health and their dependence on flood characteristics and population vulnerability. It demonstrated that the long-term consequences cannot be fully explained yet. In the first year after the flood, mortality rates can increase essential, the risk of epidemiological disease outbreaks in the areas of population movement can increase as well.

An analysis of waterborne disease outbreaks, depending on the frequency, intensity and duration of extreme weather incidents related to precipitations for the period 1910-2010, showed that the outbreaks were preceded by heavy rainfalls and floods in 55.2 and 52.9% of extreme weather incidents (Cann et al. 2013). Most of the outbreaks were caused by Vibrio spp. (21.6%) and Leptospira spp. (12.7%) pathogens due to contamination of potable water storages.
Various aspects of the methodology to identify precipitation extremes and to enable their simulation by global climate models were discussed in many studies (for instance, (Allan and Soden 2008; Groisman et al. 1999; Leander et al. 2014; Kiktev et al. 2003; Zolina and Bulygina 2016)). Precipitation extreme changes under the Global Warming conditions were examined worldwide and locally in the numerous studies (eg, (Alexander et al. 2006; Frich et al. 2002; Groisman et al. 2005; Klein Tank and Können 2003; Zolina et al. 2009)). It was found that in general the intensity of precipitation extremes in Russia grew for the period from 1966 to 2012 what increased the risk of flood incidents (Zolina and Buligina 2016). An increasing number of days with precipitation exceeding the 95% percentile in winter was found at stations of European Russia and Western Siberiain for the 1977-2006 period (Bulygina et al. 2007). According to observations for the 1966–2010 period, the maximal snow cover depth rose in the large parts of Western and Eastern Siberia, on the coast of the Okhotsk Sea and in the southern Russian Far East and in the central and north-eastern regions of the European Russia (Bulygina et al. 2011). On the other hand, the number of medium and heavy snowfalls increased in the east of the European Russia and in the west of Siberia and reduced in the northeast of Siberia (Borzenkova and Shmakin 2012).

The objective of this exploration is to study regional peculiarities of the changes in characteristics of precipitation extremes, increasing the risk of floods and waterborne diseases for the modern warming period of 1991-2013 compared to the 1961-1990 climate norms. The peculiarity of the study is that in addition to general assessments for the whole territory of Russia, analysis of the changes was conducted in the most sensitive areas with high population density, where precipitation extremes lead to negative consequences for the environment and human vital activities.

DATA AND METHODOLOGY

The objective of the study is in assessment of changes in seasonal characteristics of precipitation extremes in Russia for the modern warming period of 1991-2013 compared to the 1961-1990 climate norms and the evaluation of their trends for the 1961-2013 period. It is suggested to analyze characteristics of precipitation extremes in the regions with increased incidents of floods and waterborne diseases.

In this paper, we analyze total daily precipitation extremes in the territory of Russia allocated by daily observations on the base of 95% percentile value and calculated for each meteorological station per season for the period 1961-1990 (threshold value). The following seasonal characteristics of precipitation extremes were calculated for each year from 1961 to 2013 based on climate records of daily precipitation totals from 527 meteorological stations in Russia (http://meteo.ru/): (1) average daily precipitation totals exceeding the threshold value (mm/day); (2) frequency of daily precipitation total exceeding the threshold value. These annual characteristics were averaged for the climate periods of 1961-1990 and 1991-2013. Time series with gaps not exceeding 10% were accepted for consideration. The significance of changes was estimated at 95% (Student's t-test). In addition, climatic trends of the same characteristics were estimated for the 1961-2013 period. As for the linear trend coefficients, we refer to the time regression. The statistical significance of trends was evaluated according to the method described in the study (Seber 1977). Our study was focused on detection of number of stations: (1) with significant linear trend coefficients for the 1961-2013 period; (2) with significant changes of precipitation extreme characteristics, where significant increase of frequency and intensity of seasonal precipitation extremes was observed in the period between 1991 and 2013 compared to the climate norm. In spring and summer, the population of Russia is more vulnerable to waterborne diseases. In addition to spring and summer seasons the changes in precipitation extreme characteristics were studied for winter, because spring floods in regions with a stable snow cover are dependent essential on quantities of winter precipitations.

Precipitation extreme changes were analyzed throughout the country territory, which includes the main settlement and economic development area of Russia with the highest population density of 10-100 person per square km, as well as with lightly and low populated areas with a density of 1-10 person/km^2 and below 1 person/km^2 respectively. The most densely populated Russian territory occupies only 1/5 of the whole area of the country, however more than 4/5 of the population is living there. The major part of this territory is located in the European area of Russia. The natural conditions of population vital activities in the most populous parts are comfortable (favorable) for living and are divided into three zones depending on the degree of comfort (Zolotokrylin et al. 2012). The rest of the area, including mountain landscapes is inhabited very poorly and some places are unsettled at all. Four most uncomfortable areas for living are located there. The discomfort increases towards the North (Zolotokrylin et al. 2012).

Zoonotic diseases are infectious and helminthic diseases that exist in natural ecosystems due to persistent pockets of infection and invasion, supported by wild animals. Waterborne diseases include the following bacterial infections: (1) tularemia (disease agent – Francisella tilarensis); (2) leptospirosis (disease agent – leptospira from Spirochaetaceae family). Parasitic helminthic infections hold a specific place, they include: (3) diphyllobothriasis (disease agent is a parasitic warm tapewarm, of the Genus Diphllbothrium, intermediate hosts are fresh-water maxillopods of the Genus Cyclops and Diaptoms, and fishes; (4) opisthorchiasis (disease agent is a parasitic trematode Opisthorchisfelineus, intermediate hosts are fresh-water shell fish Bithynia Leachi and fishes; (5) clonorchiasis (disease agent is a trematode Clonorchis sinensis, intermediate hosts are shell fishes); (6) paragonimosis (disease agent – tape fluke Paragonimus westermani, intermediate hosts are shell fishes and crawfishes). Infectious human diseases, including transmission ones (i.e., transmitted by vectors), are distributed throughout the whole territory of Russia (Medico-geographical Atlas 2015). Pathogens and vectors of zoonotic diseases are the part of natural ecosystems. They circulate within the systems, regardless of human species, and pose a serious threat to a human health. Current climate changes lead to transformation of their distribution conditions and growing of the numbers of risk factors (Second Assessment Report 2014). In this connection in the paper we present the results of studies for regions with frequent incidents of spring and summer rain floods in the densely populated part of Russia as well as for the regions with high number of incidents of waterborne zoonotic infectious and helminthic diseases. Note that due to latent disease progression the impact of the observed extremes on the incidents of the discussed diseases can be evaluated only indirectly. The characteristics of precipitation extreme changes were considered, taking into account a spatial distribution of incidents of dangerous floods throughout the territory of Russia (Map: Incidents of dangerous river floods and snow-melt floods 2008). Also, the selected characteristics were analyzed using information on the spatial distribution of water-borne zoonotic diseases throughout the territory of Russia (Map: Sanitary and environmental assessment of the territory of Russia 2008; Medico-geographical Atlas 2015).

RESULTS AND DISCUSSION

The analysis of the spatial distribution of the daily precipitation extreme frequency for the 1991-2013 period compared to the 1961-1990 period showed that the winter precipitation extreme frequency increased in most parts of Russia. The number of meteorological stations with significant changes of the winter precipitation extreme frequency is 33.3% out of the total quantity of the examined stations (Fig. 1 a). The growth of precipitation extremes prevailed in the areas with the highest population density. Widespread areas of most homogenous changes in the daily precipitation extremes in winter were detected in the West and the East of Russia. Statistically significant increase by 20-40% compared to the norm was observed in the central part of European Russia. Note that the same increase of precipitation extremes was recorded by the meteorological stations located on the banks of the great Siberian Rivers Yenisei and Lena. At the same time, a significant loss in the precipitation extreme frequency, by 40% in average was observed on the coast of the Arctic and the North-East of Russia (including the Chukotski Peninsula).

As well as in winter, increased daily precipitation extremes prevailed in spring throughout the territory of Russia for the 1991-2013 period compared to 1961-1990 (Fig. 1 b). The number of meteorological stations with significant changes of the winter precipitation extreme frequency is 31.1% out of the total quantity of the examined stations. A spatial structure and values of precipitation extreme frequency in winter and in spring are well correlated (Fig. 1a and 1b respectively). The spatial distribution of precipitation extreme frequency in spring outstands with the shift in the area of significant frequency increase from the center of European Russia to its eastern part. At the same time, the most significant growth by 20-40% (as in winter) was observed in the eastern part of European Russia. Perhaps the most significant difference between the winter and the spring situations is that the loss in frequency of precipitation extremes in the north east of Russia (including the Chukotka Peninsula) in the 1991-2013 winter period gave a way to a slight increase in the spring. The obtained results show not only the dynamic of changes in precipitation extreme frequency but also indicate that the peaks of snow water equivalent throughout the Russia territory were achieved in the 1991-2010 period (see Fig. 5a in the paper by Bulygina with co-authors (Bulygina et al. 2011) for the 1966-2010 period).

It was revealed that the spatial pattern of daily precipitation extreme frequency in summer was different than winter and spring one. The number of stations where significant changes of precipitation extreme frequency were observed in summer reduced to 19.6% as compared to the winter period (Fig. 1 c). In contrast to winter and spring, when positive changes of precipitation extreme frequency were substantially prevailed, 47% of significant changes were positive in summer time, but 53% of the ones were negative. On the other hand, the positive frequency changes in the most densely populated territory of Russia prevailed at most stations in summer as well as in winter. However, these changes were not statistically significant in general. The number of stations with significant positive changes of the frequency decreased on the Arctic coast and in the north eastern part of Russia, with the exception of the Chukotski Peninsula.

Thus, the frequency of precipitation extremes for the period of 1991-2013 compared to 1961-1990 significantly increased in winter and spring. This occurred both in sparsely and in densely populated regions of Russia. The revealed changes affected the growth of snow cover (Bulygina et al. 2011) and led to increasing of spring flooding risks especially in the regions with higher than usual frequency of dangerous floods. However, an uncertainty is remaining on the territory of European Russia, as the higher winter temperatures have led to a reduction in the depth of soil freezing and have improved its draining properties. In some areas in the west and in the south of European Russia the number and duration of winter thaws, during which snowmelt occurred, increased in the first decade of 21-st century compared to 1961-1990 (Krenke et al. 2012). In turn, the

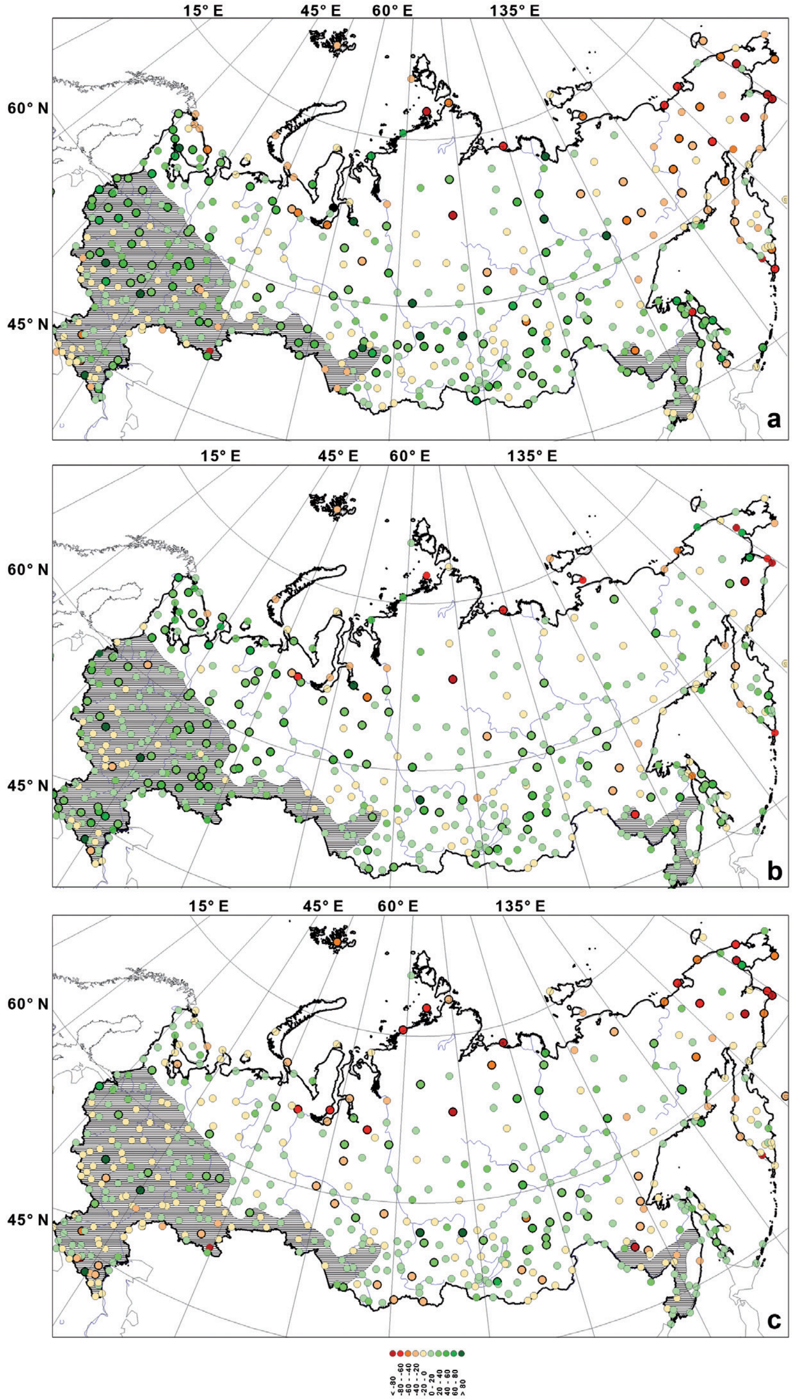

Fig. 1. Difference of daily total precipitation extreme frequency (%) in winter (a), in spring (b) and in summer (c) for the period of 1991-2013 compared to 1961-1990. Conditionally favorable area with the highest population density (4/5 of the Russia's population) is shaded (source: National Atlas of Russia 2008c). Significant differences are denoted with the black border of colored symbols

loss of water storages in the snow cover in early spring enables reducing of spring flood runoff (Roshydromet second assessment report 2014).

The peculiarity of the spatial distribution of significant trend coefficients for daily precipitation extremes on the territory of Russia for the 1961-2013 period is that a positive trends were detected at two third of meteorological stations in all seasons. Thus, the number of stations with significant positive trend coefficients for daily precipitation extremes (59.4% in winter, 65% in spring, 64.4% in summer and 66.7% in autumn) exceeds the corresponding number of stations with negative trend coefficients (41.2% in winter, 35% in spring, 35.6% in summer and 33.3% in autumn). For all seasons, in most parts of the study area the steady tendency of increasing in precipitation extreme changes, not exceeding 1.2 mm/day/decade in winter, 1.5 mm/day/decade in spring, 2.7 mm/day/decade in summer and 2.4 mm/day/decade in autumn, was observed.

As shown in Fig. 2a, the negative trends of changes in winter precipitation extremes were observed mainly on the sparsely populated Arctic coast of the country, including the Chukotski Peninsula. Conspicuous is the fact that negative significant trends (from 0.2 to 0.6 mm/ day in a decade) prevail in the densely populated southern part of European Russia (especially in the basin of the Don River), affected by spring floods of mixed sources (snow and rain). According to an analysis described in the study (Roshydromet second assessment report 2014), the spring runoff of the Don River decreased to 30% for the past few decades. Reduced runoff is caused by lower water storage in snow cover by early spring thaw that is a result of not only reducing of precipitations, but also increasing number and duration of winter thaws. In summary, the full-flowing spring floods on the Don were not occurred for almost 16 years. In the other area of dangerous spring floods - the Kuban River basin - negative trends also prevailed in winter (Fig. 2a), but they were statistically non-significant.

In winter, in the area of spring snowmelt floods, located in the South Urals region, the number of stations with positive (0.1-0.2 mm/day per decade) trends and negative (0.2 mm/day per decade) trends was approximately equal (Fig. 2a). However, the positive trends (0.2 mm/day per decade) were observed mainly in the Altai region with frequent dangerous river floods on tributaries of the Ob River (once in 3 years) and in the middle reach of the Yenisei (once in 6 years). The last biggest catastrophic flood over past half of century occurred in the spring of 2014 in the Altai region, due to the simultaneous combination of rapid snowmelt and heavy precipitation fall. This resulted in an increasing risk of chemical and biological contamination of water intended for human consumption, changes in the distribution of disease vectors and rodents throughout the territory. Loss of raw water supply and its quality degradation in turn affected the efficiency of water treatment processes and the stability of distributed potable water. Increased turbidity of surface water and growth of the number of pathogens (and their indicators) resulted in additional loads for wastewater treatment plants, especially for the facilities of surface water treatment. The damage caused by the destructive floods happened in spring, 2014 in the Altai region was estimated at almost five billion Rubles. Less destructive flood compared to 2014 happened again in some areas of the Altai region in 2016.

In summer, the number of stations with a significant negative trend of changes in daily precipitation extremes for the period of 1961-2013 on the Arctic coast, including the Chukotski Peninsula, decreased in comparison with winter (Fig. 2b). However, in the same time, the number of meteorological stations with a significant negative trend (up to 0.6-1.1 mm/day per decade) increased in the south-eastern part of European Russia. There was revealed essential increase in the frequency of droughts in this region for the past few decades (Cherenkova 2013). It is important to stress that non-significant trends prevailed in the areas of most frequently repeated rainfall floods (Amur River region, Transbaikalia). Strong positive trends of

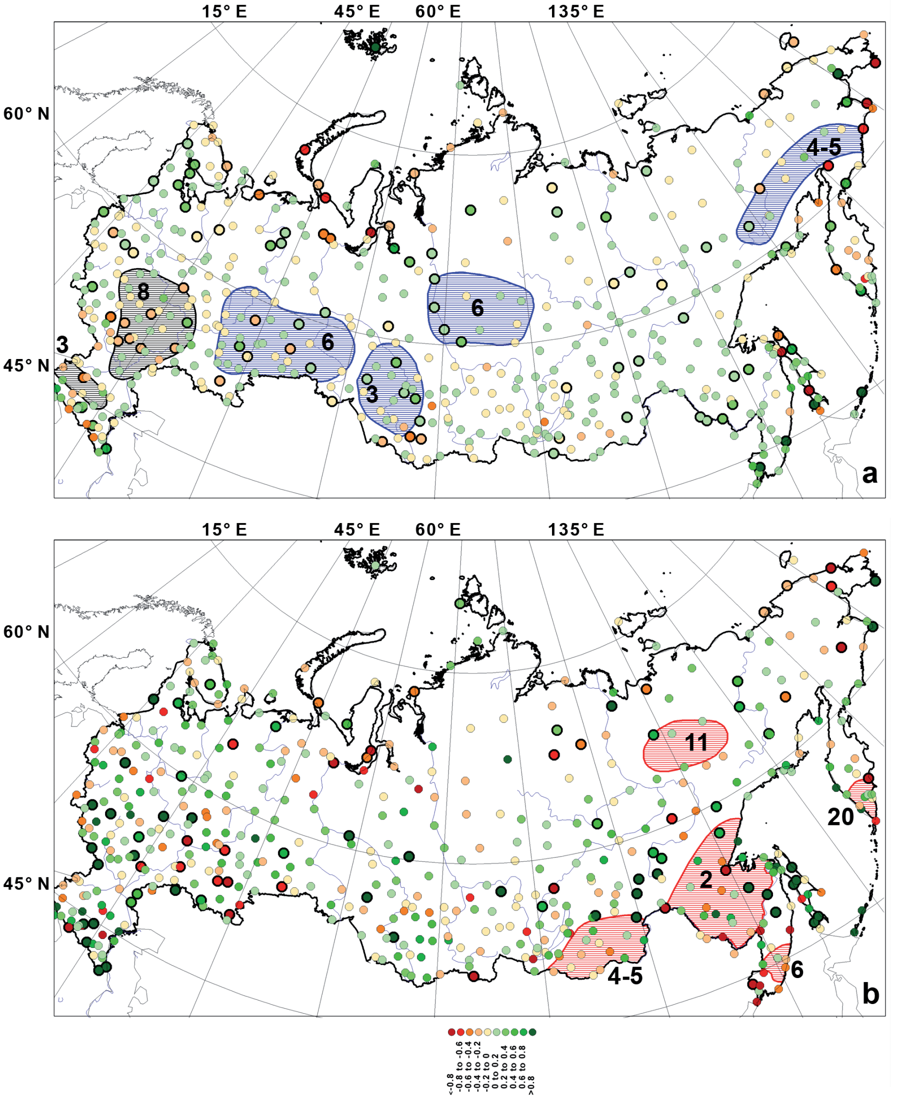

Fig. 2. Decade trends of changes in daily precipitation extremes in winter (a) and in summer (b) for the 1961-2013 period (mm/day/decade). Significant trends are denoted with the black border of colored symbols. Areas of increased frequency of dangerous floods originated by snow (marked with Blue), originated by snow and rain (mixed origin) (marked with Black). Areas of increased frequency of dangerous floods originated by rainfall are indicated with Red (source: National Atlas of Russia 2008a). A number of incidents per year are shown within or near areas

changes in precipitation extremes (increase up to 1.5-1.7 mm/day per decade) were observed in the southern part of the Russian Far Eastern of the Amur River Basin (Fig. 2b). It indicates the growing risk of floods in the region. The summer floods of 2013 spilled over vast areas of the Russian Far East and China's northeast has become one of the biggest natural disasters of the last decade - in view of duration, distribution area, casualties and economic losses (527 billion Rubles) (Danilov-Danilyan and Gelfan 2014). The abovementioned results obtained correspond to conclusions of the study (Zolina and Bulygina 2016).

It should be noted that the floods in the southern part of the Primorye Territory occur frequently in late summer - early autumn (Fig. 2b). Most of them are caused by tropical typhoons passing over the Japan Sea at this time. The last destructive flood in this area occurred under the influence of typhoons Lionrock (late August 2016) and Nam Teun (early September 2016). According to the preliminary assessment of the Khabarovsk region Administration, the flood damage amounted by 1.2 billion Rubles (http://www.primorsky.ru/news/). As consequence of the flood, many inhabited localities were flooded, internal infrastructure was destroyed, including power supply facilities, transport and waterworks. The flood caused losses of the crop and a large number of livestock. Population health risks were increased significantly due to contamination of potable water by the infiltration of pathogens. The abovementioned results in increased risks of human contacts with waterborne disease agents.

Statistically significant coefficients of the trend of daily precipitation extremes frequency in the winter accounted for nearly 40% out of the trend coefficients at all considered meteorological stations in Russia. In addition, 70.7% out of them were positive. The tendency to increase the daily precipitation extreme frequency for the 1961-2013 winter periods observed almost in the entire territory of Russia. At the same time the meteorological stations of the Chukchi Peninsula were an exception: observations at these stations showed a reduced trend in daily precipitation extremes (did not exceed two days per 10 years). The number of stations with positive significant trend of daily precipitation extreme frequency (did not exceed two days per 10 years over study area) slightly decreased in summer to 63.3% in comparison with winter in the whole territory of Russia (Fig. 3a). Positive coefficients of the trends identified in winter are kept in summer as well, in most parts of East Siberia and West Siberia and in European Russia. Note that the seasonal patterns demonstrate the consistency between the trends in the daily precipitation extremes frequency in the European part of Russia for the period of 1961-2013 and monthly precipitation in the same region for the period of warm anomalies of Northern Atlantic sea surface temperature (1995-2012) relative to its cool period (1962-1994) which were analyzed in the previous study (Cherenkova 2017).

The Fig. 3a and 3b show the areas (marked by number 1) of wooded steppe and meadow-steppe plain ecosystems of the Central Chernozem region located in the center of European Russia where incidents of bacterial infectious diseases tularemia and leptospirosis were reported. As shown in Fig. 3b, the lowest number of incidents of leptospirosis (less than 1 incident/year) for the period of 1997-2010 was observed in the Kursk and Lipetsk region, as well as in the north of the Saratov region. The annual average incidents in the same period in the Tambov region amounted to 1-5 cases/year and 5-15 cases in Belgorod, Voronezh and Penza region. The highest incidents of leptospirosis were reported in the north and east of the study area: 15-40 cases/year in Orel and Ryazan regions, and 40-80 cases/year in the Tula region and in the Republic of Mordovia. It should be noted that the highest incidents were observed in the areas with significant positive trends of the precipitation extreme frequency in summer for the period of 1961-2013. Similar to the conclusion made in the work (Sann et al. 2013) using the example of the United States, the majority of above-mentioned incidents in the regions of Russia were caused by pathogens Leptospira spp. as a result of contamination of drinking water sources.

Among other waterborne infections, only the tularemia appears in sub-boreal forest and forest-steppe essentially swamped plain ecosystems of Western Siberia (Fig. 3a, area number 2). The positive significant trend of precipitation frequency (4 day per 100 years) was revealed in observations of only one meteorological station in this region, although local summer rain floods are observed almost every year.

Negative trends of precipitation extreme frequency prevailed in the regions with frequent summer floods in the Amur region

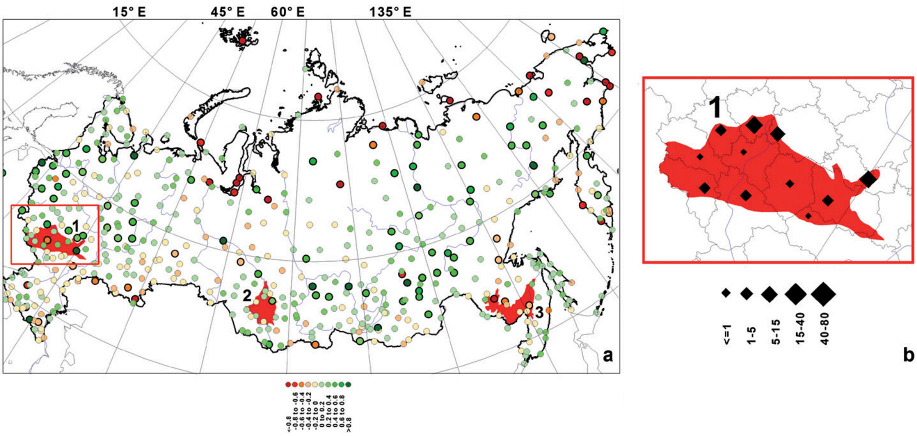

Fig. 3. Decade trends of frequency of changes in daily precipitation extremes in summer for the period of 1961-2013 (day/decade) (a). Significant trends are denoted with the black border of colored symbols. Areas with observed incidents of tularemia and leptospirosis: center of European Russia (1), south of Western Siberia (2), Russian Far East (3) are marked with Red (source: National Atlas of Russia, 2008b). The average annual number of leptospirosis incidences in European Russia for the 1997-2010 period (source: Medico-geographical Atlas 2015) is marked by rhombs (b)

(up to 3-12 day per 100 years). Lowland broad-leaved forest ecosystems of the Amur region located in Far East of Russia (Fig. 3a, area number 3), are the large center of parasitic helminthic infections, namely: (1) diphyllobothriasis; (2) opisthorchiasis; (3) clonorchiasis and (4) paragonimiasis. The agents of these diseases are parasitic worms that change two or three hosts in the process of lifecycle. In this case the last host is a human. Eating of raw, lightly salted or poor cooked fish causes human infection. Formation of the centers is caused by well warmed, low-flow shallow places, favorable for expansion of small crustaceans. That is why the negative trend of precipitation extreme frequency is not critical in these helminth centers.

CONCLUSIONS

The analysis of seasonal characteristics of the precipitation extremes for the period of 1961-2013 in Russia allocated by daily observations on the base of 95% percentile allowed to obtain the following results. The frequency of precipitation extremes in winter and spring for the period of 1991-2013 increased significantly by 20-40% on average compared to the 1961-1990 climate norms, both in sparsely and in densely populated regions of Russia. The only exception was the coast of the Arctic in winter and spring, and the north-east of Russia (including the Chukotski Peninsula) in winter. There was observed a significant decrease in the frequency of precipitation extremes in these regions, by 40% on average for the period of 1991-2013. The changes in daily precipitation extremes revealed in winter and spring in the period of 1991-2013 compared to the climate norms affected the growth of snow storages (Bulygina et al. 2011). In summer, the positive statistically insignificant changes in the frequency of precipitation extremes in the most densely populated territory of Russia prevailed at most meteorological stations.

Significant positive trends of changes in daily precipitation extremes in Russia in the period of 1961-2013 are revealed on two thirds of meteorological stations in all seasons. A steady increasing tendency of changes in daily precipitation extremes (not exceeded 3 mm/day per decade) was observed for all seasons of the year in most parts of Russia for the 1961-2013. In the same time, prevalence of essential trends to reduction of daily precipitation extremes in winter in the densely populated southern part of European Russia in the same period has resulted in lower runoff of the Don

River. Positive trends of changes in daily precipitation extremes were observed in the Altai region where dangerous river floods on tributaries of the Ob River and in the middle reach of the Yenisei River are happened frequently. In view of positive trends of changes in daily precipitation extremes revealed in winter and in spring, the risks of catastrophic spring floods (similar to the flood in the Altay region in the spring of 2014 are growing, especially in the areas with a higher recurrence rate of dangerous floods. Consequently, the risks of chemical and biological contamination of water are increased. In summer, strong positive trends of changes in precipitation extremes were observed in the southern part of the Russian Far East (in the Amur River Basin). It indicates the growing risk of floods in the region. Substantiation of the abovementioned is the summer floods of 2013, spilled over vast areas of the Russian Far East and China's northeast and caused the huge economic losses as well as the destructive flood in late August, early September 2016 in Khabarovsk region.

Increasing frequency of daily precipitation extremes in winter for the period 1961-2013 was observed almost in the entire territory of Russia. Positive coefficients of trends occurred in the winter time were kept also in the summer in the most parts of Eastern Siberia and West Siberia as well as in European Russia.

In summer the positive significant trend of the precipitation extreme frequency in the Central Chernozem region in the center of the European part of Russia in the years 1961-2013 enabled increasing of leptospirosis disease incidences. It is the result of contamination of potable water sources.

A significant threat to sustainable vital activities and in particular to the health of the Russian population is associated with return of these phenomena and with revealed trends in hydrological cycle changes that are not relevant to meteorological and hydrological regimes typical for the local area.

ACKNOWLEDGEMENTS

The study was supported by the Russian Science Foundation (project 16-17-10236 «Impact of climate changes on population vital activity in Russia («areas with specific climatic conditions»)»).

REFERENCES

Alexander L., Zhang X., Peterson T., Caesar J., Gleason B., Klein Tank A., Haylock M., Collins D., Trewin B., Rahimzadeh F., Tagipour A., Rupa Kumar K., Revadekar J., Griffiths G., Vincent L., Stephenson D., Burn J., Aguilar E., Brunet M., Taylor M., New M., Zhai P., Rusticucci M., Vazquez-Aguirre J. (2006). Global observed changes in daily climate extremes of temperature and precipitation. J. Geophys. Res., 111, D05109. doi:10.1029/2005JD006290

Alderman K., Turner L., Tong S. (2012). Floods and human health: A systematic review. Environment International, 47, pp. 37-47. doi:10.1016/j.envint.2012.06.003

Allan R., Soden B. (2008). Atmospheric warming and the amplification of precipitation extremes. Science, 321, pp. 1481–1484. doi:10.1126/science.1160787

Auld H., MacIver D., Klaassen J. (2004). Heavy rainfall and waterborne disease outbreaks: The Walkerton example. J. Toxicol. Environ. Health, A 67, pp. 1879-1887. doi:10.1080/15287390490493475

Borzenkova A., Shmakin A. (2012). Changes in the snow depth and the daily intensity of snowfall, impacting on the cost of cleaning highways in the Russian cities. Ice and snow, 2(118), pp. 59-70. (in Russian)

Bulygina O., Razuvaev V., Korshunova N., Groisman P. (2007). Climate variations and changes in extreme climate events in Russia. Environ. Res. Lett., 2(4):045020.

Bulygina O., Groisman P., Razuvaev V., Korshunova N. (2011). Changes in snowcover over Northern Eurasia since 1966. Environ. Res. Lett., 6:045204.

Cann K., Thomas D., Salmon R., Wyn-Jones A., Kay D. (2013). Extreme water-related weather events and waterborne disease. Epidemiology & Infection, 141, pp. 671-686. doi:10.1017/s0950268812001653 l

Cherenkova E. (2013). Quantitative Evaluation of Atmospheric Drought in Federal Districts of the European Russia. Izvestiya RAN. Ser. Geogr., 6, pp. 76-85. (in Russian)

Cherenkova E. (2017). Seasonal precipitation in the East European Plain during the periods of warm and cool anomalies of the North Atlantic Surface temperature. Izvestiya RAN. Ser. Geogr., 5, pp. 72-81. (in Russian)

Curriero F., Patz J., Rose J., Lele S. (2001). The association between extreme precipitation and waterborne disease outbreaks in the United States, 1948–1994. American Journal of Public Health, 91, pp. 1194-1199. doi:10.2105/AJPH.91.8.1194

Danilov-Danilyan V., Gelfan A. (2014). National disaster. Science and life, 1, pp. 32-39. (in Russian)

EEA (2008). Impacts of Europe's changing climate – 2008 indicator-based assessment. Copenhagen, European Environment Agency (Report No. 4/2008) http://www.eea.europa.eu/publications/eea_report_2008_4, accessed 7 July 2010.

EM-DAT (2009). EM-DAT International disaster database [online database]. Brussels, UniversitéCatholique de Louvain Centre for Research on the Epidemiology of Disasters (CRED) (http://www.emdat.be/database, accessed 5 April 2010).

Frich P., Alexander L., Della-Marta P., Gleason B., Haylock M., Klein Tank A., Peterson T. (2002). Observed coherent changes in climatic extremes during the second half of the 20th century. Climate Res., 19, pp. 193–212.

Groisman P., Karl T., Easterling D. Knight R., Jamason P., Hennessy K., Suppiah R., Page C., Wibig J., Fortuniak K., Razuvaev V., Douglas A., Forland E., Zhai P. (1999). Changes in the probability of heavy precipitation: Important indicators of climatic change. Climatic Change, 42, pp. 243–283.

Groisman P., Knight R., Easterling D., Karl T., Hegerl G., Razuvaev V. (2005). Trends in intense precipitation in the climate record. J. Clim., 18, pp. 1326–1350.

Kiktev D., Sexton D., Alexander L., Folland C. (2003). Comparison of modeled and observed trends in indices of daily climate extremes. J. Clim., 16, pp. 3560–3571.

Klein Tank A., Können G. (2003). Trends in indices of daily temperature and precipitation extremes in Europe, 1946–99. J. Clim., 16, pp. 3665–3680.

Krenke A., Cherenkova E., Chernavskaya M. (2012). The stability of the snow cover in Russia under climate change. Ice and snow, 1(117), pp. 29-37. (in Russian)

Leander L., Buishand T., Klein Tank A. (2014). An alternative index for the contribution of precipitation on very wet days to the total precipitation. J. Clim. 27, pp. 1365-1378. doi: http://dx.doi.org/10.1175/JCLI-D-13-00144.1

McMichael A., Woodruff R., Hales S. (2006). Climate change and human health: present and future risks. Lancet, 367(9513), pp. 859–869. doi: http://dx.doi.org/10.1016/S0140-6736(06)68079-3

Medico-geographical Atlas of Russia «Natural Focal Diseases» (2015). Edited by Malkhazova S.M. Faculty of Geography, Lomonosov Moscow State University. Moscow. 208 p. (in Russian)

Meusel D., Menne B., Kirch W. (2004). Public health responses to extreme weather and climate events – a brief summary of the WHO meeting on this topic in Bratislava on 9–10 February 2004. J. Public. Health, 12(6), pp. 371.

Miettinen I., Zacheus O., von Bonsdorff C., Vartiainen T. (2001). Waterborne epidemics in Finland in 1998–1999. Water Sci. Technol., 43(12), pp. 67–71.

National Atlas of Russia (2008a). Map: Frequency of dangerous floods. Scale 1:40,000,000. Federal Agency of Geodesy and Cartography. Moscow, 2:196-197. (in Russian)

National Atlas of Russia (2008b). Map: Sanitary and ecological assessment of Russia. Scale 1:45,000,000. Federal Agency of Geodesy and Cartography. Moscow, 2:446. (in Russian)

National Atlas of Russia (2008c). Map: Zoning the territory of Russia on the natural conditions of life. Scale 1:45,000,000. Federal Agency of Geodesy and Cartography. Moscow, 3:172. (in Russian)

Roshydromet second assessment report on climate change and its consequences in the Russian Federation (2014). The Federal Service for Hydrometeorology and Environmental Monitoring of Russia. Moscow, 1009 p.

Seber G. (1977). Linear Regression Analysis. New York: John Wiley and Sons, 496 p.

Shmakin A. (2010). Climatic characteristics of snow cover of Northern Eurasia and their variation in the last decades. Ice and snow, 1(109), pp. 43–57. (in Russian)

USGCRP (2016). The Impacts of Climate Change on Human Health in the United States: A Scientific Assessment. Crimmins A, Balbus J, Gamble JL, Beard CB, Bell JE, Dodgen D, Eisen RJ, Fann N, Hawkins MD, Herring SC, Jantarasami L, Mills DM, Saha S, Sarofim MC, Trtanj J, Ziska L, Eds. U.S. Global Change Research Program, Washington, DC, 312 pp. doi:http://dx.doi.org/10.7930/J0R49NQX

WHO Regional Office for Europe (2005). Health and climate change: the now and how. A policy action guide. Copenhagen, WHO Regional Office for Europe.

Zolina O., Simmer C., Belyaev K., Kapala A., Gulev S. (2009). Improving estimates of heavy and extreme precipitation using daily records from European rain gauges. Journal of Hydrometeorology, 10, pp. 701–716.

Zolina O., Bulygina O. (2016). Current climatic variability of extreme precipitation in Russia. Fundamental and Applied Climatology, 1, pp. 84-103. (in Russian)

Zolotokrylin A., Krenke A., Vinogradova V. (2012). Zoning the territory of Russia on the natural conditions of life. Moscow: GEOS. 156 p. (in Russian)

Received on October 27th, 2017 Accepted on November 22nd, 2017

Alexander N. Zolotokrylin is DSc. in Geography, Professor, Chief Scientist at the Department of Climatology of the Institute of Geography of the Russian Academy of Sciences. He is a well-known Russian climatologist-geographer. The main areas of expertise include the influence of climate changes on human life conditions, desertification, polar climatology and response of vegetation on climate change using remote sensing data. He is the author of more than 210 scientific publications, including monographs, head of the scientific projects supported by Russian foundations. The most popular publications of Prof. Zolotokrylin are monograph "Climate desertification", 2003 (in Russian) and joint monograph «Zoning by natural living conditions in Russia», 2012 (in Russian).

Elena A. Cherenkova is a Senior Researcher at the Department of Climatology, Institute of Geography, RAS. She graduated in 1987 from the applied Mathematics at the Lomonosov Moscow State University. In 2009 she received the PhD in Geography (Thesis "Changing of humidification of sub-boreal plain landscapes of Russia in the 20th and 21st centuries"). Her research is focused on long-term dynamics of extreme meteorological events under changing climate, change of hydrological regimes and climatology of semi-arid regions.

Rhoda Olanrewaju[1], Buku Ekiotuasinghan[1], Godwin Akpan[1*]
[1]Department of Geography and Environmental Management, University of Ilorin, P.M.B.1515, Ilorin, Nigeria
*** Corresponding author:** godisgood885@gmail.com

ANALYSIS OF RAINFALL PATTERN AND FLOOD INCIDENCES IN WARRI METROPOLIS, NIGERIA

ABSTRACT. Climate change has led to changes in the known patterns of rainfall and other climatic variables as well as increase in the frequency and magnitude of natural disasters including floods in different parts of the world; and flood is indeed a global environmental issue that had destroyed lives and property amidst other untold hardships. The study examined rainfall characteristics in Warri metropolis for the past 30 years (1986-2015) vis-à-vis the flood situation in the metropolis; as well as the factors responsible and adaptation strategies to flood in the area. Dividing the study area into four zones after Sada (1977), the researchers collected rainfall data from the archives of Nigerian Meteorological Agency; 268 copies of questionnaire and oral interview were used. The result of the correlation analysis performed showed a negative relationship of -0.156 between rainfall and time (years), this implies that rainfall is decreasing over time. The trend line regression equation Y=243.75-0.4572X, confirms that rainfall in Warri Metropolis is decreasing at the rate of -0.45 per year. However, the p-value 0.412 is greater than 0.05, hence, the trend is not statistically significant at 95% level of confidence. It was discovered that rainfall, absence of drainage and poor urban planning practices (as factor 1) contributed 51.09% while overflowing of rivers, blocked/poor drainage and untarred roads (as factor 2) contributed 44.10% variance to flood occurrence in the metropolis. Recommendations given included continual monitoring and study of rainfall characteristics and other climatic data and dissemination of such information for planning purposes; construction of integrated drainage system and river rechannelisation, legislation against dumping of refuse on roads and drainages; proper urban planning including implementation of the metropolitan urban drainage master plan.

KEY WORDS: Rainfall, flood, climate change, disaster and metropolis

CITATION: Rhoda Olanrewaju, Buku Ekiotuasinghan, Godwin Akpan (2017) Analysis of rainfall pattern and flood incidences in warri metropolis, nigeria. Geography, Environment, Sustainability, Vol.10, No 4, p. 83-97
DOI-10.24057/2071-9388-2017-10-4-83-97

INTRODUCTION

The earth's climate has not been static since inception but the rapidity, frequency and severity of the consequences of climate change in the last few decades are however, alarming (NRC, 2010). According to Afangideh, et al. (2013), the current and projected manifestations of climate change include global warming (increase in temperature), rise in sea level, shifting of global climate zones, changes in the intensity, quality, duration and general pattern of rainfall leading to drought, desertification, and flooding; melting of glaciers/polar ice and increased incidences and severity of extreme weather events, among other effects.

As different parts of the world experience different types of extreme weather events and disasters, the one that cut across all continents is flood. The term flood as defined by Sada and Odemerh (1988) represents high rate of water discharge which often lead to inundation of land adjacent to stream often caused by intense or prolong rainfall. Zbigniew et al (2013), however went further to describe flooding as overflowing of the normal confines of a stream or other body of water or accumulation of water over areas that are not normally submerged. It could then mean a flow of water over areas which are habitually dry which can be resulted from storm surge, melting of glacier, snow melt or heavy rainfall. Increasing flood risk is now being recognized as the most important threat from climate change in most parts of the world (Afangideh, et al., 2013). This view was equally supported by Bhanumurthy and Behera (2008) which asserted that flood is the most common and widespread of all natural disaster, accounting for about 46% of fatalities.

On the global scale flood is said to regularly claim over 20,000 lives per day and adversely affected about 75 million people (Smith and Ward, 1998). The United Nations Disaster Relief Coordination (UNDRC, 1976) stated that flood accounted for second only to typhoon and tidal waves as causes of mortality. To corroborate this, the study of Efe and Mogborukor, (2010), showed that over 173,000 deaths occurred from various flood occurrences between 1947 and 1970. The European space agency (ESA, 2004) reported further that flood incidences accounted for almost 55% of all disasters in the year 2004, adding that flood incidences have increased by 10-folds in the last 5 decades from only 206 cases in 1990 to about 1,900 incidences in 2005, with each incident having different levels of severity among continents and Asia being the worst hit (Raji, Adeniyi and Odunuga, 2014).

Flooding is a major problem in African cities. According to Action Aid (2006) projection, by 2030 majority of Africa's population will live in urban areas. Climate change will increase the vulnerability level of the urban poor throughout Africa because urbanization aggravates flooding by its paved surfaces which hinder water percolation and hence increase surface runoff.

Nigeria the giant of Africa has witnessed several flood disasters in different parts of the country, both in coastal, inland, rural and urban areas; they include those of Ibadan, Yobe, Akure, Kafachan, Markudi, Lagos, etc. However, the Niger Delta has been recognized by far the largest single area subject to annual flooding in Nigeria (see Fig. 1). This is because of its disposition as flat, low-lying swampy area of alluvial deposition across which the tributaries of the Niger meander, (Agbonkhese et al. 2014).

Flood is arguably the most common and severe natural disaster in the Warri Metropolis like most coastal cities in the Niger Delta, it has become an annual environmental problem during every rainy season. Umuteme and Orusi (2012) reported that in July 2012 over 300 people were render homeless in Warri due to an early morning rain that lasted for several hours (Fig. 1). According to Efe and Mogborukor (2010), the 4th – 6th August 2002 flood in Warri which resulted from rainfall submerged several houses, workshops in the metropolis. It reoccurred in the following years leading to the destruction of properties worth over 3.6 million of naira and rendering over 3,250 people homeless. Other notable incidences of floods recorded in the metropolis included those of 1999, 2000, 2002, 2003, 2005, 2006 and 2007.

Fig. 1. Flood incident in Warri (Information Nigeria 2012)

Since the major causal factor of Warri flood is heavy rainfall as observed above, this study aimed at analyzing the pattern of rainfall characteristics and flood incidences in Warri metropolis with the view to providing lasting solution to flood menace in the city through various adaptive and mitigation strategies that can be adopted to cope with flood challenges in the study area.

THE STUDY AREA

Warri Metropolis is geographically located between 5°30′ N to 5°35′ N and 5°29′ E to 5°48′ E. The study area is bounded to the north by Okpe and Sapele Local Government Areas; to the southern axis by Warri South West and the Atlantic Ocean; to the east, the metropolis is bounded by Ughelli South Local Government Area while it shares its western boundary with Warri North Local Government Area (Fig. 2).

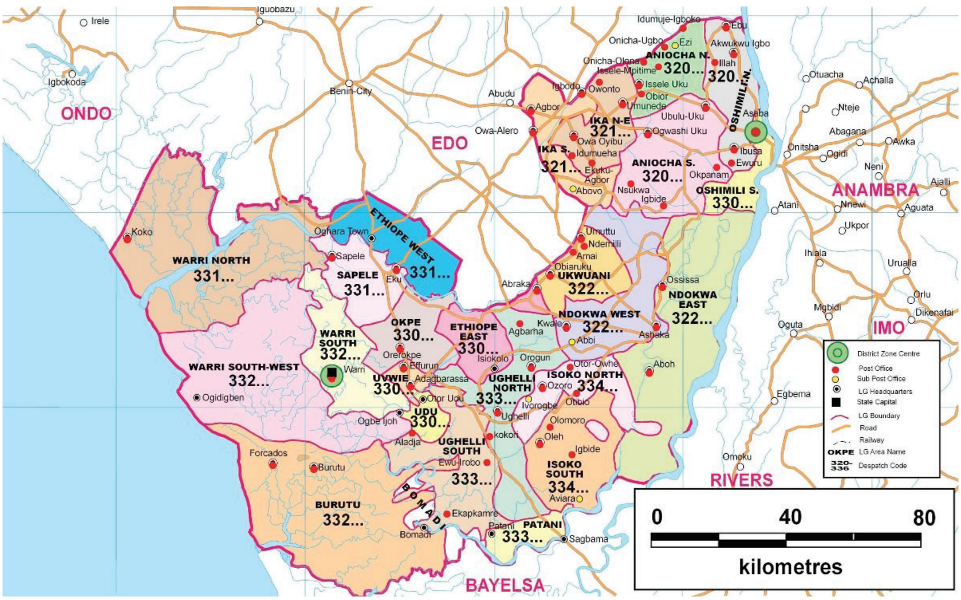

Fig. 2. Study Area (Ministry of Land and Survey, Delta State/Google)

Warri is directly underlained by a quaternary formation, the Somebreiro-Warri Deltaic Plan Sand consisting of fine and coarse-grained unconsolidated sediments – sands, peats, gravel, etc. The rock types that formed the geology of this area are the sedimentary rocks with silty clay and sand on the top (4-6m), followed by a thick layer of about 17m, the silt then become coarse and pebbly at that depth below. Having a flat terrain devoid of hills and mountains, with average height of about 6m above sea level (Olabaniyi and Efe, 2007); the area is traversed by networks of many creeks, rivers and streams all draining water into the Atlantic Ocean.

Warri is characterized with the tropical equatorial type of climate and just like most cities of the Niger Delta is influenced by two air masses namely the southwest monsoon wind and the northeast trade wind. The former is responsible for the long rainy season experienced in the metropolis lasting from March to October. The latter ushers in short dry season in the city which lasts from November to February. The city has an annual total rainfall of about 3000mm and temperature of 280C Mean monthly rainfall value is as low as 20.4mm in January and as high as over 499.1mm in September. Warri city enjoys two rainfall peaks every year. The first is observed in the month of July and the second occurs in September with a short period of dry spell in between termed August break. The metropolis mostly experiences the convectional type of rainfall, with a relative humidity that oscillates between 80%-90% as well as dense cloud cover (Obafemi, et al, 2012; Abotutu and Ojeh, 2013; Aderoju, et al. 2014).

MATERIALS AND METHODS

Rainfall data from 1986-2015 were collected from the Nigeria Meteorology Agency (NIMET), Warri station. Rainfall characteristics used include daily, monthly and yearly amount of rainfall, intensity, frequency, variability, trends, return period and fluctuation of rainfall. Data on frequency of flood incidences was sourced from available literature while questionnaire and oral interview were employed to collect data on residents' perception and understanding of causes of flood in the area and their mitigation strategies.

In order to ensure widest coverage of questionnaire administration, the Warri Metropolis was zoned into four areas. This is taken after Sada's (1977) four physical divisions in most developing cities in Nigeria. Consequently, the four zones-designates Warri Metropolis is divided into for this study were; (a) Government Reserved Areas (GRA)/ Bendel Estate; (b) Warri Core; (c) Effurun; and (d) Udu.

Equal number of respondents (67) was selected from each zone; residents in the 1st street and every 3rd street was systematically picked in this consecutive order in all the zones until the required sample size was derived.

Coefficient of variation was used to determine the percentage deviations in rainfall values for the study period; it showed the degree of variability in the monthly and yearly means of rainfall. To calculate the intensity of rainfall, both yearly and a monthly run of 30 years, the formula below (1) was adopted after Afangideh, et al (2013);

$$\text{Intensity of rainfall} = \frac{\text{annual rainfall amount (mm)}}{\text{annual rainfall duration (days)}} \quad (1)$$

The Simple Linear Regression analysis method was used to determine the patterns/trends of rainfall in the study area. Igweze et al. (2014) and Ologunorisa (2006) had adopted this tool in similar studies. While factor analysis was employed to assess the dominant factors responsible for flooding in the area.

RESULTS AND DISCUSSION

Monthly and Annual Rainfall Intensity in Warri Metropolis

Table 1 shows the monthly rainfall intensity for the period of study, and the results show that the month of July recorded the highest rainfall intensity (21.10mm/d, i.e. per day) in the study area. This result indicates that the month with the highest total monthly rainfall is also the month with the highest rainfall intensity in the study area. The followings were the next highest monthly intensities, the months of September, August and April with 18.95mm/d, 18.18mm/d and 17.02mm/d respectively. On the other hand, the month of December recorded the lowest rainfall intensity (9.61mm/d), followed by the months of November and January with 10.23mm/d and 11.44mm/d respectively (Fig. 3).

Trend/Pattern of Rainfall in Warri Metropolis

The trend in rainfall amount over time was determined using regression analysis (table 3). The p-value for the rainfall slope of 0.412 obtained is greater than 0.05, hence, there is no statistically significant relationship between rainfall and year at 95% confidence level for the 30 years period of study. The R-squared statistic shows that the model, as

Table 1. Case studies and used methods

Months	Rainfall Intensity (mm/d)
January	11.44
February	13.59
March	13.82
April	17.02
May	16.33
June	16.57
July	21.10
August	18.18
September	18.95
October	16.60
November	10.23
December	9.61

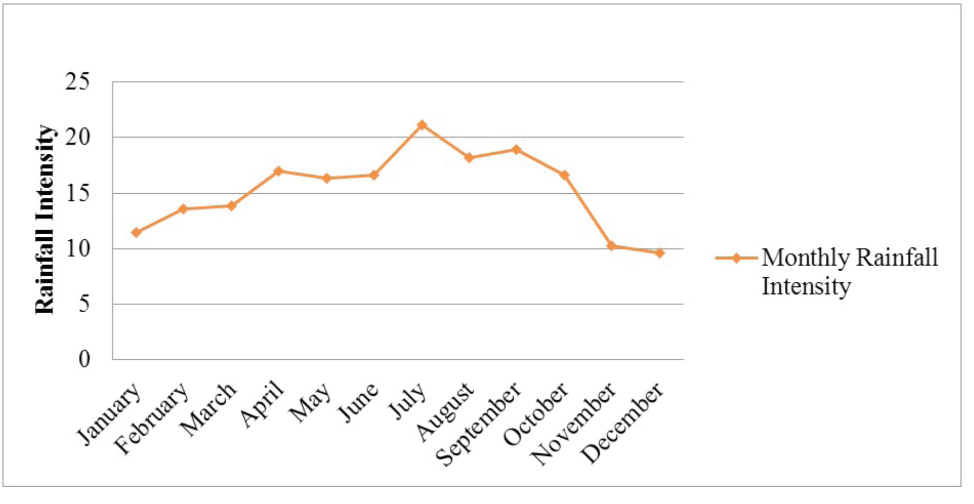

Fig. 3. Mean Monthly Rainfall Intensity in Warri Metropolis from 1986-2015 (Authors' Computation 2017)

Table 2. Mean Annual Rainfall Intensity for the Period 1986-2015 (Authors' Computation 2017)

Years	Rainfall Intensity (mm/d)
1986	19.84
1987	19.28
1988	15.44
1989	15.22
1990	18.82
1991	16.54
1992	18.86
1993	18.09
1994	17.53
1995	20.34
1996	16.13
1997	18.84
1998	16.84
1999	18.81
2000	15.86
2001	15.52
2002	20.74
2003	14.83
2004	18.05
2005	14.10
2006	14.26
2007	16.40
2008	19.19
2009	13.67
2010	15.22
2011	16.36
2012	16.04
2013	12.42
2014	16.84
2015	17.59

fitted, explains 2.40 % variability in rainfall in the study area. The correlation coefficient of -0.156 reveals a negative relationship between the rainfall and time (year). This suggests that rainfall is decreasing over time in the study area. Since the decreasing trend observed is not statistically significant (that is, the trend is random), decrease in the future cannot be categorically predicted or ascertained and the trend cannot be attributed to a particular causative factor in the study area.

Fig. 4 is obtained from the plotting of the mean annual rainfall amount against time. The graph reflects fluctuation in mean annual rainfall pattern of the study area however,

Table 3. Trend/Pattern of Rainfall Derived from Regression Analysis (Authors' Computation 2017)

Variables	Regression Equation	P-value	Statistically Significant	Sample Correlation	R^2
Warri	Y=243.75-0.4572X	0.412	No	-0.156	2.4%

the trend is on the decline since the last three decades. This is further corroborated by a negative trend line obtained. From the trend line equation, it can be concluded that the rainfall amount is decreasing at a rate of -0.45mm per year during the 30 years period under consideration. This method of analysis, according to Ologunorisa (2006) has been used by Sharon (1979, 1981); Adelekan, (1998) and several others in the study of rainfall trends.

Standardize Rainfall Anomalies Index (SAI) was used to establish the dry and wet episodes in the study area for the period of study (table 4). For critical analysis the thirty years under consideration were divided into three periods of ten years (decade) and the number of dry and wet episodes (years) within these ten years period were identified. The results revealed great insight into the nature of rainfall vis-à-vis the seasons (rain and dry) in Warri Metropolis for the past three decades.

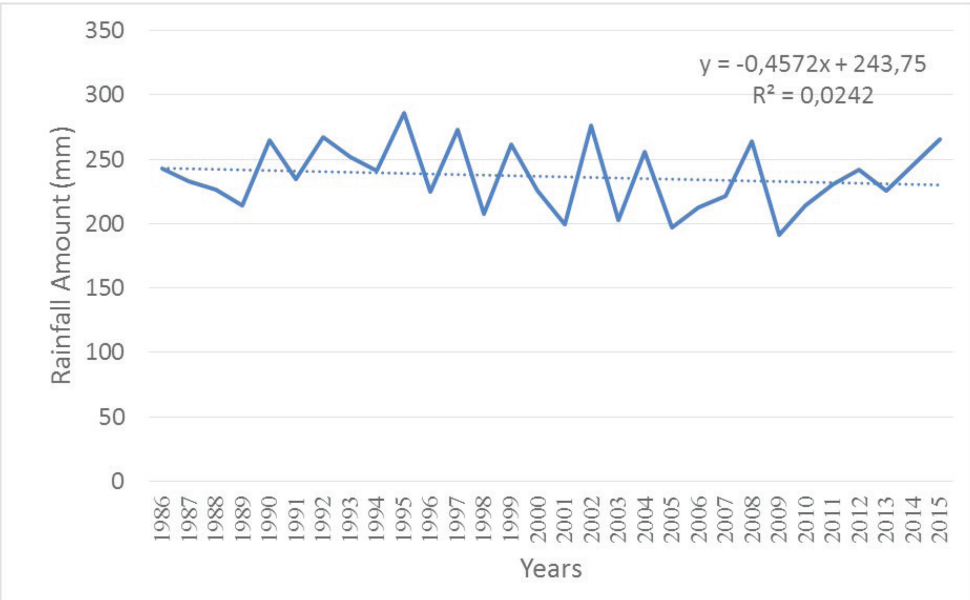

Fig. 4. Mean Rainfall Trend in Warri (1986-2015) (Authors' Computation 2017)

On the whole, there were 16 dry years out of the thirty years period considered in this study. Table 4 further revealed an average of six dry years in every ten years in the last twenty years in the study area. Fig. 5 reveals the pattern of rainfall anomalies in the study area for the thirty years period with the sixteen dry years and fourteen wet years on the negative and positive sides of the graph, respectively.

Implications of the Rainfall Characteristics on Flood Occurrence in the Metropolis

The information on table 5 was used to crosscheck the analyzed rainfall characteristics in the study area to see if there is any relationship between rainfall pattern and flood incidents in the study area. According to Ologunorisa and Tersoo (2006) this method has been used by Babatolu (1996) and they too equally adopted it in similar studies

Table 4. Dry and Wet Episodes in Warri in the last Three Decades (1986–2015) (Authors' Computation 2017)

Periods (Decades)	Dry Years	Wet Years
1986-1995	1987 (-0.14), 1988 (-0.39), 1989 (-0.86), 1991 (-0.09)	1986 (0.24), 1990 (1.10), 1992 (1.18), 1993 (0.58), 1994 (0.17), 1995 (1.93)
1996-2005	1996 (-0.47), 1998 (-1.12), 2000 (-0.41), 2001 (-1.45), 2003 (-1.31), 2005 (-1.52)	1997 (1.41), 1999 (0.97), 2002 (1.54), 2004 (0.73)
2006-2015	2006 (-0.92), 2007 (-0.59), 2009 (-1.75), 2010 (-0.86), 2011 (-0.24), 2013 (-0.43)	2008 (1.05), 2012 (0.20), 2014 (0.35), 2015 (1.10)

**Standard Rainfall Anomalies Indices are italicized in parentheses.

Available flood records (table 5 below) indicate that flood occurs in Warri and surrounding environments only in the months of April, May, June, July, August, September and October. This corresponded with the analyzed monthly rainfall intensity for the study (see tables 1, 2, and Fig. 3) which showed that these months marked the limit of wet season in Warri metropolis. No available flood showed that flood occurred in any of the months with least rainfall intensities, that is, December, November and January; these months with the addition of February equally represented the dry season in the study area.

The flood incidence of August 4th-6th, 2002 (table 5) corresponded with both the annual rainfall intensity and annual mean rainfall in table 2 as the highest rainfall recorded in that year. The year 2002 recorded the highest annual intensity (20.74mm/d) in the study period, and among other causes floods are equally induced by high rainfall intensity and consistent long duration of rains. A look at the daily rainfall amount for the days 4th-6th of August 2002 shows that each day had 144.2mm, 119.8mm and 7.3m respectively, and this individual amount especially the last two have the capacity to generate floods, and Olaniran (1983) confirmed that heavy rains have the capacity to induce

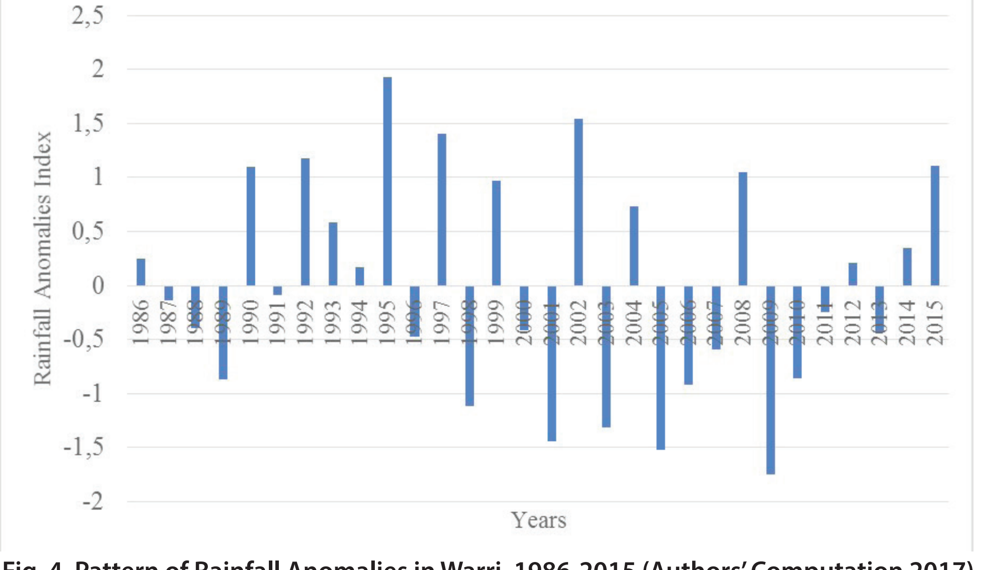

Fig. 4. Pattern of Rainfall Anomalies in Warri, 1986-2015 (Authors' Computation 2017)

Table 5. Chronology of past flood events in Warri metropolis (Authors' Compilation 2017)

SS/N	Date/Year	Location/Area	Cause(s)	Impacts/Effects	Source(s)
1	1999	Warri metropolis	Long and continuous rains	Over 5,000 houses affected	Efe and Mogborukor, (2010)
2	2000	Warri metropolis	Long and continuous rainfall	Property worth millions destroyed, several people displaced	Efe and Mogborukor, (2010)
3	August 4th-6th, 2002	Warri metropolis	Heavy rains	Several houses, shops worth millions of naira were submerged under 1meter floodwater	Efe and Mogborukor, (2010)
4	June, 2003	Warri and its environs	Rains	Property worth over 3.6millions destroyed; over 5,250 people rendered homeless	Efe and Mogborukor, (2010)
5	July, 2005	Warri metropolis	Heavy rains	Unspecified level of destruction	Vanguard, July 2005
6	August, 2006	Warri metropolis	Rains	Several houses, shops, worth millions destroyed	Efe and Mogborukor, (2010)
7	September, 2007	Warri metropolis	Rains	Several houses, shops, worth millions destroyed	Efe and Mogborukor, (2010)
8	July 10th -13th, 2011	GRA Effurun, Orhuwhorun	Heavy torrential rains	Unspecified levels of destruction (affected all southern states including Lagos, where 10 deaths were recorded)	Aderobga (2012)
9	July-October, 2012	Warri (and several other parts of Nigeria)	Heavy rains; Release of Lagdo dam in Cameroun due to excess water from rains there	People were killed and several displaced in the metropolis	Udo, et al (2015); Wikipedia (2016)
	July 12, 2012;	Asheshe layout, Jakpa, Igbudu axis, Mowoe	Heavy rains	Over 300 people displaced	Umuteme and Orusi (2012)
	September 20th, 2012	Several parts of the metropolis	Torrential rains	Property worth millions of naira swept away	Ogoigbe, et al, (2012)
10	May 21st-22nd, 2013	Several parts of the metropolis	Burst of water supplying reservoir/pipe	Unspecified levels of damage	Urhobo Today (Thursday 23rd May, 2013)
11	October, 14th, 2014	3rd Marine Gate, Warri	Heavy midnight rains	Residents trapped for several days; vehicular movements halted	Urhobo Today Newspapers (October, 2014)
12	April 26th; May 10th, 2015	Cemetery road, Warri Stadium	3hours heavy downpour	Submerged many parts of the road, including the Warri City Stadium in which an NNF league match between Warri wolves and Nassarawa Utd were delayed	The Guardian Newspapers (May 11th, 2015)

flood in a place when they occur several times in one month. This also confirms the findings of Ologunorisa and Tersoo (2006) which suggest that extreme daily rainfall events especially heavy rains can result in overland flow. Hence, the ability of these extreme daily rains to have caused flood in the reported days in the area cannot be doubted.

The flood incidences of October 14th 2014; April 26th, 2015 and May 10th, 2015 as shown in table 5 first corresponded with the period high annual rainfall intensities of both years. Secondly the individual daily rainfall amount for the three respective days, that is, October 14th, 2014 with 29.0mm, April 26 2015 with 66.0mm and May 10th 2015 with 62.6mm indicate their capacity to induce floods in the area especially when the accumulative effects of previous days of rainfall amount in the same area as well as other environmental conditions of the metropolis are considered.

In considering the results of decadal analysis (see table 4) available flood records show that flood incidences were reported in 4 of the 14 wet years of 1999, 2002, 2014 and 2015. However, many flood incidences were equally reported even in those years termed 'dry' such as the cases of 2000, 2003, 2005, 2007 and 2011 as shown in table 4. This suggests that dryness is relative, and Warri metropolis is one of the highest rainfall zones in Nigeria having rainy season that last for over 7-8 months. Though there are no available reported cases of flood in some of both the dry and wet years, however, individual daily rainfall events in some of the years have the capacity to induce flash floods.

The flood records in table 4 and 7 however, show that the May 21st-22nd, 2013 flood was caused by damage to water reservoir, water supplying scheme in the metropolis. The implication is that rain may not be the only cause of flood in the area, there are other contributory factors ranging from attitudes of inhabitants, nature of topography and the urban space among others.

Factors Responsible for Flood in Warri Metropolis

To identify the dominant factor responsible for flood occurrence in Warri, eight (8) flood causing variables were identified in the study area and were subjected to factor analysis statistical method. After vari-max rotation, only two (2) factors dominated the explanation of the variance in the flood occurrence experienced in Warri metropolis. **Factor I:** This factor has the highest loading on rainfall, absence of drainage and poor town planning. It is tagged nature of rainfall occurrence and urban design. This has the highest contribution to flood occurrence in Warri. This factor is an index of nature of rainfall incidences and poor urban planning which contributed 51.09% variance to flood occurrence in Warri metropolis. As seen in most cities of Nigeria, the nature of rainfall occurrence and poor urban planning are the major causes of flooding (leading factors). This is as a result of excess rainfall being disrupted from flowing directly to the river channels. In addition, the absence of artificial drainage which is part of poor urban planning play major role in flood incidence.

Factor II: This factor loaded highest on overflowing of rivers, blocked/poor drainage and untarred road, it is tagged river overflow and poor drainage. This factor is an index of poor natural/artificial drainage network management which contributed 44.10% variance to flood occurrence in Warri metropolis. Hence, poor natural (river) and artificial (gutters/culverts) drainage network management combined to form the second most dominant factor of flood occurrence in Warri metropolis. This is in terms of the drainage networks not properly linked, various waste items deposited in the drainage systems that leads to its blockage. Also, the topsoil washed from the untarred road during rain end up in river channel, increased the river sedimentation and caused the river to overflow its bank leading to flood.

The rotated component scores of spatial patterns of factors responsible for flooding in Warri using the two (2) identified factors as criteria is presented in table 6. The table

Table 6. Factors Responsible for Flood Occurrence in Warri Metropolis (Authors' Computation 2017)

SN	Parameters	Factor 1	Factor2
1	Rainfall	0.98	-0.65
2	Overflowing of Rivers	0.549	0.903
3	Nature of Topography	-0.76	0.02
4	Blocked/Poor Drainage	0.141	0.969
5	Absence of Drainage	0.782	0.389
6	Poor Town Planning	0. 902	0.475
7	Untarred Road	0.291	0. 817
8	Impervious Surfaces	-0.824	-0.553
Factor defining Variable		**Rainfall amount& urban design**	**River overflow & poor drainage**
Factor Description		Index of nature of rainfall incidence and urban planning	Poor natural/artificial drainage network management
Total Eigen value		4.087	3.528
% Variance		51.092	44.103
% Cumulative variance		51.092	95.20

revealed that factor I (Nature of rainfall incidence & urban planning) contributed highest to the flooding in Effurun with a factor score of 1.09 and lowest to flooding in GRA with a factor score of -1.23. Factor II (Poor natural/artificial drainage network management) contributed highest to flooding in Warri core with a factor score of 1.12 and lowest to flooding in GRA with a factor score of -0.82.

The study revealed that the month of July had the maximum monthly rainfall intensity of 21.10mm/d while the least monthly intensity was recorded in December (9.61mm/d). The yearly analysis shows that year 2002 observed the highest annual rainfall intensity of 20.74mm/d while the year 2013 was found to have the lowest annual rainfall intensity of 12.42mm/d for the study period.

Trend analysis revealed the R2 statistics of 02.4, and this is able to explain about 2.40% of rainfall variability in the metropolis. The correlation coefficient shows -0.156 which indicates a negative relationship between rainfall and time (years). This means that rainfall is decreasing over time in Warri metropolis. From the trend line regression equation Y=243.75-0.4572X, it can be concluded that rainfall in Warri Metropolis is decreasing at the rate of -0.45 per year. However, the p-value 0.412 is greater than 0.05, hence, the trend is not statistically significant at 95% level of confidence, that

Table 7. Rotated Component Scores of Factors Responsible for Flooding in Warri Metropolis (Authors' Computation 2017)

Zones	Factor I	Factor II
GRA	-1.2365	-0.8291
Warri Core	-0.2882	1.12426
Effurun	1.09826	-0.8565
Udu	0.42641	0.56132

is, the trend is random. By implication, future decrease in rainfall amount in subsequent years in the metropolis cannot be assured. Factorial analysis of some identified factors responsible for flood in Warri showed that rainfall, absence of drainage and poor urban planning practices (as factor 1) contributed 51.09% while overflowing of rivers, blocked/poor drainage and untarred roads (as factor 2) contributed 44.10% variance to flood occurrence in the metropolis. By implication these two factors explained 95.19% of all flood occurrences while the 4.81% could be attributed to impervious/concreted surfaces, nature of topography and every other possible factor as causative agents of flood in Warri and its environs.

CONCLUSION AND RECOMMENDATIONS

The rainfall situation in the area as well as other climatic variables should be continually studied and monitored since they have major effects on flood occurrence and frequency, and such information should be made readily available to the urban planners, road engineers and other concerned professional and individual alike in the metropolis for effective planning purposes.

The management of flood starts with available of relevant data/information relating to its history, remote and immediate causes, impacts, frequencies, etc, therefore, it is recommended that concerned government agencies, ministries and parastatals both at the federal, state and local levels especially the Ministries of Environment and Works; National Emergency Management Agency (NEMA) and the Delta State Emergency Management Agency (DESEMA) should keep comprehensive record of flood incidences, and such records should be updated periodically.

The Delta State environmental laws should be reviewed and updated and check to see if there is a legislation against dumping of refuse on drainage channel and on roads. If there is none then it should be incorporated, modalities of its implementation and punishments for defaulters be clearly spelt out. Most importantly is the strict enforcement of such legislation because most several environmental laws do not go beyond the paper works.

Proper urban space planning and management is vital to controlling flood in any place, therefore, it is important that Delta State Ministry of Lands, Survey and Urban Development and any other relevant governmental body should rise up to the challenge of ensuring strict compliance with the original Master Plan of the Warri Metropolis. Ensuring enforcement of existing town planning laws and constant monitoring of the urban space is needed to prevent activities like unauthorized development, the practice of citizens changing residential structures to commercial and vice versa, erecting of structures on flood prone areas, among others. Furthermore, as matter of urgency, it is very imperative for relevant government authorities to implement the Urban Drainage Master Plan of Warri Metropolis immediately.

REFERENCES

Abotutu A. and Ojeh N. (2013). Structural Properties of Dwelling and Thermal Comfort in Tropical Cities: Evidences from Warri, Nigeria. International Journal of Science and Technology 2(2), pp. 67-98.

Action Aid (2006). A Report on Climate Change, Urban Flooding and the Right of the Urban Poor in Africa – Key Findings from Six African Cities.

Aderogba A. (2012). Global Warming and Challenges of Floods in Lagos Metropolis, Nigeria. Academic Research International 2(1):448-468.

Adejuwon O. (2011). Rainfall Seasonality in the Niger Delta Belt, Nigeria. Journal of Geography and Regional Planning 5(2):51-60. Available online at DOI: 10.5897/JGRP11.096. [Accessed on 15th July,2016].

Afangideh I., Ekpe A., Offiong A. (2013). Implications of Changing Rainfall Pattern on Building Loss in Calabar. International Journal of Innovative Environmental Research. 1(2):10-18.

Agbonkhese O., Agbonkhese G., Aka O., Joe-Abaya J., Ocholi M., Adekunle A. (2014). Flood Menace in Nigeria: Impacts, Remedial and Management Strategies. Civil and Environmental Research. 6 (4): pp. 32 – 40. Available on line at www.iiste.org. [Accessed on 29th June, 2016].

Ayoade O. (2003). Tropical Hydrology and Water Resources. Ibadan: Macmillan Publishers Limited.

Bhanumurthy V. and Behera G. (2008). Deliverables from Space Data Sets for Disaster Management, Present and Future Trends. The International Archives of the Photogrammetry, Remote Sensing and Spatial Information Sciences. Vol. Xxxvii. Part B8, Beijing 2008.

Efe I. and Mogborukor A. (2010). Flood Hazards in Warri A Third World City, Nigeria. Journal of Social and Management Sciences. 5(2):83-93.

European Space Agency (2004). "Space and Public Safety, Civil Protection Assistance", Available online at http://www.esa.int/esaeo/SEMQFF3VQUD_environment_0.html. [Accessed on 15th August, 2016].

Igweze H., Amagohm N., Ashinze N. (2014). Analysis of Rainfall Variations in the Niger Delta of Nigeria. Journal of Environment, Science, Toxicology and Food Technology (IOSR-JESTFT) 8(1) Version VI. 25-30. Available online at www.Iosrsjournals.Org. [Accessed on 15th August, 2016].

Mogborukor A. (2012). "Flooding Problems in Auchi and its Environs, Edo State, Nigeria". In Efe I. and Atubi O. (eds) Environment and Socioeconomic Impacts of Natural Resources Exploitation in Auchi and Environs, Edo State Nigeria. Abraka: An Occasional Publication Series of the Department of Geography and Regional Planning, Delta State University, Abraka.

National Research Council (NRC, 2010). America's Climate Choices: Panel on Advancing the Science of Climate Change. Advancing the Science of Climate, Washington, DC.

Obafemi A., Eludoyin S., Akinbosola M. (2012). Public Perception of Environmental Pollution in Warri, Nigeria. Journal of Applied Science, Environment and Management 16(3) 233-240.

Ogundele B. (2015). "Why Warri Residents Dread the Rains". The Nation Newspapers, Saturday 7th, March 2015.

Olabaniyi B. and Efe I. (2011). Comparative Assessment of Rainwater and Groundwater Quality in an Oil Producing Area of Nigeria; Environmental and Health Implications. JEHR 6(2).

Ogoigbe E., Osuyi P., Kings K. (2012). "Rain, Flood Sack Delta Communities" Sun Newspapers (September 21, 2012). Available online at www.sunnewsonline.com. [Accessed on on 21st April, 2015].

Ologunorisa E. (2006). Flood risk Assessment and Management in Nigeria: Perspectives from the Niger Delta. Markudi: Selfers Educational Books.

Raji A., Adeniyi O., Odunufa, S. (2014). Multi-criteria Flood Risk Analysis of Lower Ogun River Basin. Journal of Environment and Earth Science. 4(13):112-124.

The Guardian (2015). "Glo Premier League: Warri Wolves Whip Nassarawa United 4-1 After Flood Induced Delay." The Guardian Newspapers. Available online at www.m.guardian.ng. [Accessed on 11th July, 2016].

The Nigerian Meteorological Agency (NIMET, 2016). "Records of Daily Rainfall Data in Warri from 1986 to 2015". Retrieved from the Nigerian Meteorological Agency (NIMET), Warri Station.

Sada P. and Odemerho F. (1988). Environmental issues and management in Nigeria development. Evans, Ibadan.

Udo A., Baywood N., Gift A., Ojinnaka C. (2015). Flood Hazard Analysis and Damage: Assessment of the 2012 Flood in Anambra State Using GIS and Remote Sensing Approach. FIG Working Week 2015. Wisdom of the Ages to the Challenges of the Modern World, Sofia, Bulgaria. pp.17-20.

Umuteme B. and Orusi K. (2012). Flood Rendered Hundreds Homeless in Warri. Frontiersnews, Wed 18th, July 2012.

Urhobo Today (2013). "Delta: Part of Warri Floods as Water Reservoir Burst Again". Urhobo Today Newspapers (Thursday 23rd, May, 2013). Available online at www.urhobotoday.com. [Accessed on Saturday 26th September, 2015].

Urhobo Today (2014). "Delta: Flood Submerged Warri as Drainage System Collapsed". Urhobo Today Newspapers (14th, October, 2014). Available online at www.urhobotoday.com. [Accessed on Monday 11th July, 2016].

Wikipedia (2015c). "The Water Cycle". Available online at www.wikipedia.com. [Accessed on 20th June, 2015].

Zbigniew W. Kundzewice S.K., Sonia I.S., John H., Newille N., Pascal P. (2013). Flood Risk and Climate Change: Global and Regional Perspective. Hydrological Science Journal 59 (1) 1 -28

Received on August 10th, 2017 Accepted on November 22nd, 2017

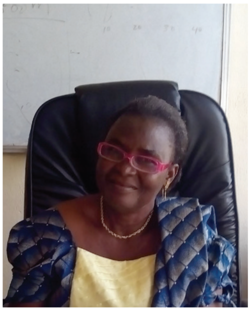

Dr. Rhoda Mojisola Olanrewaju, a Senior lecturer in the Department of Geography and Environmental Management, University of Ilorin, Kwara State, Nigeria had her Ph.D in Applied Meteorology from the Federal University of Technology, Minna, Niger State, Nigeria. She teaches courses such as Climatology, Applied Climatology, Air Photo Interpretation and Remote Sensing at Undergraduate level while at Postgraduate level she teaches Agrolimatology, Urban Climatology and Remote Sensing. She has published over 40 papers in both international and local Journals and books. Her broad area of research is in Applied climatology. Most of her research work is in the field of Agroclimatology.

Buku Ekiotuasinghan is a post-graduate student of the University of Ilorin, Nigeria. He had his NCE from College of Education Warri, Nigeria, B.Sc., Delta State University Abraka, Nigeria. His research focus is in Climatology and Environmental Management. Other areas of interest are GIS, Remote Sensing and Soil Studies. He has published many papers in his field of interest.

Godwin Peter Akpan is a PhD student of the University of Ilorin, Nigeria, Department of Geography and Environmental Management. He had his B.Sc. Degree from the Department of Geography and Regional Planning (now Dept. of Geography and Natural Sources Management), University of Uyo, Nigeria in 2004. He teaches physical geography in College of Advanced Studies, Kebbi State, affiliate of Ahmadu Bello University, Zaria, Nigeria. His research interest is in the area of Climate Change, Agroclimatology and Environmental Management. He has published over 20 papers in outstanding international and local journals and has contributed numerous chapters in books.

Oksana Klimanova[1]*, Alexey Naumov[1], Yulia Greenfieldt[1], Rachel Bardy Prado[2], Daria Tretyachenko[1]
[1]Lomonosov Moscow State University, Moscow, Russia. Russian Federation, Moscow, GSP-1, Leninskie Gory, Faculty of Geography, 119991
[2]EMBRAPA National Soils Research center (Embrapa Solos), Rio de Janeiro, Brazil; Rua Jardim Botânico,1024, CEP: 22460-000, RJ
*** Corresponding author:** oxkl@yandex.ru

RECENT REGIONAL TRENDS OF LAND USE AND LAND COVER TRANSFORMATIONS IN BRAZIL

ABSTRACT. Regional trends of land use/land cover transformation in Brazil during 2001—2012 were analyzed in the following order: 1) identification of the types of transitions for different land use and land cover categories and aggregated groups of transformation processes based on the Global Land Cover Facility datasets, 2) analysis of national agricultural and forestry statistics to find out the principal socioeconomic drivers, 3) land cover and land use data merging to elaborate comprehensive typology of land use/land cover changes on a regional level. The study evealed 96 types of transitions between land cover categories, aggregated into 10 groups corresponding to driving processes. It was found that the main processes of land cover transformations is related to both natural and anthropogenic origins. Cropping and deforestation are anthropogenic processes, flooding and draining are the principal natural ones. Transformation of cultivated lands and reforestation are combined natural and anthropogenic. The contribution of natural factors is higher in the states of the North (Amazonia) and the Northeast macroregions; in the Center-West and the South anthropogenic factors make larger contribution. We have also detected considerable land use/land cover changes caused by agricultural development in densely populated states of the Southeast and the South. In both macroregions planted area expands due to increase of soybeans and sugar cane production, while area of pastures is shrinking. The trends of transformations of agricultural land use revealed as a result of statistical data analysis, match with transitions of land cover categories belonging to the aggregated group of cropping processes. Transformations of land cover types with predominance of shrub vegetation were the most problematic to interpret because of lack of comparable statistical data on pastures.

KEY WORDS: land use/land cover regional dynamics, Brazil, MODIS, agriculture, forestry

CITATION: Oksana Klimanova, Alexey Naumov, Yulia Greenfieldt, Rachel Bardy Prado, Daria Tretyachenko (2017) Recent regional trends of land use and land cover transformations in brazil. Geography, Environment, Sustainability, Vol.10, No 4, p. 98-116
DOI-10.24057/2071-9388-2017-10-4-98-116

INTRODUCTION

Conversion of virgin lands for agriculture followed by soil degradation, indiscriminate use of fertilizers and water pollution, loss of biodiversity, along with climate change has exerted strong pressure on terrestrial and aquatic ecosystems, compromising their sustainability. Over the past 50 years, humans were changing ecosystems more rapidly and extensively than in any comparable period of time before. This has resulted in a substantial and largely irreversible loss in the diversity of nature on Earth (MEA 2005).

The above mentioned transformations, mostly related with development of agriculture and forestry, require elaboration of appropriate action strategies, e.g. agri-environmental sustainability (Stallman 2011). Aiming the sustainability of rural landscapes as reconciliation of ecosystems preservation and satisfaction of demand in food, fiber, energy, water, raw materials and other goods and services, is a fundamental approach for studies of dynamics and functions of ecosystems and landscapes (Barkmann et al. 2004).

Modern studies of land use and land cover (LULC) transformation processes and specific features of land resources utilization are based on the analysis of remote sensing data of various spatial resolutions. Land cover means a present-day mosaic of vegetation cover, both natural and anthropogenic, the last one including agricultural crops, of settlements, industries and infrastructure, of lands without vegetation (fallow, glaciers, etc.) and water surfaces (Channan et al. 2014). Satellite imagery is a tool for highly precise identification of areas where land cover transformations are caused by particular anthropogenic and/or natural factors. However the interpretation of obtained results and the discovery of reasons of LULC changes, especially at the regional level, are possible only through the complex analysis of natural and socio-economic features of the territories.

In this context, characteristics of agriculture are considered as research priority for LULC studies. Geographical analysis reveals spatial heterogeneity of agricultural development, and provides bases for assessment of its role in land cover changes within different regions. This could be done with a great level of precision as statistical data on land use by administrative-territorial units become available for the increasing number of countries. As estimated in 2006, agricultural censuses were held in 134 countries of the world, and most of them contained data by states, provinces and similar units. For 2020, the UN Food and Agricultural Organization (FAO) plans to launch global data collection through the World Agricultural Census (World Programme FAO for the Census of Agriculture).

In recent years, several attempts were made to integrate the statistical and remote sensing data in order to evaluate geographical variety of agricultural production systems. An example is the project on global mapping of the differences in productivity of the main crops fulfilled by US and Canada researchers (Monfreda et al. 2008; Ramankutty et al. 2008). Factors influencing the yield differences, such as water and nutrients supply, were also taken into account. However, the yield was considered as a function of biological productivity, and the socio-economic features of agricultural production were ignored. A number of similar global projects are carried out under the auspices of FAO: the GLC2000 (studying the global land cover for the assessment of the state of ecosystems), the Global Livestock Information System, and the so-called Agro-maps project, involving compilation of universal cartographical database on agriculture at the "subnational" level (Agro-maps). The International Food Policy Research Institute (IFPRI) also has launched the program of global localization of harvest data (Global Mapping... 2006).

Joint analysis of remote sensing and agricultural statistics is also applied at the national level. E.g., in Brazil, the Companhia Nacional do Abastecimento uses remote sensing and analysis of the municipal statistical data for estimate crops productivity, being the GeoSafras (yield forecasting) and SIGABrasil (mapping of agricultural indicators) projects two basic components of this research (CONAB).

LULC studies are quite common at the level of one country, but usually they emphasize only main drivers of land use and land cover changes. E.g. publications on land use dynamics in Brazil focus on deforestation, expansion of soybeans and other commercial crops (Naumov 2005; Lapola et al. 2014). More often, rather short periods of time, usually 3—5 years are covered (Richards et al., 2014). At the same time, large-scale studies concerned with the detailed analysis of land cover changes basing on the remote sensing data for certain territories are common (Ferreira et al. 2009).

The objective of our paper is to evaluate regional trends of land use/land cover transformations in Brazil during 2001—2012, focusing on agricultural and forestry development as their driving forces. The methodology was based on the GIS assisted extrapolation of the big array of statistical data for small administrative-territorial units to the natural (soil and landscape) areas identified through the interpretation of space imagery.

STUDY AREA

Extensive territory of Brazil (8.5 million sq. km) consists of both densely populated areas and natural ecosystems of global value in different biomes (Fig. 1). It is rapidly colonized and developed, generally because of agricultural expansion. Understanding the current LULC dynamics will enable assessment of anthropogenic impact on the natural-territorial complexes and could serve as a base for the forecast of the future LULC changes.

Fig. 1. Brazil: biomes (Ferreira et al. 2013)

Brazil possess extremely high biodiversity, estimated the number of species from 1 to 8 million (Lewinsohn and Prado 2005) At the same time, it is one of global leaders in agricultural production (FAO 2015), playing an increasingly important role supplying food to the humanity (Foley et al. 2011). Reconciling agricultural production and environmental conservation is one of the greatest challenges this country currently faces (Ferreira et al. 2012).

Brazil ranks high in the rates of such processes as deforestation (mainly because of agricultural development and logging), conversion of natural pastures into cultural ones and cultivated fields, and the urban sprawl, which are the most important in the context of LULC changes. According to the Brazilian Institute of Geography and Statistics (IBGE), in 2010—2014 the forested area in the country was reduced by 2%. The area of natural pastures was also rapidly decreasing: in 2010—2012 its size dropped by 7.8%, and in 2012—2014 – by 9.4%. During the same two periods of time the area of agricultural lands has increased by 8.6% and 8.2%, respectively. Increase of the area of improved pastures (ameliorated and planted by cereals and leguminous forage crops) has slowed down (11.1% in 2010—2012, and 4.5% in 2012—2014), and some of them were converted to agricultural lands. At the same time, there was a significant increase in the area of planted forest (by 23.8% during 2012—2014), which substituted cleared forests and/or pastures (IBGE. Mudanças... 2016). Degradation of pastures is one of the main environmental issues in Brazil. Besides the low efficiency of cattle ranching, from the total of 190 million ha of improved pastures it is estimated that some 27—42% are degraded (Ferreira et al. 2014).

MATERIAL AND METHODS

The methodological scheme of the study includes three main stages: 1) identification of the types of transition between the land use and land cover categories and of aggregated groups of transformation processes on the basis of the Global Land Cover Facility (GLCF) data, 2) analysis of national agricultural and forestry statistics aiming to find out the principal socio-economic LULC drivers, 3) integration of both kinds of above mentioned data and elaboration of a complex typology of LULC changes. Our research is based on data, generalized for states of Brazil (26 states and 1 Federal district). As data source, we have used official publications and web pages of IBGE (this institute is responsible on population and agricultural censuses in Brazil, hold each 10 years), CONAB, and other institutions. The cycle of agrarian production in Brazil because of its geographical location mainly in the Southern hemisphere passes over the calendar New Year, therefore 2001–2002 and 2011—2012 agricultural seasons are the starting and the ending points of the studied period.

Understanding LULC transformation at different territorial levels requires to use remote sensing data (space imagery along with databases derived from their interpretation). The use of global land cover databases projected at the regional level seems quite adequate for such big countries as Brazil, which territory ranks fifth in the world. The state of land cover in Brazil during 2001—2012 was evaluated using the open data of the Global Land Cover Facility (GLCF) obtained through the MODIS satellite survey with the resolution of 5′x5′. These sources were considered as the most reliable basing on the comparison of a series of heterochronous global land cover data (Alekseeva et al. 2017). The data were analyzed using the environment of the ArcGIS Desktop for Desktop Spatial Analyst.
The legend to the land cover map compiled on the basis of MODIS data includes 17 classes, corresponding to the classification of the International Geosphere-Biosphere Program (IGBP) (Loveland et al. 2000). The classes were identified according to the height of trees and shrubs, canopy coverage of a forest stand, etc. (Table 1).

To find out social and economic drivers of LULC transformation, the analysis of national agricultural statistics was carried out. Changes in the harvested area under main grains (soybeans, corn, sorghum, wheat, rice, beans and others) and under other

Table 1. Classification of LULC of the International Geosphere-Biosphere Program (IGBP)

Classes with a predominance of woody vegetation	Classes with a predominance of shrubby and grassy vegetation	Classes with antropogenic transformed vegetation	Other categories
1. Evergreen Needleaf Forest	6. Closed Shrublands	12. Croplands*	11. Permanent Wetlands
2. Evergreen Broadleaf Forest	7. Open Shrublands	13. Urban and Built-up	15. Snow and Ice
3. Deciduous Needleaf Forest	8. Woody Savannas	14. Croplands/Natural Vegetation Mosaic	16. Barren and Sparsely Vegetated
4. Deciduous Broadleaf Forest	9. Savannas		17. Water surface
5. Mixed Forest	10. Grasslands		

* Any fields in which seasonal crops are grown, including minimal and zero plowing.
Source: Modified from Loveland et al. 2000.

commercial crops (soybean, sugar cane, cotton, coffee) were analyzed. The above-mentioned crops, except rice, account for a considerable share of cultivated land in Brazil, and the essential changes of growing and harvested area were typical for all of them during the studied period. According to the Ministry of Rural Development of Brazil, in 2009 soybeans covered 37.3% of all acreage under seasonal cultivation, sugar cane — 14.6 rice — 4.9 and cotton — 1.4% (Estatísticas... 2011). Sugar cane is cultivated on the same field during 4—5 years; it grows up after harvest and is poorly distinguishable from perennial crops on the space imagery. Rice is particularly interesting for our study, because the expansion of this irrigated crop causes a specific type of land cover transformation. Corn accounted for 23.4% of seasonally cultivated lands, however in Brazil it is most often grown up in one-year crop rotation with soybean. Because of overlapping of cropping area under these two crops it was not possible to consider data on corn cultivation separate from soybean. Coffee ranked first among perennial crops accounting for 35.4% of the total area (Estatísticas... 2011). Statistical data on afforestation were also used. Unfortunately, data on the area of pastures in Brazil are not published annually; they are available only in census years which do not coincide with the first and the last years of the period under our study. Therefore it was impossible to analyze the dynamics of areas under pasturing.

The processes described on the basis of statistical data analysis, i.e. expansion of agriculture and creation of forest plantations, do not cover all the types of changes identified through the use of MODIS data. However, we decided it was feasible to consider these two processes as the main drivers of LULC changes in Brazil.

RESULTS AND DISCUSSION

Structure and main process related to the LULC dynamics

The comparison of data for 2001—2012 made it possible to identify the types of land cover changes; each of them was assigned a two-digit index according to the IGBP classification (Table 1). The first digit corresponds to the land cover type in 2001, and the second — to the same in 2012. For example, type "2/9" means the change "evergreen broad-leaved forest — savanna"; 12/5 — "croplands — mixed forest". In total, 96 types of changes were identified and subsequently combined into 10 groups according to the processes causing the changes (Fig. 2, Table 2).

Table 2. The main processes of LULC transformation and corresponding types of changes

№	Process	Types of changes
1.	Draining	All changes for transitions from the 0 category; 11/2, 11/8, 11/9
2.	Flooding and partial flooding	All changes resulting in transitions to categories 0 and 11
3.	Conversion to cropland*	All changes resulting in transition to category 12 and changes causing the transition of non-cultivated lands to category 14
4.	Agricultural transformations (changes of vegetation cover on agricultural lands)	All changes relating to categories 12 and 14
5.	Deforestation	2/14, 2/10, 2/8, 2/9, 8/9, 8/10, 9/10
6.	"Savanization" (savanna vegetation replacing the deciduous forests)	4/9, 4/8, 5/8
7.	Decreasing share of shrubs in the vegetation cover	7/10, 6/7, 6/9, 6/8
8.	Increasing share of tree vegetation (in some cases, reforestation)	7/8, 7/9, 8/2,8/4, 8/14, 9/2, 9/4, 9/8, 9/14, 10/2, 10/8, 10/14, 14/2, 14/8,
9.	Increasing share of shrubs in the vegetation cover	9/7, 10/9, 10/7
10.	Construction and other forms of anthropogenic transformation within settlement territories	2/13, 8/13, 9/13, 10/13, as well as all transitions from category 13**

* Including minimum and zero plowing. ** To avoid the distortion of results because of relatively small size of areas of settlements, the impact of urbanization process is not specially considered in this study.

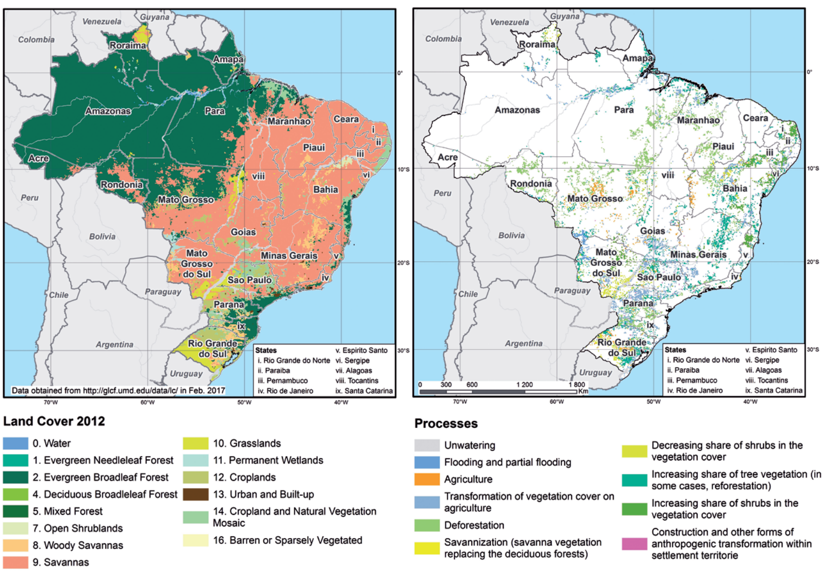

Fig. 2. Brazil: land cover, 2012 and LULC changes (by processes), 2001—2012. Data Source: GLCF, MODIS 2001—2012

Each type of changes and group of processes were characterized by: 1) area of changes; 2) share of each type of changes and group of processes in the area of each state; 3) share of each type of changes and group of processes in the total area of all types of changes in particular state. Similar approach was already used on the global scale, data generalized for the main biomes (Klimanova et al. 2017). Final results of the complex analysis of LULC changes are presented in Table 3.

The area of changes revealed by comparison of land cover data on MODIS space imagery for all categories of lands in the states of Brazil differs significantly: in 3 states of 27 (Mato Grosso, Bahia, Pará) it exceeds 100.000 sq. km, in 8 states it is less than 10.000 sq. km. Minimum area of changes registered was 1.600 sq. km in the Federal District Brasilia. However, the total area of this units just 5.800 sq. km. Minimum share of the area of change in the total area of the state is 0.9% (Amazonas) and the maximum – 36.2% (Paraná). In the North and Northeast there are states with low, average and high degree of land cover change, and in all states of the South the share of the area of changes is the highest in the country.

Regional differences are also legibly traced in the basic processes causing land cover changes. In the states of the North deforestation makes the greatest contribution to these changes. The contribution of agriculture is the most valuable in the state of Tocantins, which is located on the transition zone between the Amazon forest (port. Amazônia) and Savanna (port. Cerrado) biomes. In the states of Northeast processes of shrub vegetation change (considered in the our analysis as "others") have the greatest value; these states differ markedly from the rest of the country. Interpretation of driving forces of these changes is complicated; perhaps, they are caused by the natural transformation of shrubby vegetation. We can also assume that a considerable proportion of areas here were converted into pastures, which could hardly be distinguished from shrubby savannas or grasslands, especially during first years. In some states of the Northeast (Maranhão and Piauí) deforestation plays the most important role, in some other states of this macroregion (Pernambuco and Alagoas) the main process is conversion of deforested lands to agriculture.

The states of the Center-West which lay in the area of predominance of the Savanna biome, since 1980s are characterized by the most intense agricultural development, causing drastic changes in the structure of land use. In the state of Mato Grosso the deforestation is very important accounting for a half of area of all land cover changes. In the South and Southeast the role of agricultural development is also high, and the considerable proportion of already cultivated land is characterized by the transformation of land cover as a consequence of replacement by traditional crops by the new ones, also of conversion to cultural pastures.

The contribution of flooding or, on the contrary, draining as driving forces of transformation processes is more complicated to determine and requires verification. The pattern of these processes could be related to the annual changes of river flow and respective expansion or shrinking of wetlands. It could be implicitly proven by the greatest contribution of such processes to the structure of land cover changes in the states of the North, where they are obviously caused by natural factors. Reforestation could be considered as a result of both expansion of forest plantations establishing and natural vegetation dynamics.

MAIN DRIVERS OF LULC CHANGES

The calculations reflecting the dynamics of agricultural and planted forest areas by the states of Brazil made it possible to reveal the main types of changes in agricultural and forestry LULC. The results of this analysis can be found in Table 4.

AGRICULTURE

Analysis of agricultural development is most important for understand the reasons of land

Table 3. Structure and the main processes of land cover changes in the states of Brazil during 2001—2012

States by Macroregions	All land cover changes		Components of land cover changes in 2012*, %							Statistical data	MODIS data	Statistical data	MODIS data	CAS+FAS/ CAM+FAM, %***
	1.000 sq.km	% of total area of the state	Draining	Flooding (also partial)	Conversion to cropland	Agricultural transformations	Deforestation	Afforestation	Other processes**	Increase of cropland area, 2001—2012, % of total area of the state		Increase of planted forest area, 2001—2012, % of total area of the state		
										CAS	CAM	FAS	FAM	
North (Amazonia)														
Acre	4.6	3.3	0.0	0.0	0.0	9.9	78.1	9.8	2.3	-0.0	0.0	0.0	0.3	0.0
Amazonas	14.2	0.9	7.9	7.9	1.2	0.0	14.01	31.7	3.6	-0.0	0.0	0.0	0.3	0.0
Amapá	16.6	12.0	0.6	0.6	3.7	6.2	2.6	67.1	1.0	0.0	0.4	-0.3	8.0	0.0
Para	105.4	8.5	0.0	0.0	1.7	14.1	52. 6	22.4	0.3	-0.1	0.2	0.1	1.9	1.1
Rondônia	35.6	15.0	0.0	0.0	0.0	0.9	91.2	5.1	0.3	0.4	0.0	-0.5	0.8	2.5
Roraima	13.2	5.9	0.0	0.0	2.0	0.8	34.9	48.0	-0.0	0.1	0.1	0.0	2.9	0.1
Tocantins	7.2	2.6	0.0	0.0	9.6	3.6	27.7	47.0	1.0	2.0	0.2	0.4	1.2	91.5
Northeast														
Alagoas	8.9	32.5	0.0	0.0	6.8	46.4	0.0	2.4	44.4	-3.8	6.8	0.0	0.8	0.0
Bahia	115.8	20.6	0.0	1.6	15.2	16.3	17.8	17.2	31.9	0. 8	3.1	0.6	3.5	6.8
Maranhão	41.9	12.9	0.3	2.9	4.0	24.6	65.1	2.4	0.6	1.6	0.5	0.5	0.3	16.8
Paraíba	4.9	8.7	0.0	0.0	31.2	12.6	3.6	8.8	43.8	-2.5	2.6	0.0	0.7	0.0

Pernambuco	12.9	13.0	0.0	1.3	2.8	21.9	1.9	7.6	64.5	-2.8	0.4	0.0	1.0	0.0
Piauí	24.8	9.8	0.1	0.2	2.4	0.9	90.8	2.4	3.2	2.2	0.2	0.1	0.2	23.3
Rio Grande do Norte	12.5	23.9	0.0	1.3	8.0	1.5	0.0	9.8	79.4	-2.8	1.9	0.0	2.4	0.0
Ceará	3.1	2.1	0.0	9.3	6.8	18.8	5.5	16.7	42.9	-3.0	0.1	0.0	0.4	0.0
Sergipe	7.3	33.7	0.0	0.0	22.6	12.4	0.9	0.0	64.1	4.2	7.6	0.0	0.0	12.4
Center-West														
Goiás	36.0	10.6	0.1	0.9	19.4	36.8	1.2	40.8	0.8	4.9	2.1	0.2	4.3	48.0
Mato Grosso	129.8	14.3	0.1	5.9	20.6	4.8	50.9	14.8	3.0	8.5	2.9	0.1	2.1	59.8
Mato Grosso do Sul	72.4	20.2	1.1	11.7	11.9	6.9	6.6	35.4	26.5	4.9	2.4	1.5	7.2	68.2
Fed. District	1.6	27.5	0.0	0.0	13.9	24.2	0.0	51.3	10.7	8.4	3.8	0.0	14.1	30.6
Southeast														
Minas Gerais	91.0	15.5	0.3	2.4	12.64	24.8	8.5	50.9	0.4	0.99	0	2.5	0.0	0.0
Rio de Janeiro	3.8	9.2	0.0	1. 9	15.48	8.9	27.4	42.1	4.2	0.35	1.4	0.1	3.9	4.5
Espírito Santo	7.6	16.9	0.0	0.0	16.73	28.6	10.0	44.7	0.0	-0.86	2.8	0.6	7.6	3.7
São Paulo	55.6	22.4	0. 9	2.0	33.35	33.3	12.1	16.3	2.0	-1.38	7.5	3.2	3.7	14.2
South														
Paraná	72.0	36.2	0.2	1.04	38.85	31.6	21.6	5.8	1.0	10.33	14.1	2.5	2.1	35.5
Rio Grande do Sul	84.5	32.2	0.0	1.02	22.95	20.5	32.7	21.0	1.9	5.37	7.4	1.4	6.7	21.2
Santa Catarina	25.2	27.0	0.0	0.99	19.43	29.6	41.3	8.4	0.3	-1.48	5.3	5.6	2.3	20.7

* Total area of changes within each state equals 100%.** Other processes include numbered as 6,7,9,10 in the Table 2. *** Hereafter types of transitions match with the processes listed in Table 2. *** Comparison of the sum of cropland and planted forest area changes estimated by analysis of statistics (CAS and FAS) and remote sensing data (FAS and FAM), %.

Table 4. Main types of changes in agricultural and forestry land use in the states and regions of Brazil, 2001/2002 — 2011/2012[1]

Process (according to remote sensing data)	Type of changes[2]	Regions
Deforestation	Insignificant	The North: Acre (NA), Amazonas (NA), Amapá (N), Roraima (A)
Conversion to cropland	Forests → seasonal crops	The North: Rondônia (A)
Conversion to cropland	Savannas → seasonal crops	The Northeast: Maranhão (A), Piauí (A), Sergipe (NA)
Conversion to cropland	Savannas →seasonal and perennial crops	The Northeast: Bahia (A)
Agricultural transformations	Seasonal crops → perennial crops	The North: Pará (NA) The Southeast: Rio de Janeiro (A) Espírito Santo (A)
Agricultural transformations	Seasonal crops → pastures	The Northeast: Alagoas (A), Paraíba (A), Pernambuco (A), Rio Grande do Norte (NA), Ceará (NA)
Agricultural transformations	Seasonal crops, pastures → seasonal and perennial crops	The Southeast: São Paulo (A)
Agricultural transformations	Perennial crops → seasonal crops	The North: Tocantins (A)
Conversion to cropland, afforestation	Pastures → seasonal and perennial crops, forest plantations	The Southeast: Minas Gerais (NA)
Conversion to cropland, afforestation	Pastures → seasonal crops, forest plantations	The South: Rio Grande do Sul (NA); The Central-West: Mato Grosso (NA), Mato Grosso do Sul (NA), Goiás (A), Fed. District (A)
Agricultural transformations, afforestation	Pastures, perennial crops → seasonal crops, forest plantations	The South: Paraná (A)

[1] – N – natural processes, A – anthropogenic processes, NA – both natural and anthropogenic processes.
[2] - Only changes caused by agricultural development and creation of forest plantations.

cover changes in Brazil, being this sector a trigger of the recent economic growth of the country and providing 28% of the total national value of exports (FAO 2012). Its contribution to the LULC changes can be considered as of highest value for the states of the Center-West and the South, but it was also significant for different states in all other macroregions.

In the North (Amazonia) the LULC changes were not so significant in relation to the size the states, which make part of this macroregion. The only exception is the state of Tocantins, where the cultivated area under seasonal crops during 2001—2012 nearly doubled and has reached more than 0.5 million ha, or nearly 2% of the total agricultural area in this state. More than 90% of this area was planted by soybeans. The area under this crop has also increased significantly in the other Amazonian state Rondônia (by more than 40% or, 140.000 ha). At the same time, the area of coffee plantations in this state decreased by 119.000 ha (49% comparing with 2001), which suggests that perennial plantations could be converted into fields.

In the Northeast, the change of the area under seasonal crops involves from 0.8 to 4.2% of the area of each state of this macroregion. The most profound changes have occurred in the state of Alagoas (-57.3%), where seasonal crops planted area has considerably decreased (by 106.700 ha), while the area under coffee trees increased by 42.600 ha. In Bahia, Maranhão, Piauí and Sergipe states the seasonal crops area considerably increased: by 18.5% (544.000 ha) in the first one, and in two others it has almost doubled, increasing by 549.000 and 92.000 ha respectively. This is due to both the formation of a new large agricultural region of MATOPIBA[1] where soybean and cotton are expanding, also due to increase of the area of sugar cane plantations in a coastal strip along the Atlantic Ocean. At the same time, the area under seasonal crops decreased significantly in the states of Alagoas, Pernambuco, Rio Grande do Norte and Ceará. In the state of Bahia, particularly in its western part, the area of coffee plantations increased. In this state, and also in the state of Maranhão, large areas of forest plantations (307.000 and 168.000 ha respectively) were created during the first decade of the 21st century.

In the states of the Southeast different directions of the dynamics of the LULC changes was detected. In the state of Minas Gerais, area under grains (mainly soybeans), sugar cane, and both coffee and forest plantations increased considerably. The total increase of the area under seasonal crops and sugar cane amounts to about 1% of this state area; coffee and forest plantations area registered 2.5% increase. The most developed parts of this state have experienced conversion of pastures into agricultural lands; at the same time, unused slopes of the Plateau of Brazil started to be used for new plantations of coffee, which made the Minas Gerais state ranking first in Brazil by the volume of coffee harvest. Expansion of the area of sugar cane plantations by 1.3 million ha, or by 40% compared with 2005, was the main process of land use changes in the state of São Paulo, harvesting this state ¾ of this crop in Brazil. At the same time, the area of coffee plantations decreased both in São Paulo and in the Espírito Santo states. A considerable increase of the area under forest plantations in Minas Gerais, São Paulo and Espírito Santo states (855.000, 240.000 and 78.000 ha respectively) is worth attention. It can be explained by both the growing demand for wood charcoal, and the development of and the cellulose and paper production.

In the South, the state of Paraná registered a significant increase in the area under grains and sugar cane (by 2 million and 200.000 ha respectively), along with reduction of the area of coffee plantations by 60.000 ha and growth of the area of forest plantations by 0.6 million ha during 2001—2012. In the state of Rio Grande do Sul, similar changes in agricultural land use were recorded, but in this subtropical state sugar cane is not planted. At the same time, the areas under irrigated rice have increased here by 126.000 ha; the growth of the area under this crop accounts to 0,4% of the total area of the state. In another state of the South, Santa Catarina, planted area of irrigated rice also has increased, though not so considerably, while the area under grains decreased almost by 10%. In all states of this macroregion, large forest plantations were established (743.000 ha in Rio Grande do Sul, 489.000 ha in Santa Catarina and 221.000 ha in Paraná).

The Center-West macroregion faces prompt agricultural development of the Savanna areas, including both colonization of virgin lands and conversion of natural pastures. Therefore, a considerable increase of the area under seasonal crops is characteristic of all states of this macroregion: it grew by 8.5% of the total state area in Mato Grosso and

[1]Acronym, meaning the first letters from the names of four states: Maranhão, Tocantins, Piauí and Bahia.

almost by 5% in Mato Grosso do Sul and Goiás states. The area under sugar cane has also considerably expanded here. In all states of this macroregion large forest plantations were established, reaching those nearly 1 million ha in the state of Mato Grosso do Sul.

To conclude, agricultural colonization can be considered as the main driving force of the LULC changes in Brazil, being of continuous influence not only in 2001—2012, but also earlier. Half a century ago an attempt of agricultural development in Amazônia was made, which, however, didn't become as large-scale as it was thought (Naumov 1983). In the 1980s, colonization of the Savanna has started, mainly in the Center-West (Naumov 2010). This colonization campaign brought more notable results; according to the estimates, about 90 million ha, including 60 million ha of cropland, were developed (MMA, 2009). This campaign is still under way, mostly at the transition zone between Savanna and Amazon forest. At the same time, considerable changes occurred in agricultural specialization and land use in the previously developed Southeast and South macroregions (Naumov 2005; Naumov 2012). In general, the most considerable recent changes in agricultural land use in Brazil were almost everywhere caused by the expansion of soybean; during 2001—2012 its planted area in Brazil has doubled, reaching 28 million ha by 2012 (CONAB). Particularly noteworthy are the changes in the area under coffee plantations. By 2012, the coffee planted area in Brazil has dropped by 129.500 ha, or 6% compared with 2001. In the meantime, the main coffee plantations have shifted to Minas Gerais, increasing in this state by 137.300 ha during 2001—2012, and also have expanded in the Northeast, in Bahia. In the Amazon macroregion, in Rondônia state, coffee plantations area has dropped twice compared with 2001, when it was lager there, then in São Paulo, formerly main coffee producing state in Brazil. The area of rice cultivation changed considerably. In the South this crop is mostly planted in Rio Grande do Sul (more than 2/3 of the gross national harvest of this crop), being this subtropical region historically the area of irrigated rice cultivation (CONAB). In the 1980-s due to colonization of the Savanna the upland rice became a pioneer culture in the Center-West. However, in 2015 only 13% of the total planted area of this crop was located in the tropical part of Brazil, and even there 11% of the total area was under irrigated rice. This is a consequence of implementation after 2012 of nature protection laws, limiting the development of forests and declaring tropical rivers valleys as water protection zones (Acts 12.651 of May 25, 2012 and 12.727 of October 17, 2012 (Codico..., 2012). As a result, the acreage under rice decreased considerably nearly everywhere, except Rio Grande do Sul and Santa Catarina.

Unfortunately it was not possible to consider data on the area of pastures. The problem stems from the lack of available statistical data for the studied period, as the area of pastures by states is reported only during agricultural censuses, the latest one held in 2006. Another reason is considering pasturing as non-agricultural land use. The area of natural pastures in Brazil, meanwhile, permanently decreases. According to IBGE, after 2006 the area of improved in Brazil exceeded that of "natural" ones. The total area of the improved pastures, considered to appear "in good state" is estimated at 9.25 million ha, other 9.9 million ha are "degraded" improved pastures. Total area of "natural" pastures is estimated at 52.7 million ha, while 44 million ha were under seasonally cultivated croplands, 11 million ha under perennial plantations, 36 million ha under planted forests, and 51 million ha under nature protection areas and natural reserves (IBGE. Mudanças..., 2016).

FORESTRY

Processes related to forestry and other commercial and subsistence use of forests (the second ones still are important in Amazonia) play an essential role in LULC changes in Brazil (22 of 96 identified types of changes). According to national statistics, in 2012 Brazil ranked 2nd in the world by forest area amounting to 561 million ha, or about 60% of the national territory (IBGE 2002). Throughout the history of economic

[2] *In Brazil, soybean is considered as a grain crop.*

development forests were actively cleared in Brazil. Consequently, it is estimated in the Amazon biome between 15 and 18% loss of natural environments; in the Savanna, Pampas and Caatinga biomes 50% and in the Atlantic Forest 88% (GEO Brazil 2002; MMA 2012; UNEP 2016).

After 1970-s, when the large-scale colonization of Amazonia started, the problem of deforestation in Amazonia draw great attention of the world community. Nowadays, Brazilian government implemented public policies and environmental control which enabled reducing the deforestation of the Amazon (Laurance et al. 2002; Chazdon 2008; INPE 2015). In 2016, the Environmental Monitoring Program of the Brazilian Biomes was created by the Ministry of the Environment (MMA), whose purpose is to expand the mapping and monitoring of deforestation and land cover for all Brazilian biomes.

It is also important to stress, that regional differences in deforestation rates in Brazil depend on the nature protection legislation and public policies. Forest Code (BRASIL 2012) established a legal protection norm of 80% of total area of each rural land property for the Amazon forest biome, of 35% for the areas under Savanna, located in the so-called Legal Amazon region, and of 20% for the other areas under Savanna for the rest of biomes. Moreover, the protection of native vegetation in public reserves is consistently low outside the Amazon and below 5% for most biomes. As the largest part of area under native vegetation in each Brazilian biome is still found in private ownership, it is hard to control the accomplishing of the nature protection legislation (Ferreira et al. 2012), and to get the data for LULC analysis. In total, from 21 to 30 million ha is the estimated size of areas in Brazil, where natural vegetation should be restored and/or protected (Sparovek et al. 2010; Soares-Filho 2014)

The analysis of statistical data on protected areas of Brazil allows to evaluate their possible contribution, in particular, on reforestation processes (Protected Planet 2015). During 2002–2012, 17 natural reserves, 80 national parks, 205 managed natural areas, 83 protected areas with sustainable use of natural resources were established, mostly in the North and Southeast macroregions. However, the status of approximately 700 protected areas is not defined yet. We can assume, that the reforestation processes were driven mainly by expanding of protected areas in Amazonian states and in three states of the Northeast (Maranhão, Pernambuco, Piauí).

Forest plantations, created for production of commercial timber, cellulose and wood charcoal, which rapidly expands in Brazil, is another driving force of the LULC changes. In 2003 total national area of forest plantations in Brazil reached 1.6 million ha, 73.7% under eucalyptus and 25.3% under pine, with minor share of araucaria plantations (mostly in the state of Paraná) and acacia (in the state of Amapá) (BRASELPA 2003). By 2012, total area under plantations of eucalyptus and pines in Brazil reached 6.7 million ha (ABRAF 2013).

CONCLUSIONS AND FINAL REMARKS

The complex analysis of LULC changes in Brazil during 2001—2012 comprised land cover dynamics study based on satellite imagery data, and land use dynamics study, based on agricultural statistics data. For both approaches, the results were generalized at the regional level, being the states of Brazil basic units of research. Most of these states, surpass by area medium and even large European countries, which allowed to draw general conclusions on LULC changes and their driving forces. Nevertheless, we got reliable results, which can be discussed and developed in the further studies.

According to the data on conditions of land cover, in 2001—2012 the main processes of its transformation in the states of Brazil were driven by both natural and anthropogenic factors. Agriculture and, in large extent, deforestation are among the processes of anthropogenic origin, flooding and unwatering are the principal natural processes. Changes of vegetation cover on agricultural lands and reforestation are the processes of mixed natural and anthropogenic nature as they depend from both natural dynamics of vegetation, along with creation of forest plantations and conversion of pastures.

In general, the contribution of natural factors on LULC changes in Brazil is higher in the North (except Tocantins) and the Northeast (except Piauí and Pernambuco) macroregions. In Center-West and South macroregions anthropogenic factors make larger contribution. The latter are: development of agriculture, generally colonization as the country still has the considerable resources of undeveloped lands, and only 1/3 of its territory is used for cropping; conversion of pastures into agricultural lands; conversion of natural pastures into improved ones.

Comparison of the data on particular types of land cover changes and on the LULC transformation processes related with agricultural development shows for the most densely populated and developed states of Brazil the general correlation in trends, rather than the complete coincidence. According to the MODIS data, the areas with an increase of forest cover are larger by size, than statistics gives for forest plantations expansion. We assume that this is an evidence of the dualistic nature of this process, which depends from both natural and anthropogenic factors. Generally, the size of area of changes in the structure of cultivated lands is statistically less, than the area of transitions included in the "cultivation" category estimated assessed through the remote sensing data.

The suggested technique of comparative analysis of land use changes basing of the remote sensing data of medium spatial resolution and the data of agricultural statistics has shown its potential for identification of the main drivers of LULC transformation at the macro-regional level. Based of comprehensive geographical approach, it could be applied for different purposes, such as environmental assessment and territorial planning.

ACKNOWLEDGEMENTS

The research project was financially supported by the RFBR (Project 15-05-06186) and research project «Geographical problems of social and economic development of countries of the world» at the Faculty of Geography of MSU.

REFERENCES

Alekseeva N., Klimanova O., Hazieva E. (2017). Global databases on land cover and prospects of their application for the present-day landscape mapping. Izvestiya RAN. Seriya geograficheskaya, №1, pp. 126-139. (In Russian)

Associação Brasileira de Produtores de Florestas Plantadas (ABRAF) (2013). Anuário estatístico 2013 ano base 2012. ABRAF. – Brasília.

Barkmann, J., Helming, K., Muller, K., Wiggering, H. (2004) Multifunctional landscapes: towards an analytical framework for sustainability assessment of agriculture and forestry in Europe. Müncheberg: Centre for Agricultural Landscape and Land Use Research, 422 p.

Barten, F., Fustukian, S., Haan, S. (1996). The occupational Health Needs of Workers: The Need for a New International Approach. Social Justice, 23(4), pp. 152-163.

BRASELPA (2003). Asociaçao do Selvicultores do Brasil. Available at: http://www.braselpa.com [Accessed 20 Nov. 2017].

BRASIL (2012). LEI 12.651, DE 25 DE MAIO DE 2012. Diário Oficial da República Federativa do Brasil. Poder Legislativo, Brasília, DF: 28 de maio, 2012.

Channan, S., Collins K., Emanuel W. (2014). Global mosaics of the standard MODIS land cover type data. University of Maryland and the Pacific Northwest National Laboratory, College Park, Maryland, USA.

Chazdon, R. (2008). Beyond deforestation: restoring forests and ecosystems services on degraded lands. Science 320, 1458–1460. DOI: 10.1126/science.1155365.

Companhia Nacional de Abastecimento (CONAB). Available at: http://www.conab.gov.br/conteudos.php?a=533&t=2 [Accessed 20 Nov. 2017].

Departamento Intersindical de Estatística e Estudos Socioeconômicos (2011). DIEESE. Estatísticas do meio rural 2010-2011. 4.ed. / Departamento Intersindical de Estatística e Estudos Socioeconômicos; Núcleo de Estudos Agrários e Desenvolvimento Rural; Ministério do Desenvolvimento Agrário. -- São Paulo: DIEESE; NEAD; MDA.

Food and Agriculture Organization of the United Nations (2015). FAO. Statistical pocketbook-world food and agriculture. Rome: FAO. 231 p.

Ferreira C., Pardo R., Benites V., Polidoro J., Naumov A. (2009). Classificação semi-automática de imagens multitemporais Landsat-5 para análise do padrão de uso agrícola das terras do Sudoeste Goiano. In: XIV Simpósio Brasileiro de Sensoriamento Remoto, Natal. Anais XIV Simpósio Brasileiro de Sensoriamento Remoto. São José dos Campos: INPE, pp. 5781-5788.

Ferreira, J., Pardini, R.; M. J. P., Fonseca, C. , Pompeu, P. , Sparovek G., Louzada, J. (2012). Towards environmentally sustainable agriculture in Brazil: challenges and opportunities for applied ecological research. Journal of Applied Ecology, 49, pp. 535–541. DOI: 10.1111/j.1365-2664.2012.02145.x

Ferreira Manuel E., Ferreira J., Latrubesse E., Miziara F. (2013). Journal of Land Use Science: Considerations about the land use and conversion trends in the savanna environments of Central Brazil under a geomorphological perspective. DOI: 10.1080/1747423X.2013.845613

Ferreira, L. G., Sousa, S. B., Arantes, A.E. (2014). Radiografia das pastagens do Brasil. Goiânia: LAPIG/UFG. 214 p.

Foley, J., Ramankutty, N., Brauman, K., Cassidy, E., Gerber, J., Johnston, M., Mueller, N., O'Connell, C., Ray, D., West, P., Balzer, C., Bennett, E., Carpenter, S., Hill, J., Monfreda, C., Polasky, S., Rockstrom, J., Sheehan, J., Siebert, S., Tilman, D., ,Zaks, D. (2011) Solutions for cultivated planet. Nature, 478, pp. 337–342. DOI: 10.1038/nature10452

Global Land Cover Facility (GLCF). MODIS Land Cover. Available at: http://glcf.umd.edu/data/lc/ [Accessed 20 Nov. 2017].

Global Mapping of Agricultural Production Systems (2006). Pro-Poor Livestock Polity Initiative Meeting Report. Bangkok, 4–6 April 2006. Ed. by Robinson T., Thronton P. FAO, 2006. 79 p.

GEO Brazil (2002). Global Environment Outlook in Brazil. Brasilia, p.101

Instituto Nacional de Pesquisas Espacias (INPE) (2015). Monitoramento da Floresta Amazonica Brasileira por Satelite e Projeto Prodes. Instituto Nacional de Pesquisas Espaciais, Sao Jose dos Campos.

IBGE. (2016) Mudanças na cobertura e uso da terra do Brasil 2000 — 2010 — 2012 — 2014. Rio de Janeiro, 30 p.

Insituto Brasileiro de Geografia e Estadistica. (IBGE) (2002). Available at: www.ibge.br [Accessed 20 Nov. 2017].

Klimanova O., Tret'yachenko D., Alekseeva N., Arshinova M., Kolbovskij E., Grinfel'dt Yu. (2017) Changes of land cover on the continental and zonal levels: classification and mapping. Landshaftnye izmereniya ustojchivogo razvitiya: Issledovanie – Planirovanie – Upravlenie. — Tbilisskij gosudarstvennyj universitet Tbilisi. (In Russian)

Lapola, D., Martinelli, L., Peres, C., Ometto, J., Ferreira, M., Nobre, C., Aguiar, A., Bustamante, M., Cardoso, M., Costa, M., Joly, C., Leite, C., Moutinho, P., Sampaio, G., Strassburg, B., Vieira, I. (2014). Pervasive transition of the Brazilian land-use system. Nature Climate Change, v.4, pp. 27-35.

Laurance, W., Albernaz, A., Schroth, G., Fearnside, P., Bergen, S., Venticinque, E. (2002). Predictors of deforestation in the Brazilian Amazon. Journal of Biogeography, 29(56), 737-748. DOI:10.1046/j.1365-2699.2002.00721.x

Lewinsohn, T.; Prado P. (2005). How many species are there in Brazil? Conservation Biology, 19, pp. 619–624.

Loveland T., Reed B. , Brown J. , Ohlen D. , Zhu Z., Yang J L., Merchant W. (2000). Development of a global land cover characteristics database and IGBP DISCover from 1 km AVHRR data. International Journal of Remote Sensing. 216–7, pp. 1303–1330.

MMA (2009). Relatorio tecnico de monitoramento do desmatamento no bioma Cerrado, 2002 a 2008: dados revisados. Centro de sensoriamento remoto, IBAMA, Brasília.

Monfreda C., Ramankutty N., Foley J. A. (2008). Farming the planet: 2. Geographic distribution of crop areas, yields, physiological types, and net primary production in the year 2000. Global Biogeochem. Cycles. V. 22. 19p. DOI:10.1029/2007GB002947

Millenium Ecosystem Assessment (MEA). Ecosystems and human well-being: Synthesis. Washington: Island Press, 2005. 155p.

Naumov A. (2005) Land use in Brazil: Major contemporary changes and their driving forces. Understanding Land-Use and Land-Cover Change in global and Regional Context. Ed. E.Milanova, J. Himiyama, I. Bičik. Enfield (NH), USA, Plymouth, UK. Pp. 208–223.

Naumov A. (2010).Spatial scenarios of the world agriculture development: the modern agricultural colonization in South America. Geografiya mirovogo razvitiya. Pod red. L. M. Sincerov, N. A. Sluka. T. 2. KMK Moskva, pp. 407–422. (In Russian)

Naumov A., Oliveira Ronaldo P., Pardo P., Turetta A. (2012). Balanced fertilization for sustainable development of agriculture in the savannas of South America: Towards a geographical approach. Geography, Environment, Sustainability. 5(4), pp. 84–95.

Naumov A. (1983). Agricultural development of Brazilian Amazonia. Latinskaya Amerika, №6, pp. 50-59. (In Russian)

Naumov A. (2013). Problems and prospects of the modern agricultural colonization in South America. Latinskaya Amerika. T. 466, № 7. pp. 36–49.(In Russian)

Richards, P. D., Walker, R. T., Arima, E. Y. (2014). Spatially complex land change: The Inderet Effect of Brazil's agricultural sector on land use un Amazonia. Global Environmental Change, Nov. 1; 29: 1-9. DOI: 10.1016/j.gloenvcha.2014.06.011.

Protected Planet. Available at: https://www.protectedplanet.net [Accessed 20 Nov. 2017].

Ramankutty N., Evan A. T., Monfreda C., Foley J. (2008). Farming the planet: 1. Geographic distribution of global agricultural lands in the year 2000. Global Biogeochem. Cycles. V. 22. 19 p. DOI:10.1029/2007GB002952

Stallman, H. R. Ecosystem services in agriculture: Determining suitability for provision by collective management. Ecological Economics, Vol. 71, 2011, pp. 131-139. DOI: 10.1016/j.ecolecon.2011.08.016

Sparovek, G., Berndes, G., Klug, I.L.F., Barretto, A.G.O.P. (2010) Brazilian agriculture and environmental legislation: status and future challenges. Environmental Science and Technology, v.44, pp. 6046–6053. DOI: 10.1021/es1007824

Soares-Filho, B., Rajao, R., Macedo, M., Carneiro, A., Costa, W., Coe, M., Rodrigues, H., Alencar, A. (2014) Cracking Brazil's Forest Code. Science, v. 344, pp. 363-364. DOI: 10.1126/science.1246663

Uhling A., Goldemberg J., Coelho S.T. (2008) O uso de Carvalho vegetal na indústria brasileira e o impacto sobre as mudancas climáticas. Revista Brasileira de Energía, 14(2), pp. 67—85.

UNEP (2016). GEO-6 Regional Assessment for Latin America and the Caribbean. United Nations Environment Programme, Nairobi, Kenya.

World Programme for the Census of Agriculture. Available at: http://www.fao.org/economic/ess/ess-wca/ru/ [Accessed 20 Nov. 2017].

Received on November 18th, 2017 Accepted on November 22nd, 2017

Yulia Greenfieldt is Senior Scientist at the Department of World Physical Geography and Geoecology, Faculty of Geography, Lomonosov Moscow State University. She received her Ph.D. in Geography from Lomonosov Moscow State University in 2005. Her research work deals with ecological problems, transformation of land cover and natural environment, geoecological assessment of land changes at regional and local levels, land-use planning in South America.

Oksana Klimanova is Associate Professor at the Department of World Physical Geography and Geoecology of Lomonosov Moscow State University, lecturer for courses "Physical Geography of World", "Geoecology", "Urban ecology and sustainable cities". Her research interests focus on spatial aspects of man-nature interactions at different spatial levels, regional environmental assessment, cultural landscapes and urban a planning. Main publications: Environmental Challenges for Tropical Areas (2012, with Alexeeva N.), Regional Environmental Studies: Natural and Anthropogenic Factors of Regionalization (2014), Multiscale Dimensions of Cultural Landscapes: mapping and typology at different levels (2015, with Kolbowsky E.), Global Land Cover Databases and its use for Present-day Landscapes Mapping (2017, with co-authors).

Alexey Naumov was graduated from the Faculty of Geography of Lomonosov Moscow State University (MSU), where in 1990 he also got his Ph.D degree. Dr. Naumov is Associate Professor and Head of Department of Social and Economic Geography of Foreign Countries at the Faculty of Geography of MSU, lecturer for courses "Geography of World Agriculture" and "Social and Economic Geography of Latin America". In 2001-2011 he also served as Coordinator of programs of the International Potash Institute in Latin America. His research interests focus on spatial aspects of land use, agricultural development, and modeling of agricultural systems. Main publications: Land Use in Brazil: Major Contemporary Changes and Their Driving Forces (2005), Agricultural geography of the world (2004), Spatial scenarios of world agriculture development: contemporary agricultural colonization in South America (2010), Balanced fertilization for sustainable development of agriculture in the savannas of South America: Towards a geographical approach (2012, with co-authors), Problems and prospects of the modern agricultural colonization in South America (2013).

Rachel Bardy Prado is graduated in Biological Sciences from the Federal University of São Carlos, has master and doctor degree in Science in Environmental Engineering from the University of São Paulo, specializing in Planning and Water Management from the Federal University of the Amazon (Brazil). She is currently a researcher at Embrapa Soils since 2003 and has been working in monitoring and planning of ecosystem services, especially water resources. She leads the Ecosystem Service Embrapa Research Network. Currently she is accredited in the Post-Graduation in Engineering of Biosystems of the Fluminense Federal University in Rio de Janeiro, Brazil.

Darya Tretyachenko graduated in 2001 from the Faculty of Geography of the Lomonosov Moscow State University (MSU). She is a GIS-specialist at the Department of World Physical Geography and Geoecology, Faculty of Geography, Lomonosov Moscow State University. Her research interests focus on GIS-mapping and spatial analysis of land-use/land cover patterns at global and regional level.

Yosef Akhtman[1], Elena Golubeva[2], Olga Tutubalina[2], Mikhail Zimin[2]*
[1]Geodetic Engineering Laboratory of École Polytechnique Fédérale de Lausanne (EPFL), Switzerland
[2]Faculty of Geography, M.V. Lomonosov Moscow State University, Russia
*** Corresponding author:** ziminmv@mail.ru

APPLICATION OF HYPERSPECTURAL IMAGES AND GROUND DATA FOR PRECISION FARMING

ABSTRACT. Crops, like other plants, clearly react to various changes in both natural and anthropogenic factors (herbicides, pesticides, fertilizers, etc.), which affects the amount of phytomass, its fractional composition, and developmental and physiological state of the plant, and, accordingly, is reflected in the spectral image. Data on spectral characteristics of plants allow users to determine quickly and with a high degree of reliability various indicators of the state of agricultural crops and thus improve the efficiency of agro-technical practices and the use of land resources and facilitate the implementation of the precision farming concept. Reflective properties of plants (and hence crops) carry a large amount of meaningful information about the species, stage of development, and morpho-physiological state, allowing determination of the interrelations between the spectrometric characteristics and temporal physiological parameters.

The paper presents the results of monitoring of the state of winter wheat and corn in experimental fields in southern and central Russia in the spring and summer of 2016.

KEY WORDS: remote sensing data, hyperspectral images, precision farming, spectral characteristics, agricultural crops

CITATION: Yosef Akhtman, Elena Golubeva, Olga Tutubalina, Mikhail Zimin (2017) Application of hyperspectural images and ground data for precision farming. Geography, Environment, Sustainability, Vol.10, No 4, p. 117-128
DOI-10.24057/2071-9388-2017-10-4-117-128

INTRODUCTION

Agriculture is one of the most successfully developing sectors of the Russian economy ensuring domestic needs of the country and success in foreign markets. In modern realities, sustainable development of agriculture is inextricably linked with precision farming and innovative information technologies. Geo-intellectual services enhance the effectiveness of agricultural and related activities. Satellite and aerial monitoring allows assessing the condition of crops and the results of technical and meliorative measures, reduces the cost of production, and increases yield. The effectiveness of hyperspectral remote sensing methods for diagnosing the state and course of various processes in agriculture has been widely discussed in scientific literature in recent years (Borengasser et al. 2007; Thenkabail 2011; Thenkabail 2014; Haboudane 2004; Liebisch 2015 etc.). A new generation of compact, light and relatively inexpensive hyperspectral cameras (Constantin 2017) installed on unmanned aircraft systems (UAS) (Liebisch et al. 2015; Constantin et al. 2015) has emerged. A significant reduction in the cost of these technologies has facilitated the use of hyperspectral remote sensing data (RSD) in precision farming.

Precision farming is a combination of technologies, tools, and decision-making systems in the integrated production and information system of agriculture, aimed at long-term improvement of efficiency and productivity for specific local conditions and minimization of the negative impact on the environment. The concept of precision farming is based on the concept of heterogeneity of plant growth characteristics within a single field. In this regard, various land management activities (e.g., application rates of fertilizers, lime, herbicides, and pesticides, irrigation, etc.) are carried out on each individual small plot. To implement the concept of precision farming, constantly updated high-detail cartographic material is necessary, which can be provided by remote sensing, particularly, UAS and hyperspectral methods. Timely assessment of the agricultural land conditions based on RSD is a key tool in implementing agro-services for regular monitoring of large areas.

The tasks of precision farming in relation to operational monitoring and agro-technical practices can be facilitated by RSD, especially ultra-high resolution imagery based on the analysis of sets of statistically reliable empirical information on the spectral characteristics of agricultural plants. Spectral images of agricultural plants vary depending on the heterogeneity of both natural conditions of the fields (e.g., hydrothermal, soil, geomorphological) and the agro-technical practices (tillage methods, irrigation, use of fertilizers, herbicides, pesticides, etc.) (Yakushev and Petrushin 2013; Thenkabail et al. 2014).

An important element of this crop monitoring system is based on specific identified relationships between the spectral characteristics and physiological parameters of plants in different periods of vegetation growth (Sidko et al. 2009). Such information allows users to determine quickly and with a high degree of reliability the various indicators of the state of agricultural crop and improve the efficiency of agricultural practices and the use of land resources in general (Zimin et al. 2014; Knizhnikov et al.2011).

The purpose of this study is to analyze the results of monitoring of the state of agricultural crops (winter wheat and corn) based on hyperspectral surveying and ground measurements. The following tasks have been addressed:

- ground measurements of the morphometric and spectral parameters and characteristics of winter wheat and corn in different vegetation periods and various applications of agro-technical practices were conducted;

- the technology of agricultural crops monitoring using a miniature hyperspectral camera was tested;

- correlation dependency between ground and aerial data using these quantitative data was obtained; and

- maps for experimental fields, reflecting the current state of agricultural crops, were compiled.

MATERIALS AND METHODS

The crops subjected to various agro-technical practices on the experimental fields of Syngenta company were studied in southern and central Russia in the spring and summer of 2016. In the Krasnodar region, on the experimental fields of winter wheat, the effects of various seed dressing were considered on test sites. To assess the drought resistance of various corn hybrids, three remote sensing surveys and ground-based studies were conducted on experimental fields in the Krasnodar and Stavropol regions of Russia. The ground-based studies included: spectroradiometric measurements (ASD FieldSpec 3 Hi-Res, OceanOptics Flame, and OceanOptics USB2000+ spectroradiometers), identification of the morphometric parameters of plants (height, density of crops, size, the number of ears of wheat or corn, etc.), measurement of the production of green phytomass (wet and absolutely dry weight), determination of the presence of weeds, and collection of samples for biogeochemical analyzes to obtain reference data. Hyperspectral survey of agricultural crops was carried out by a miniature hyperspectral camera Gamaya (41 spectral channels in the range 470-904 nm), installed on the "Geoscan" UAS, in different phenological stages of plants.

Our approach implied the simultaneous acquisition of ground and remote data. The ground-based spectroradiometric measurements were performed using calibration panels to obtain reflectance values. This allowed us to compare material from different studies and to obtain highly reliable results.

For the purpose of calibrating the UAS-obtained hyperspectral survey data, ground-based spectroradiometric measurements were used; these surveys were conducted synchronously on the calibration sites represented by open surfaces with average brightness (homogeneous sections of dirt roads or parts of fields with insignificant projective vegetation cover).

Investigations on winter wheat crops were carried out in an experimental field in the Krasnodar region in April-June, 2016, on six strips where seeds were treated with various dressings. On each of these strips, test plots (Fig. 1) measuring 5x5 m were marked, within which, during the hyperspectral survey (April 8-9, May 6-7, and June 29), ground measurements were taken to obtain obtain the reference data. Ground work included measurements of the morphometric characteristics of vegetation cover, sampling of plants (for further geochemical research and assessment of phytomass and moisture), and vegetation spectroradiometry in natural conditions.

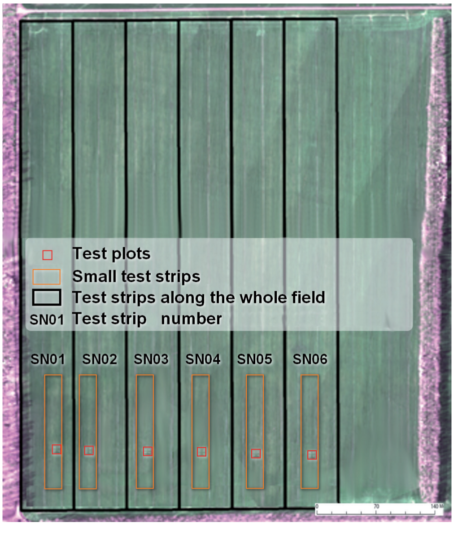

Fig. 1. An orthophotomosaic fragment of Gamaya camera images in natural colors, April 8, 2016, and the schematics of the locations of the test strips and plots

Because of specific characteristics of corn associated with its considerable height, the method of conducting fieldwork was somewhat different from the work with wheat. After the samples were taken, the cut plants were divided into parts (leaf surface, stem, ears) and separate morphometric measurements were conducted. Spectroradiometric studies were carried out only for the leaf surface of corn by placing leaves to create a 100% canopy under natural light conditions.

Thus, based on the combination of ground and remote sensing methods, reliable data have been obtained, which made it possible to identify the interrelationships between the spectral, geochemical, and morphometric characteristics of the studied plant species. The use of a series of integrated field studies is important for describing the correlation dependencies and understanding the relationships between spectral characteristics and vegetation developmental features (Bao et al. 2013; Sidko et al. 2009; Blackburn 1998), which is a reliable indicator of growing conditions (soil characteristics, meteorological conditions, relief, etc.), agro-technical practices, and vegetation stages.

Subsequent processing of the data obtained during fieldwork included spectral index, correlation, and expert approaches in the interpretation of hyperspectral imaging data, and was implemented both at the level of the test plots and strips and, in general, over the area of the experimental fields.

RESULTS AND DISCUSSION

The relative representativeness (wealth) of the information contained in the hyperspectral images compared with the multichannel imagery can be grasped by comparing the image obtained in the visible part of the spectrum, a natural color composite of the red, green, and blue channels, and the composite of the first three principal components for the 41-channel hyperspectral image (Fig. 2). Different colors in the chosen color palette correspond to the properties of the plants and here the difference in the detail of the object of the study, obtained by different types of survey, is clearly visible. The identification of such patterns and relationships of spectral characteristics with the biochemical and morphometric characteristics of the vegetation cover is one of the key directions in solving the problems of precision farming with respect to remote sensing methods and is the subject of such studies.

Hyperspectral imaging data were used to compile NDVI index maps based on two spectral channels (red [R] and near-infrared [NIR]). Fig. 3 clearly shows that when working with a wide spectral range, important differences in the state of plants are averaged and the difference in the values of the NDVI

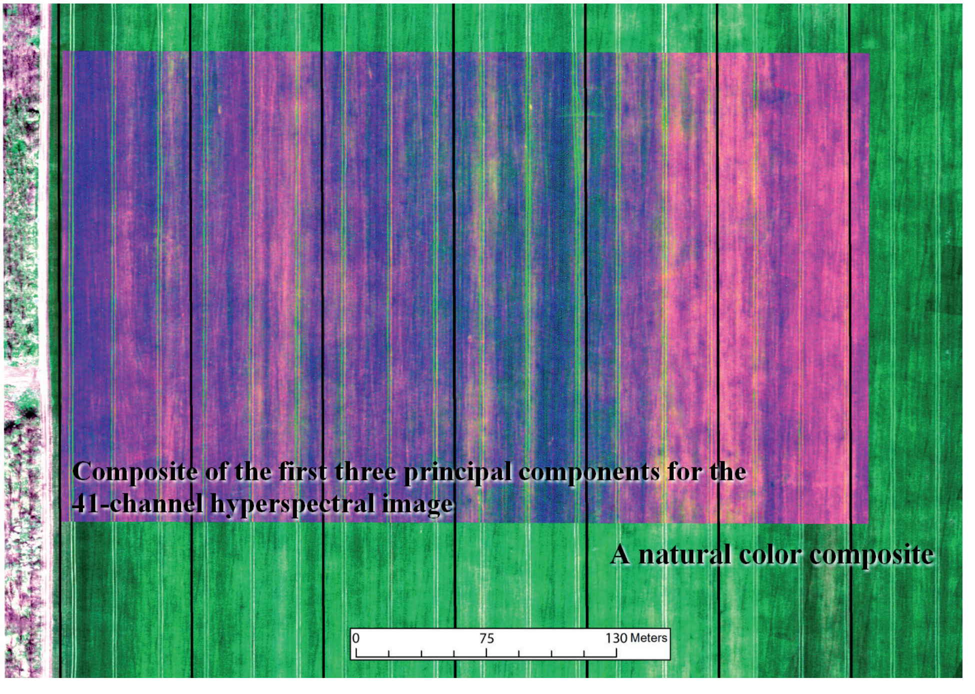

Fig. 2. The composite of the first three principal components for the 41-channel hyperspectral image (the Syngenta field). An enlarged fragment of the southern part of the field (April 9, 2016). of the locations of the test strips and plots

index is minimal. It should also be noted that the NDVI index maps represent only the relative characteristic of the phytomass value. It follows that the assessment of the state and characteristics of the vegetation cover should be based on a large number of narrow-spectral channels, which is realized by hyperspectral surveying.

The ground measurements data (spectral characteristics, phytomass, and nitrogen content in plants) and hyperspectral indices with reference to the survey data were used to compile maps of the green phytomass of the leaves of winter wheat (Fig. 4) and their nitrogen content (Fig. 5).

The maximum errors in assessing the indicators of crops on the compiled maps do not exceed 30% of the range of actually observed values. Based on the statistical processing of the data obtained at the three levels (test plots, small test strips, and test strips along the whole field (approx.1 km long) (Fig. 1), comparative diagrams were constructed (Fig. 6). As of April 8, 2016, the best state of plants was observed in the experiments SN01 and SN02, gradually deteriorating from SN03 to the worst conditions in SN05, and then sharply improving in SN06, almost to the level of SN01 and SN02. The experimental 5x5 m test plots, despite the heterogeneity of the state of the plants within each experiment, were representative for comparing the state of plants in various experiments, although their values were somewhat lower than on wider and longer test strips and the entire length of the strips of each seed dressing in the field.

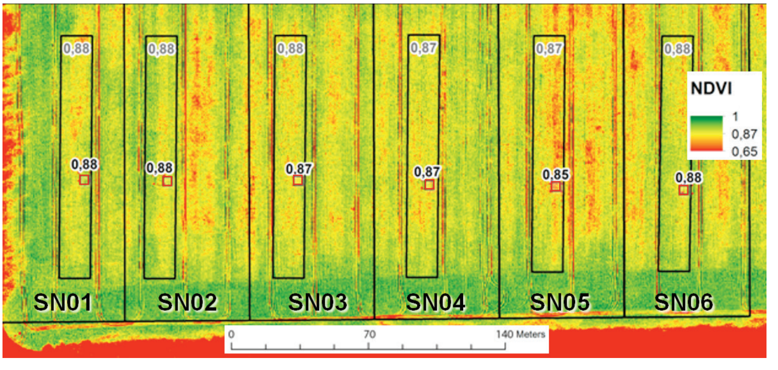

Fig. 3. Map of the NDVI index for the experimental winter wheat field, Yukka variety, April 8, 2016. Dark green, green, yellow, and red shades represent the maximum, medium, low, and zero values, respectively, of green phytomass. The numbers on the map show average NDVI values for the test plots (squares) and the larger strips (rectangles)

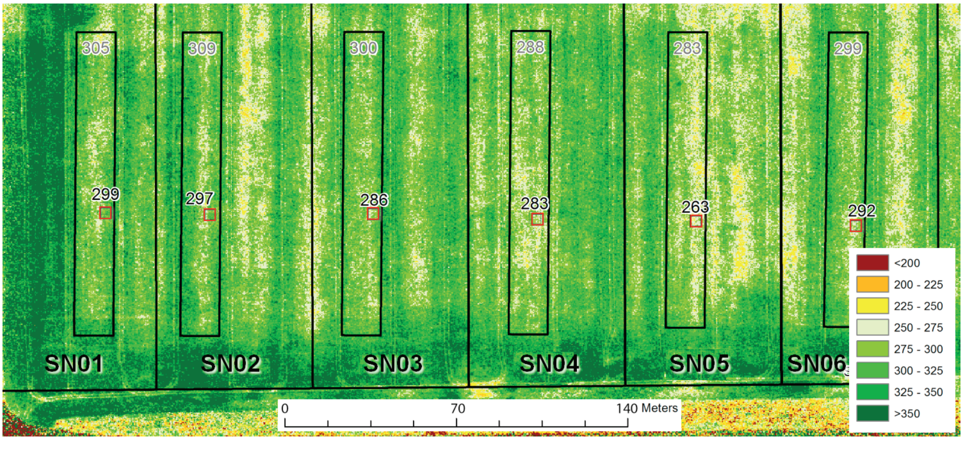

Fig. 4. Map of the green phytomass (g/sq.m.) of Yukka winter wheat leaves, April 8, 2016. An enlarged subset in the southern part of the field. The numbers on the map show the average phytomass values in the test plots (squares) and the larger strips (rectangles)

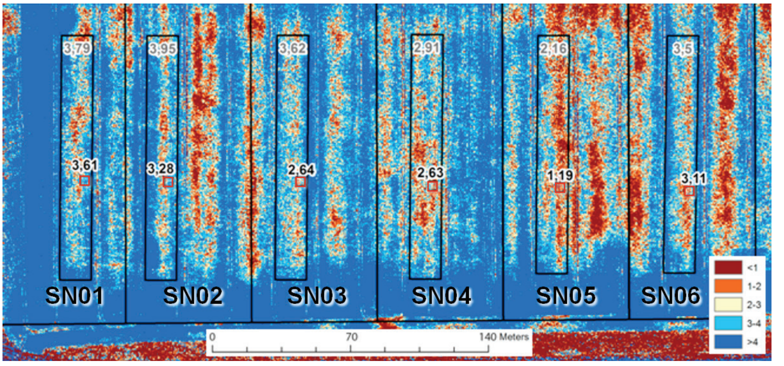

Fig. 5. Map of the nitrogen content (%) for Yucca variety winter wheat, April 8, 2016. An enlarged subset in the southern part of the field. The numbers on the map indicate the average values of nitrogen content of the plants of the test plots (squares) and the larger strips (rectangles)

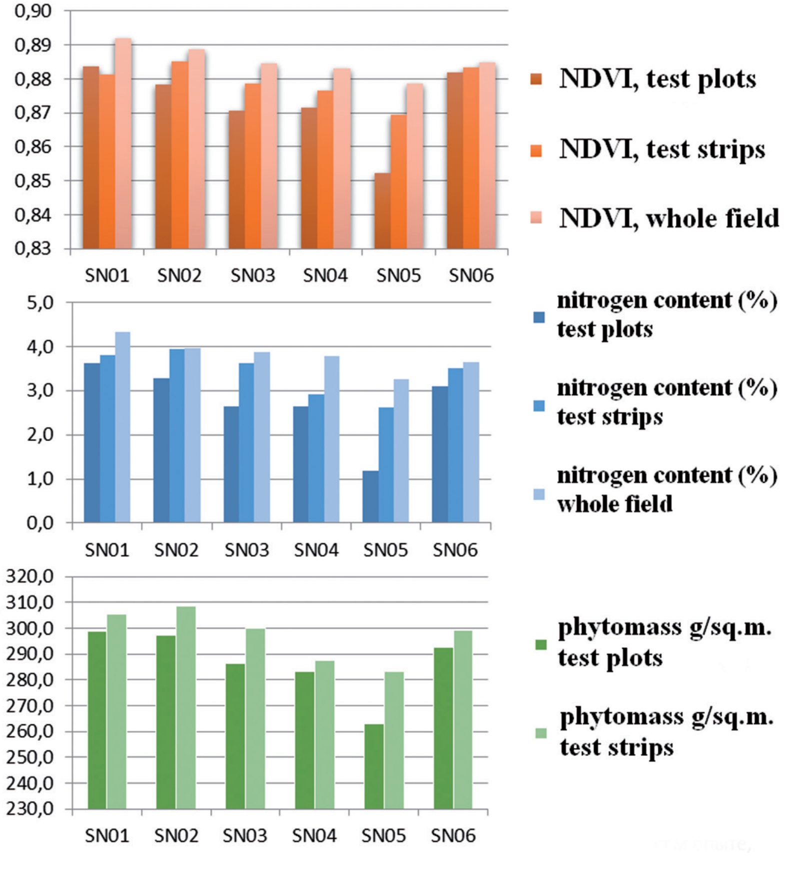

Fig. 6. The indicators of the state of crops obtained from the results of hyperspectral survey on April 08, 2016

Another way to utilize hyperspectral information is to analyze the graphs of spectral reflectance (Fig. 7). The measurements results showed that according to the data for April 8-9, 2016, the test plots SN01 and SN02, with the highest parameters, had a sufficiently high reflectance in the NIR range (greater than 750 nm) (associated with moisture and leaf

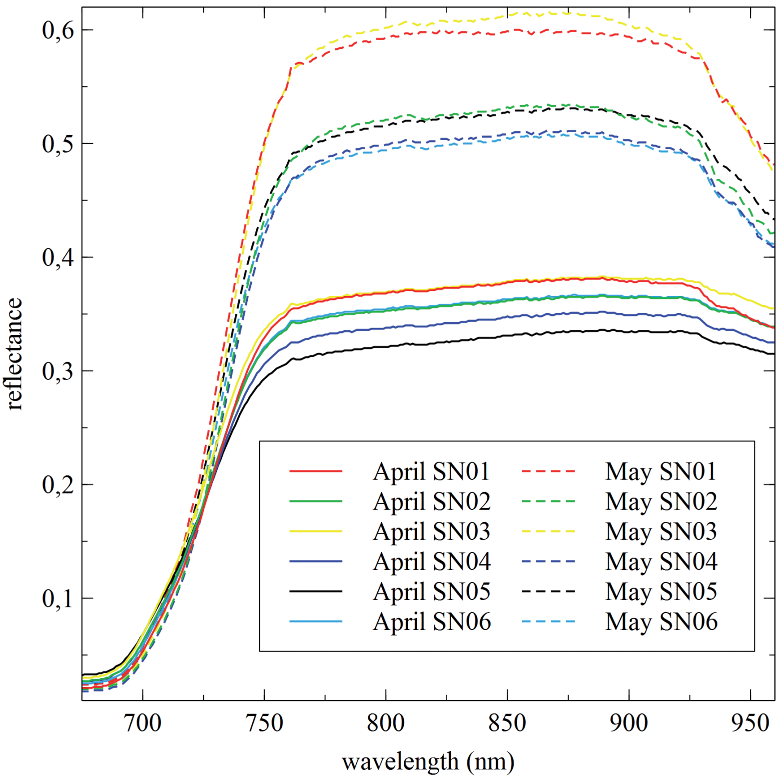

Fig. 7. Comparison of the reflectance graphs from the ground-based spectroradiometry data for Yucca variety of winter wheat. Dotted lines represent the data of April 9, 2016, and continuous lines represent the data of May 6, 2016

structure) and medium (relative to other test plots) reflectance at the red minimum (about 650 nm) (associated with the absorption of chlorophyll). The test plot SN05, with the worst state of plants, had a low reflectance in the NIR range and a high reflectance in the red spectral range. The test plot SN06, with relatively good plant condition indices, had a low reflectance in the NIR range and a low reflectance in the red spectral range, which indicates a sufficiently high chlorophyll content in plants, but poorer general conditions compared to SN01 and SN02.

To analyze the dynamics of wheat development from early April to the end of May, 2016, with the aerial survey data, we compared the results of hyperspectral surveys for April 8-9 and May 30, 2016, for the southern part of the field. Thus, by the end of May, NDVI had already fallen to an average of 0,77 compared with the beginning of April (an average of 0,88) (Fig. 8). At the same time, according to the available data from the Landsat 8 satellite, which is in good agreement with our data, the maximum NDVI was observed on April 23, 2016, and was about 0,9. According to our hyperspectral surveys on May 6, 2016, it reached 0,9-1,0. Thus, the maximum NDVI and green phytomass in the field were achieved in 2016 in late April - early May. By the end of May, the NDVI decreased to 0,77 (which was due to a decrease in the amount of chlorophyll in ripening wheat). On June 20 (according to the Tetracam camera survey), there was a decrease in NDVI to 0,40-0,60. It fell to 0,20-0,40 at the eastern margin of the field. In general, there was a good correspondence between the NDVI maps compiled from the satellite and aerial data, which makes it possible to use both types of sensors for monitoring of the general state of fields. However, NDVI did not provide sufficient differentiation between the experiments, which differ in the values of the index by only 1-2%. This, as already noted earlier, is due to the fact that the NDVI index was calculated from broad spectral bands.

The ground-based dynamics of wheat development from early April to the end of June, 2016, was obtained from the available data of the direct field measurements of spectral images of plants, as well as from the phytomass data. These data allowed analyzing the changes that have occurred in plants over one and three months. Thus, in May, the vegetation became much denser and the phytomass increased significantly, which was reflected in the increase of reflectance in the NIR part of the spectrum (Fig. 7). In May, as in April, the highest NIR reflectance was observed in the test plots SN03 and SN01. Small changes were noted in other test plots. Reflectance in the NIR range of SN02 closely followed the SN03 and SN01 values in April and May; however, in April, the identical values were associated with SN06, while in May, this test plot had the minimum reflectance values close to SN04.

SN05, which had the lowest values in April, became identical to the SN02 spectral image in May. Thus, the test plot SN05, with the strongest dressing treatment, caught up with the test plots that had average and good conditions, while the test plot SN06 (where a standard dressing treatment, as on the adjacent farm fields, was used) has slowed its development. The dynamics of the green phytomass values for the six test plots according to the April, May, and June data, is shown in Fig. 9. The dynamics of the phytomass values of the test plots has changed. In April, the highest values were observed for the test plots SN02, SN04, and SN06 and were approximately equal. The values for the test plots SN01, SN03, and SN05 were smaller and also approximately equal.

In May, there were significant changes visible in the test plot SN04, which had the largest phytomass in April, while the smallest in May. The test plot SN01 had a comparatively

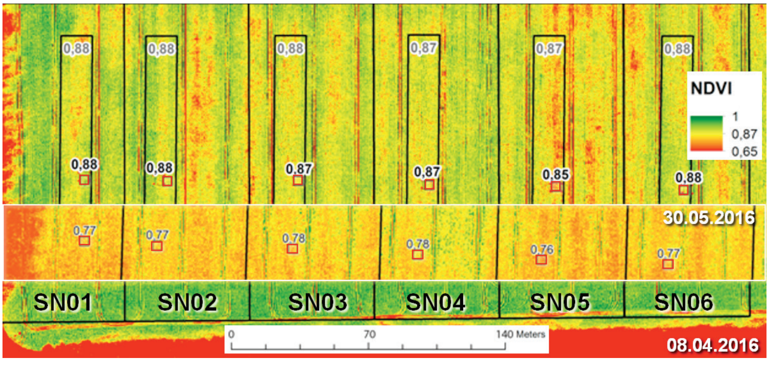

Fig. 8. The NDVI maps for April 8, 2016 and for May 30, 2016 (the enlarged fragment in the figure represent the southern part of the Syngenta filed). The numbers on the map indicate the NDVI values for the test plots (squares)

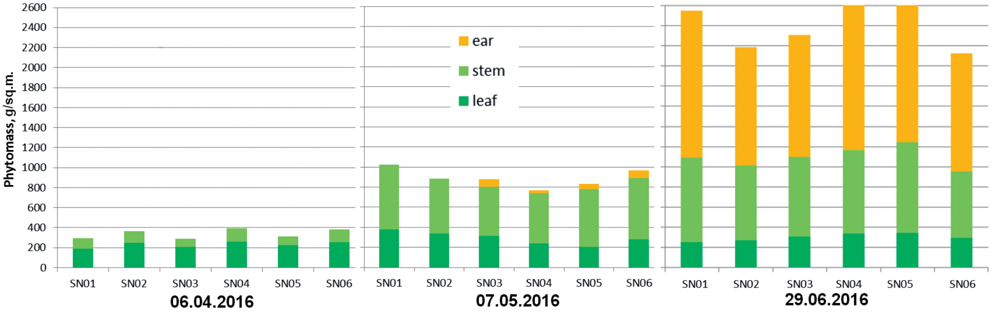

Fig. 9. Comparison of the green phytomass values for Yukka wheat variety in April (April 9, 2016), May (May 7, 2016), and June (June 29, 2016)

low phytomass in April; however, in May, it became the highest (has not yet formed ears of wheat). The test plots SN02 and SN06 that had a high phytomass value in April, retained their position in May, with one difference: ears of wheat did not yet appear on SN02. At the end of June, the situation changed again: SN05, along with SN01 and SN02, took the lead. Thus, despite the low green phytomass in early April, the wheat on SN05, treated with the strongest dressing, gradually increased the phytomass, had a high density of plants (according to the ground count), and yielded high crop, along with wheat on SN01 and SN02.

The second line of research on the assessment of drought resistance of various corn hybrids was carried out in cooperation with Syngenta company under the ARTESIAN project. The work was performed on the fields of the Stavropol and Krasnodar regions using UAS Gamaya hyperspectral survey and ground measurements of the crop state (Fig. 10).

Under conditions of stress, the NDVI index decreased and the corn hybrids differentiated according to their state, depending on the density of the crops and the efficiency of moisture intake through the root system. In addition, there was a clear deterioration in the state of crops from the middle to the end of July, 2016, due to drought (Fig. 10). In the Stavropol region, cultures had a higher green phytomass. Analysis of the crops reflectance confirmed the observed deterioration in the state of crops from the middle to the end of July, 2016, due to drought. In the Stavropol region, however, crops still had a higher green phytomass.

CONCLUSION

The study of the characteristics of spectral images of agricultural crops has enabled us to draw several conclusions. Firstly, to obtain reliable information on the state of crops, ground-based measurements of their morphometric parameters are

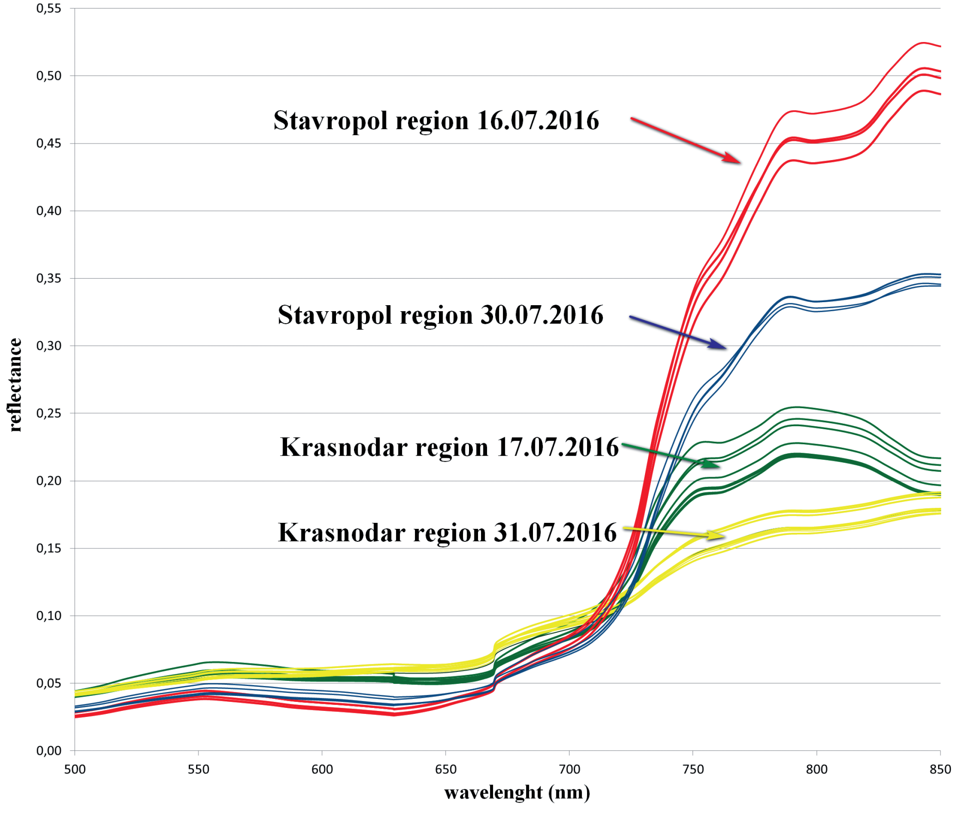

Fig. 10. The reflectance dynamics for various corn hybrids on 16-31 July, 2016, on two fields (Stavropol and Krasnodar regions)

required to obtain quantitative data and establish correlation dependencies between field experiments and hyperspectral survey results. Secondly, hyperspectral indices for the calculation of nitrogen content and plant phytomass are much more sensitive than NDVI. Thirdly, the use of a set of indicators, namely reflectance values, morphometric parameters of plants, and vegetation indices, is effective in interpreting data of aerial hyperspectral surveys and information support for precision farming. The proposed research methodology allows creating maps that reflect the current state of agricultural crops, and recommend the necessary timely agro-technical practices.

ACKNOWLEDGMENT

The research was conducted with the technical and financial support of the Program on Development Program of Moscow University through 2020, the Project "Geoportal of Moscow State University" (http://www.geogr.msu.ru/science/projects/geoportal/), and Gamaya (www.gamaya.com) and Syngenta companies (www.syngenta.com).

The authors express their sincere gratitude to A. Tenekov (Agro-Soft, LLC), A. Gorobets, D. Ogienko, S. Tsapenko (Syngenta), M. Cubero-Castan (Gamaya), the Central Agrochemical Inspection of the Krasnodar region for the data provided, logistical support and consultations, as well as to the colleagues and students from M.V. Lomonosov Moscow State University – I.I. Sereda, I.V. Sadovaya, M.K. Tarasov, A.I. Mikheeva, A.A. Derkacheva, P.G. Eremkina, for assistance in field research and data processing.

We are especially grateful to A. Trufanov for help, unmanned aircraft surveys, valuable suggestions, consultations, and discussion of research results.

REFERENCES

Bao Y., Xu K., Min J., Xu J. (2013) Estimating wheat shoot nitrogen content at vegetative stage from in situ hyperspectral measurements. Crop science, 5, pp. 2063–2071.

Blackburn G. (1998) Spectral indices for estimating photosynthetic pigment concentrations: a test using senescent tree leaves. International Journal of Remote Sensing, 19(4), pp. 657-675

Borengasser M., Hungate W., Watkins R. (2007) Hyperspectral Remote Sensing: Principles and Applications. Boca Raton, Florida, USA: CRC Press

Constantin D. (2017) Miniature hyperspectral systems. (Dirs: B. Merminod and Y. Akhtman) Thèse École polytechnique fédérale de Lausanne EPFL, n° 7647 (DOI:10.5075/epfl-thesis-7647)

Constantin D., Rehak M., Akhtman Y., Liebisch F. (2015) Detection of crop properties by means of hyperspectral remote sensing from a micro UAV. Bornimer Agrartechnische Berichte 88 (EPFL-CONF-218662), pp.129-137

Haboudane D., Miller J., Pattey E., Zarco-Tejada P., Strachan I. (2004) Hyperspectral vegetation indices and novel algorithms for predicting green LAI of crop canopies: Modeling and validation in the context of precision agriculture. Remote Sensing of Environment 90 (3), 337-352

Liebisch F., Kirchgessner N., Schneider D., Walter A., Hund A. (2015) Remote, aerial phenotyping of maize traits with a mobile multi-sensor approach. Plant methods 11 (1), 9, 2015. DOI: 10.1186/s13007-015-0048-8

Liebisch F., Rohrer B., Walter A. (2015). Evaluation of literature indices for determination of crop biophysical properties for ground and airborne hyperspectral methods. In: 9th EARSeL

SIG Imaging Spectroscopy workshop, Luxembourg. 14 – 16 April 2015. Poster. http://www.seon.uzh.ch/dam/jcr:ffffffff-9847-0310-0000-00001eb0e644/Liebisch_EARSEL_Poster_print.pdf [Accessed 2 December 2017]

Sidko A., Pugacheva I., Shevyrnogov A. (2009) A study of spectral brightness dynamics of agricultural crops in vegetation period for determination of their species composition by ground and satellite methods in the southern part of the Krasnodar region. Earth Satellite Studies, 2, pp.71-78.

Thenkabail P., Lyon J., Huete A. (2011). Hyperspectral Remote Sensing of Vegetation. Boca Raton, Florida, USA: CRC Press.

Thenkabail P., Gumma M., Teluguntla P. and Mohammed I. (2014). Hyperspectral Remote Sensing of Vegetation and Agricultural Crops. Photogrammetric Engineering & Remote Sensing, 80 (8). pp. 697-723.

Yakushev V., Petrushis A. (2013) Acquisition, processing, and use of remote sensing data for monitoring of meliorative conditions of agricultural fields. Agrophysics, 2 (10), pp. 52-58.

Zimin M., Tutubalina O., Golubeva E., Ris G. (2014) Ground spectroradiometric methodology of Arctic plants for satellite images interpretation. Moscow University Bulletin, Series 5 (Geography), 4, pp. 34–41.

Received on October 20th, 2017 Accepted on November 22nd, 2017

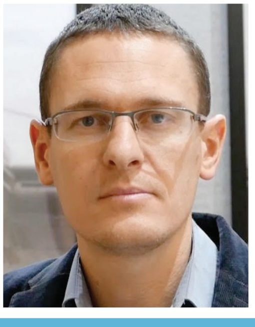

Yosef Akhtman, Ph.D., is Research Associate at the Geodetic Engineering Laboratory of École Polytechnique Fédérale de Lausanne (EPFL), Switzerland. He is the founder and CEO of Gamaya – a Swiss-based company providing precision farming solutions based on hyperspectral remote sensing and machine learning. He was Research Fellow at the Telecommunications and the Hybrid Optoelectronics Laboratories at the University of Southampton, UK, where he obtained his doctorate degree in Electronics Engineering in 2007. His main interests are focused on the development of airborne remote sensing platforms and hyperspectral imaging sensors. He has authored over 50 scientific papers and patents spanning the subjects of information theory, mobile robotics, and remote sensing of environment.

Elena I. Golubeva is Professor of the Environmental Science Department and Head of Education Programs "Ecology and Environmental Science" and "Landscape Planning and Design" at the Faculty of Geography, Lomonosov Moscow State University (1974 – M.Sc. in Biogeography, 1982 – Ph.D. in Biogeography, 1999 – D. Sc. in Biology). She is Member of the Russian Academy of Natural Science, Laureate of Russian Governmental Award in Science and Technology. Her primary research interests are in diagnostics of ecosystem health under natural and anthropogenic pressure. She is the author of over 200 scientific papers.

Olga V. Tutubalina is Leading Researcher at the Laboratory of Aerospace Methods, Department of Cartography and Geoinformatics, Faculty of Geography of M.V. Lomonosov State University. She graduated from the Faculty of Geography in 1996 and then received M.Phil in GIS and Remote Sensing in 1997 and Ph.D. in Polar Remote Sensing in 2000 from the University of Cambridge, UK. Her scientific interests are in thematic computer processing of satellite imagery and its application in geographic and ecological research. She has published over 120 scientific papers.

Mikhail Zimin is Senior Researcher at the Laboratory of Aerospace Methods, Department of Cartography and Geoinformatics, Faculty of Geography, M.V. Lomonosov State University. He graduated from the Faculty of Geography in 2001 (M.Sc. Cartography and GIS) and then received Ph.D. in Cartography and GIS (2009). His scientific interests are in remote sensing, GIS, ground spectrometry, and its application in study of vegetation and landscapes. He has published over 60 scientific papers.

INSTRUCTIONS FOR AUTHORS CONTRIBUTING TO "GEOGRAPHY, ENVIRONMENT, SUSTAINABILITY"

AIMS AND SCOPE OF THE JOURNAL

The scientific English language journal 'GEOGRAPHY, ENVIRONMENT, SUSTAINABILITY' aims at informing and covering the results of research and global achievements in the sphere of geography, environmental conservation and sustainable development in the changing world. Publications of the journal are aimed at foreign and Russian scientists – geographers, ecologists, specialists in environmental conservation, natural resource use, education for sustainable development, GIS technology, cartography, social and political geography etc. Publications that are interdisciplinary, theoretical and methodological are particularly welcome, as well as those dealing with field studies in the sphere of environmental science.

Among the main thematic sections of the journal there are basics of geography and environmental science; fundamentals of sustainable development; environmental management; environment and natural resources; human (economic and social) geography; global and regional environmental and climate change; environmental regional planning; sustainable regional development; applied geographical and environmental studies; geo-informatics and environmental mapping; oil and gas exploration and environmental problems; nature conservation and biodiversity; environment and health; education for sustainable development.

GENERAL GUIDELINES

1. Authors are encouraged to submit high-quality, original work: scientific papers according to the scope of the Journal, reviews (only solicited) and brief articles.

2. Papers are accepted in English. Either British or American English spelling and punctuation may be used. Papers in French are accepted under the decision of the Editorial Board.

3. All authors of an article are asked to indicate their names (with one fore **name** in full for each author, other forenames being given as initials followed by the surname) and the name and full postal address (including postal code) of the **establishment(s)** where the work was done. If there is more than one institution involved in the work, authors' names should be linked to the appropriate institutions by the use of 1, 2, 3 etc superscript. **Telephone and fax numbers and e-mail addresses** of the authors could be published as well. One author should be identified as a **Corresponding Author.** The e-mail address of the corresponding author will be published, unless requested otherwise.

4. The GES Journal style is to include information about the author(s) of an article. Therefore we encourage the authors to submit their photos and short CVs.

5. The optimum size of a manuscript is about 3 000 – 5 000 words. Under the decision (or request) of the Editorial Board methodological and problem articles or reviews up to 8 000 – 10 000 words long can be accepted.

6. To facilitate the editorial assessment and reviewing process authors should submit "full" electronic version of their manuscript with embedded figures of "screen" quality as a **.pdf file.**

7. We encourage authors to list three potential expert reviewers in their field. The Editorial Board will view these names as suggestions only. All papers are reviewed by at least two reviewers selected from names suggested by authors, a list of reviewers maintained by GES, and other experts identified by the associate editors. Names of the selected reviewers are not disclosed to authors. The reviewers' comments are sent to authors for consideration.

MANUSCRIPT PREPARATION

Before preparing papers, authors should consult a current issue of the journal at http://ges.rgo.ru/jour/issue/current to make themselves familiar with the general format, layout of tables, citation of references etc.

1. Manuscript should be compiled in the following **order**: authors names; authors affiliations and contacts; title; abstract; key words; main text; acknowledgments; appendices (as appropriate); references; authors (brief CV and photo)

2. The **title** should be concise but informative to the general reader. The **abstract** should briefly summarize, in one paragraph (up to 1,500 characters), the general problem and objectives, the results obtained, and the implications. Up to six **keywords**, of which at least three do not appear in the title, should be provided.

3. The **main body** of the paper should be divided into: (a) **introduction**; (b) **materials and methods**; (c) **results**; (d) **discussion**; (e) **conclusion**; (f) **acknowledgements**; (g) **numbered references**. It is often an advantage to combine (c) and (d) with gains of conciseness and clarity. The next-level subdivisions are possible for (c) and (d) sections or their combination.

4. All **figures** (including photos of the authors) are required to be submitted as separate files in original formats (CorelDraw, Adobe Photoshop, Adobe Illustrator). Resolution of raster images should be not less than 300 dpi. Please number all figures (graphs, charts, photographs, and illustrations) in the order of their citation in the text. Composite figures should be labeled A, B, C, etc. Figure captions should be submitted as a separate file.

5. **Tables** should be numbered consecutively and include a brief title followed by up to several lines of explanation (if necessary). Parameters being measured, with units if appropriate, should be clearly indicated in the column headings. Each table should be submitted as a separate file in original format (MS Word, Excel, etc.).

6. Whenever possible, total number of **references** should not exceed 25-30. Each entry must have at least one corresponding reference in the text. In the text the surname of the author and the year of publication of the reference should be given in square brackets, i.e. [Author1, Author2, 2008]. Two or more references by the same author(s) published in the same year should be differentiated by letters a, b, c etc. For references with more than two authors, text citations should be shortened to the first name followed by et al.

7. **References** must be listed in alphabetical order at the end of the paper and numbered with Arabic numbers. References to the same author(s) should be in chronological order. Original languages other than English should be indicated in the end of the reference, e.g. (in Russian) etc.

Journal references should include: author(s) surname(s) and initials; year of publication (in brackets); article title; journal title; volume number and page numbers.

References to books should include: author(s) surname(s) and initials; year of publication (in brackets); book title; name of the publisher and place of publication.

References to multi-author works should include after the year of publication: chapter title; «In:» followed by book title; initials and name(s) of editor(s) in brackets; volume number and pages; name of the publisher and place of publication.

8. Authors must adhere to SI units. Units are not italicised.

9. When using a word which is or is asserted to be a proprietary term or trade mark, authors must use the symbol ® or TM.

10. As Instructions for Authors are subjected to changes, please see the latest issue at http://ges.rgo.ru/jour/issue/current

MANUSCRIPT SUBMISSION

Authors are encouraged to submit their manuscripts on-line using the GES Journal web-site http://ges.rgo.ru/index (after registration)

SOCIALLY SCIENTIFIC MAGAZINE “GEOGRAPHY, ENVIRONMENT, SUSTAINABILITY”

No. 04 (v. 10) 2017

FOUNDERS OF THE MAGAZINE: Russian Geographical Society, Faculty of Geography, Lomonosov Moscow State University and Institute of Geography of the Russian Academy of Sciences

The magazine is published with financial support of the Russian Geographical Society.

The magazine is registered in Federal service on supervision of observance of the legislation in sphere of mass communications and protection of a cultural heritage. The certificate of registration: ПИ № ФС77-67752, 2016, December 21.

EDITORIAL OFFICE
Lomonosov Moscow State University
Moscow 119991 Russia
Leninskie Gory,
Faculty of Geography, 1806a
Phone 7-495-9391552
Fax 7-495-9391552
E-mail: GES@rgo.ru
www.ges.rgo.ru

DESIGN & PRINTING
Agency «CONNECT»
Moscow, 117452,
Artekovskaya str., 9, korp. 1
Phone: +7 (495) 955-91-53
E-mail: info@connect-adv.ru

Sent into print 25.12.2017
Order N gi417

Format 70 ½ 100 cm/16
10,83 p. sh.
Digital print
Circulation 80 ex.